YAŞAR UNIVERSITY

GRADUATE SCHOOL OF NATURAL AND APPLIED SCIENCES

MASTER THESIS

OMNIDIRECTIONAL ANTENNAS FOR SATELLITE COMMUNICATION SYSTEMS

CEYHAN TÜRKMEN

THESIS ADVISOR: ASSOC.PROF. DR. MUSTAFA SEÇMEN

ELECTRICAL AND ELECTRONICS ENGINEERING

PRESENTATION DATE: 06.01.2017

BORNOVA / İZMİR
MONTH 2016

We certify that we have read this thesis and that in our opinion it is fully adequate, in scope and in quality, as a thesis for the degree of Master of Science.

Jury Members: **Signature:**
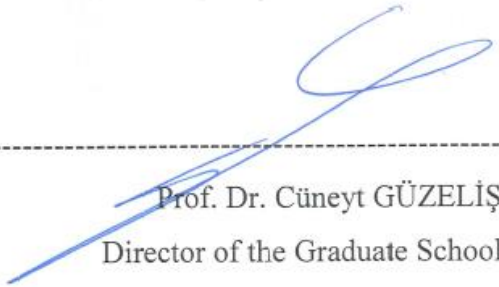
Assoc. Prof. Dr. Mustafa SEÇMEN
(Supervisor)
Yaşar University

Asst. Prof. Dr. Ali Haluk NALBANTOĞLU
Yaşar University

Prof. Dr. Korkut YEĞİN
Ege University

Prof. Dr. Cüneyt GÜZELİŞ
Director of the Graduate School

iii

ABSTRACT

OMNIDIRECTIONAL ANTENNAS FOR SATELLITE COMMUNICATION SYSTEMS

Türkmen, Ceyhan

M.Sc., Electrical and Electronics Engineering

Advisor: Assoc. Prof. Dr. Mustafa SEÇMEN

December 2016

In this thesis, the design, production and measurements of Ku-Band, omnidirectional and circularly polarized antennas, which can be used in satellite communication applications as receiver and/or transmitter, are explained. Ku-Band is a commonly used frequency band in satellite communication applications. These antennas consist of inclined slots (slotted array) placed with a circular symmetry on a circular waveguide. The antenna structures are fed by a special transition from standard rectangular waveguide to this circular waveguide, where the rectangular waveguide is the standard WR75 used frequently in Ku-Band applications. The electromagnetic wave propagates in only dominant TE_{10} mode inside the rectangular waveguide (main feed of the antenna), while propagating in the second higher order mode of TM_{01} inside circular waveguide. This TM_{01} mode is nondominant for circular waveguide; but has circular symmetry in the excitation of the slots on the antenna array, which provides omnidirectional pattern. The mentioned special transition effectively suppresses the dominant TE_{11} mode and other higher order modes such as TE_{21} in the circular waveguide, which disturbs symmetry (omnidirectionality) in the radiation pattern. In order to make the antennas circularly polarized, the slotted array elements are designed as inclined way, and parallel metallic plates (disks) are placed around the slotted arrays.

Three different versions of the proposed antenna are designed, simulated and implemented. The first one is designed just for transmitting purpose from the satellite to earth, and operates at the frequency about 11.75 GHz. Similarly, the second antenna is realized just for the receiving purpose from the ground segment to satellite. This

antenna operates at the frequency about 14.00 GHz. The last antenna design is more sophisticated than the other ones such that it works as a transceiver carrying out transmission at 11.75 GHz and reception at 14.00 GHz simultaneously.

According to results obtained for the first two designs, the return loss, which is better than 10 dB, is provided around the frequency regions of both transmitter (11.75 GHz) and receiver (14.00 GHz) within approximately 3 percent frequency bandwidth. In addition, axial ratio is lower than 1 dB in the azimuth plane and lower than 4 dB in a wide beamwidth of elevation plane at the center frequencies. Omnidirectional radiation pattern is provided at azimuth plane such that the variation of gain is about 0.7 dBi at this plane.

The transceiver version of the design has frequency bandwidth of about 350 MHz and 500 MHz for the maximum 10 dB return loss around the center frequencies of 11.75 GHz and 14.00 GHz, respectively. The axial ratio values are found to be lower than 2 dB in the azimuth plane for both center frequencies, which corresponds to good circular polarization performance. The values in the radiation patterns change at most 3 dB at the same plane.

Key Words: Satellite communication, transmit/receive antennas, circular polarization, slotted array antenna, Ku-Band, omnidirectional antennas

ÖZ

UYDU HABERLEŞME SİSTEMLERİ İÇİN YÖNSÜZ ANTENLER

Türkmen, Ceyhan

Yüksek Lisans, Elektrik Elektronik Mühendisliği

Danışman: Doç. Dr. Mustafa SEÇMEN

Aralık 2016

Bu tezde, uydu haberleşme uygulamalarında alıcı ya da verici olarak kullanılabilecek yönsüz, dairesel polarize, Ku-Band antenlerinin tasarımı, üretimi ve ölçümleri anlatılmaktadır. Ku-Bandı uydu haberleşme uygulamalarında yaygın olarak frekans bandı olarak kullanılmaktadır. Bu antenler dairesel dalga kılavuzu üzerine dairesel simetri ile yerleştirilmiş eğimli yarıklardan (yarıklı anten dizisi) oluşmaktadır. Anten yapıları, Ku- Bant uygulamalarında sıklıkla kullanılan, standart bir dikdörtgen dalga kılavuzu olan WR75 dikdörtgen dalga kılavuzundan dairesel dalga kılavuzuna özel bir geçiş yapısı tarafından beslenmektedir. Dairesel dalga kılavuzu içerisindeki elektromanyetik dalga ikinci yüksek mertebeli mod olan TM_{01} modu ile ilerlerken, dikdörtgen dalga kılavuzu içerisinde yalnızca TE_{10} baskın modu ile ilerlemektedir. TM_{01} modu dairesel dalga kılavuzu için baskın olmayan bir moddur, ancak yönsüz ışıma diyagramını sağlayan anten dizindeki yarıkların uyarılmasında dairesel simetriye sahiptir. Bahsedilen özel geçiş, dairesel dalga kılavuzu içerisinde ışıma diyagramındaki simetriyi (yönsüzlük) bozan dominant TE_{11} modunu ve TE_{21} gibi diğer yüksek mertebeli modları etkili bir şekilde batırır. Antenleri dairesel polarize yapmak için yarık anten dizisi elemanları eğimli olarak tasarlanmıştır ve yarık anten dizisi etrafına paralel metalik plakalar yerleştirilmiştir.

Önerilen antenin üç farklı sürümü tasarlanmış, simüle edilmiş ve uygulanmıştır. Bunlardan ilki yalnızca uydudan yeryüzüne verici olması amacıyla tasarlanmıştır ve 11.75 GHz frekansı etrafında çalışmaktadır. Benzer şekilde, ikinci anten yalnızca yer segmentinden uyduya bir alıcı amacıyla gerçekleştirilmiştir. Bu anten 14.00 GHz frekansı etrafında çalışmaktadır. Son anten tasarımı 11.75 GHz frekansında verici ve 14.00 GHz frekansında alıcı olarak çalışan bir dönüştürücü (alıcı/verici) anteni olmasıyla diğer antenlerden çok daha karmaşık bir yapıdadır.

İlk iki tasarımdan elde edilen sonuçlara göre, -10 dB den daha iyi olan geri dönüş kaybı verici (11.75 GHz) ve alıcı (14.00 GHz) frekans bölgelerinde yaklaşık yüzde 3 frekans bant genişliği sağlamaktadır. Ek olarak, merkez frekanslarda eksensel oran azimut ekseninde 1 dB den daha düşük iken elevasyon ekseninde geniş hüzme genişliği ile 4 dB den daha düşüktür. Azimut ekseninde yönsüz ışıma diyagramı sağlanmıştır. Bu eksendeki kazanç değişimi yaklaşık 0.7 dBi kadardır.

Tasarımın dönüştürücü sürümü 11.75 GHz ve 14.00 GHz merkez frekanslarında sırasıyla yaklaşık 350 MHz ve 500 MHz 10 dB geri yansıma kaybı bant genişliği değerlerine sahiptir. Eksensel oran değerleri her iki merkez frekans için azimut ekseninde iyi dairesel polarizasyon performansına karşılık gelecek şekilde 2 dB den daha düşük bulunmuştur. Aynı düzlemde ışıma diyagramı değerlerindeki maksimum değişim en fazla 3 dB kadardır.

Anahtar Kelimeler: Uydu haberleşmesi, alıcı/verici antenler, dairesel polarizasyon, yarık anten dizisi, Ku-Bant, yönsüz antenler

ACKNOWLEDGEMENTS

First of all, I would like to thank my supervisor Mustafa SEÇMEN for his guidance and patience during this study.

I would like to express my enduring love to my parents, who are always supportive, loving and caring to me in every possible way in my life.

I would like to thank Serdar OKUYUCU for his supports and helps during the this study.

I would like to thank Göksenin BOZDAĞ for his helps during the measurements in this study.

I would like to thank Ege University Electromagnetic Crew for their supports and motivation during this study.

<div align="right">

Ceyhan TÜRKMEN

İzmir, 2016

</div>

TEXT OF OATH

I declare and honestly confirm that my study, titled "OMNIDIRECTIONAL ANTENNAS FOR SATELLITE COMMUNICATION SYSTEMS" and presented as a Master's Thesis, has been written without applying to any assistance inconsistent with scientific ethics and traditions. I declare, to the best of my knowledge and belief, that all content and ideas drawn directly or indirectly from external sources are indicated in the text and listed in the list of references.

Ceyhan TÜRKMEN

Signature

January 30, 2017

TABLE OF CONTENTS

LIST OF FIGURES

LIST OF TABLES

SYMBOLS AND ABBREVIATIONS

ABBREVIATIONS:

RF   Radio Frequency

LHCP   Left Hand Circular Polarization

RHCP   Right Hand Circular Polarization

LOS   Line of Sight

TT&C   Tracking Telemetry & Command

TTC&M Tracking Telemetry Command & Monitoring

IMUX   Input Multiplexer

OMUX   Output Multiplexer

DHU   Data Handling Unit

TC-TX   Transmitter Test Cap

TC-RX   Receiver Test Cap

LPF   Low Pass Filter

BPF   Band Pass Filter

DUT   Device Under Test

NA   Network Analyzer

AR   Axial Ratio

TEM   Transverse Electromagnetic

TE   Transverse Electric

TM   Transverse Magnetic

CHAPTER ONE
INTRODUCTION

1.1. Scope of the Thesis

In satellite communication, satellite/spacecraft positions with respect to earth can not be exactly known at time interval between satellite/spacecraft launch from the earth and its settlement to the desired orbit. This is due to random angular motion of the satellite throughout this duration; thus, the aspect angle of the satellite/spacecraft is expected to be usually random and fluctuating with respect to earth. Even if the position of the satellite/spacecraft is random; earth station must communicate with satellite/spacecraft in order to provide proper arrangement of orientation of the satellite to its orbit. During this period, the communication from satellite to earth station is provided via a transmitter antenna, which sends signals continuously. Besides, when a satellite/spacecraft reaches to its orbit, it sends an arrival message to earth station by the transmitter antenna in general satellite applications. The orientation of the satellite/spacecraft is adjusted with a command, which is sent from earth station to the satellite/spacecraft and gathered by a receiver antenna on the satellite. Since the angular position of the satellite; consequently, the positions of transmitter and receiver antennas are random with respect to earth station, these antennas should have radiation pattern characteristics allowing transmission and reception at any aspect angle. This radiation characteristic is called as nondirectional or uniform pattern, and it belongs to an isotropic antenna. However, isotropic antenna is a hypothetical (imaginary) antenna such that real (practical) antennas do not have perfect nondirectional pattern, i.e., they have some directionalities to certain angles somehow (Balanis, 2005).

Omnidirectional antennas are very good candidates for the desired uniform radiation pattern such that they have very good (but not perfect) nondirectional characteristics. The antennas possess almost perfect uniform pattern at one principal plane (usually at the azimuthal plane) and moderate directional behavior at the other plane (usually at elevation plane). Omnidirectional antennas are frequently employed in satellite

communication systems as transmitter, receiver or transceiver antennas in order to supply uninterrupted connection between earth station and satellite/spacecraft without any significant power fluctuation. Omnidirectional patterns of these antennas make the connection between earth station and satellite/spacecraft highly independent from the instant aspect angle of the satellite/spacecraft.

Polarization mismatch (loss factor) between antennas causes an important loss especially in satellite communication systems. In a communication system with two stations being transmitter and receiver stations, when one station is fixed and the other station is mobile, one antenna has linear polarization and the other has circular polarization. This situation results in a reasonable signal level collected by the system regardless of the aspect angle of the mobile station antenna with respect to fixed antenna station. In telemetry and telecommand applications of satellite communication systems, the polarization of the transmitter and receiver antennas on the satellite are usually selected to be circular. When the antennas on the satellites belong to circular polarization, the linearly polarized incoming/outgoing signal can be received/transmitted in any orientation angle without any significant power changes (Stutzman, Thiele, 2013). Therefore, the received or transmitted signal level do not decrease significantly due to polarization loss for random aspect angles of the satellite/spacecraft along the time interval between the satellite/spacecraft is launched and settled to its orbit. The transmitter antennas on the satellite used for telemetry purpose have usually single circular polarization (left hand circular polarization-LHCP or right hand circular polarization-RHCP) due to limitation in the RF power generation. The receiver antennas on the satellite used for telecommand purpose can have single circular polarization; but they are preferably designed to give dual circular polarization (LHCP and RHCP at the same time) in order to maximize received RF power.

This thesis strives to design antennas, which can be employed in satellite communication systems as receiver (telemetry) and transmitter (telecommand) antennas. It is aimed that the antennas, which are designed, should have sufficient performance for the usage in satellite communication applications. Therefore, properties of the antennas are determined by taking general requirements and standards of satellite communication applications into account. It is decided that the antennas must have omnidirectional radiation pattern and circular polarization in order to operate effectively during from the launch of the satellite to settlement of its orbit with

proper angle. Additionally, it is aimed that antennas to be compatible as physically with satellite communication systems. Therefore, the connection port of antennas is selected as standard rectangular waveguide WR75, which is frequently used in satellite communication systems.

1.2. Motivation and Literature Search

Omnidirectional antennas are usually employed in order to provide uninterrupted connection between transmitter and receiver systems one or both of which are mobile. In this thesis, these systems are earth station part and satellite/spacecraft part where satellite part of the communication is mobile. According to definition (Balanis, 2005), the omnidirectional radiation pattern is the one having nondirectional (uniform) pattern characteristics in azimuth plane $[f(\emptyset), \theta = \pi/2]$ and directional pattern characteristics in the elevation plane $[f(\theta), \emptyset = constant]$ for the geometry and axes given in Figure 1.
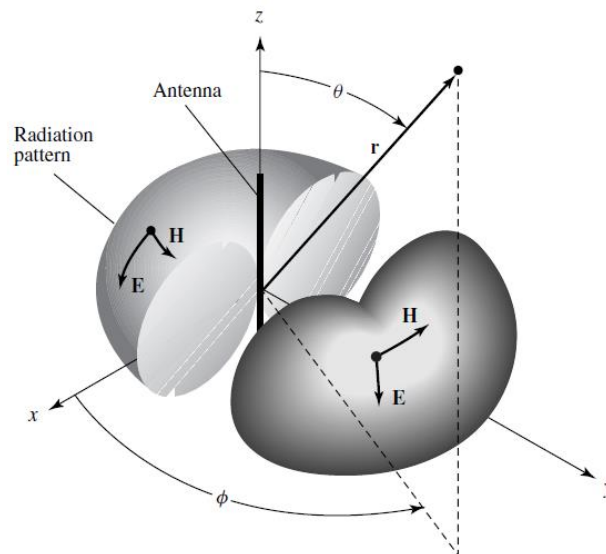
Figure 1. Omnidirectional Antenna Pattern (Balanis, 2005).

It is emphasized in (Shafai, Sharma and Rao, 2013) that the common types of antennas used in satellite systems are the omnidirectional transmit and receive antennas and the wide coverage receive and transmit horn antennas. No single antenna can achieve nondirectional (spherical) radiation in the presence of large scattering objects, such as spacecraft earth panel, structures, and waveguide feeds, it is augmented with one or more additional antennas of different configuration and combining each pattern to

form a composite radiation pattern that satisfies the spacecraft requirements in terms of antenna coverage angles and gain to provide positive radio link performance (Shafai, Sharma and Rao, 2013).

One way to acquire nondirectional (spherical) pattern is the usage of two identical hemispherical antennas, which are constituted with the addition of metallic rings around a circular aperture antenna (Lim, Nyambayar, Yun, Kim, Ahn, Bang, 2014). These antennas are placed such that one is on top platform and the other is on the bottom platform of the satellite, which results in full space (nondirectional) coverage as stated in the study of (Turkmen and Secmen, 2016) as given in Figure 2(a). Hemispherical antennas are generally used to make radiation in the satellite communication in a volume covering the elevation plane of $0° < \theta < 90°$ and the azimuth plane of $0° < \phi < 360°$ according to the geometry in Figure 1. However, the gain of these hemispherical antennas can be as low as -10 dBi at the boundary points ($\theta = 90°$). Besides, the addition of metallic rings around circular aperture makes the antennas occupying larger space in area.

(a)   (b)
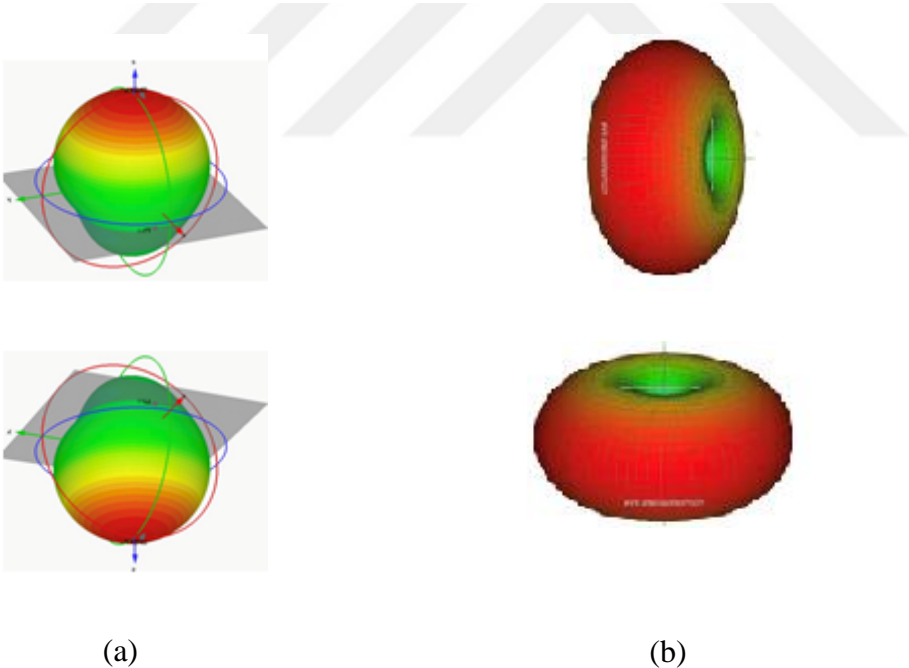
Figure 2. Full Space Coverage Methods (a) Using Two Identical Hemispherical Antennas (b) Using Two Identical Omnidirectional Antennas.

The full space coverage can be also obtained by using two identical omnidirectional antennas, which is preferred way in this thesis. The omnidirectional antennas designed

in this thesis are realized by placing slotted antenna circular array around a circular waveguide. They are generally utilized to give radiation in the satellite communication in a volume covering the elevation plane of $45° < \theta < 135°$ and the azimuth plane of $0° < \phi < 360°$ consistent with the geometry in Figure 1. In order to obtain full coverage with two identical omnidirectional antennas, they must be placed on the platform as perpendicular to each other as given in Figure 2(b). At the edge regions ($\theta = 45°\ or\ \theta = 135°$), the gain can be around -5 dBi, which is higher than the minimum gain of hemispherical antennas used for the same purpose. Besides, the omnidirectional antennas stated in this thesis have more compact structure as compared to the hemispherical antennas. This is because the omnidirectional ones contain one circular waveguide and a disk around it to provide circular polarization, which gives smaller physical cross section than that of the hemispherical antennas. The higher minimum gain and being compact structure are some of the reasons why the omnidirectional antennas are preferred instead of hemispherical ones. Omnidirectional antennas used in satellite communication systems are more common in American market, while hemispherical antennas are commonly used in European market.

It is stated in (Stutzman, Thiele 2013) that circularly polarized antennas are desired to use in satellite communication systems. Because, the wave from a linearly polarized antenna on a spacecraft will rotate due to motion or Faraday rotation in the ionosphere, but if a circularly polarized antenna is used, the incoming linearly polarized wave orientation angle will not lead to power level fluctuations. Even though a 3-dB signal loss encountered, the received signal remains constant. Satellites move with respect to ground stations. Some geometric differences may vary because of the small changing the position of the satellite with respect to ground station. In addition to atmospheric effects, geometric changings effect to communication system efficiency. Circular polarization keeps constant signals regardless of these anomalies. Circularly polarized antennas provide high performance point-to-point long run connections due to linear noise rejection. If there are any reflection in communication path, one polarization is outperform the other. Besides other RF signals in the communication path can be isolated by using a polarization in the opposite predominant high level signals. When a RF signals reflect from a smooth surface, 180° phase difference may occurs. This is a phenomena, which is known as specular or mirror image reflection. The reflected

signal may create destructively or constructively effect on Line Of Sight (LOS) signal. Circular polarization is used to this situation as an advantage since the reflected wave would have a different sense than the direct wave and block the fading from these reflections.

In literature, there are circularly polarized waveguide antennas but most of these antennas have not omnidirectional or hemispherical radiation pattern. Especially, the circularly polarized slot antenna array on rectangular waveguide type antennas exist in literature. However, these antennas based on this technique can not provide desired omnidirectional radiation pattern due to physical structure of the rectangular waveguide (Gao, Luo and Zhu, 2014).

The circular polarization can be achieved for the hemispherical antennas mentioned above with a septum polarizer, which is a microwave component attached just before the hemispherical antenna. The septum polarizer is a special component, which converts linear polarization of the rectangular waveguide or coaxial cable to the circular polarization of the square waveguide or vice-versa (Bornemann, Amari, Uher, Vahdieck, 1999), (Bertin, Piovano, Accatino, Mongiardo, 2002), (Zhong, Li, Fan, Shen, 2011). However, the septum polarizer should be carefully and specially designed to give sufficient circular polarization within the desired bandwidth, which makes the design of circularly polarized hemispherical antenna much more complex.

In this thesis, the circular waveguide slotted antenna array with omnidirectional radiation pattern is preferred. The other reason of the selection of omnidirectional antenna in addition to higher minimum gain within the coverage and compactness is the simple design to give circular polarization as compared to hemispherical antenna. In omnidirectional antenna used for the satellite communication purpose in this thesis, the polarization of the circular waveguide slotted antenna can be adjusted just with the slope of the antenna slots and the radius of metallic ring plates added around the circular waveguide. Therefore, circular polarization can be obtained by arrangement of these parameters, which results in a much simpler design.

Although there are some similar studies, there is not enough study about circularly polarized omnidirectional antennas in literature, which increases the novelty and contribution of the study performed in this thesis. The thesis is aimed to improve the results of the other similar studies. From the literature search result, there are two

similar studies, which can be taken as comparison for this thesis. The results that belong to first of these studies is given by Top and Dogan give -10 dB frequency bandwidth is about 1.005%. The gain is greater than 1 dBi in the $-10^0/+30^0$ elevation plane sector. The ripple of gain in azimuth plane is about +/- 0.75 dBi, which corresponds to 1.5 dBi gain variation. The axial ratio in azimuth plane is better than about 3.5 dB. The axial ratio in elevation plane better than 4.2 dB in $-10^o/+30^o$ and 6 dB in the $-25^o/+89^o$ region. The results that belong the other study is given by Masa-Campos, Fernandez, Sierra-Perez and Fernandez-Jambrina give -10 dB frequency bandwidth is about 1.4%. The gain is about 0.5 dBi in the azimuth plane with measured maximum ripple is 1.9 dBi. Axial ratio in azimuth plane is 3.2 dB, with a ripple of 1.5 dB. The antenna designs in this thesis are going to be shown to give wider -10 dB frequency bandwidth, smaller gain variation and better axial ratio performance.

The antenna designs/studies expressed in above paragraph including the first two antennas designed in this thesis are used only for transmitting or receiving purpose on the satellite. They can not be used to operate for transmitting and receiving purpose at the same time, in other words, transceiver purpose. This is because the transmitter and receiver frequencies in satellite communication are sufficiently far away so the antennas designs described above can not cover that kind of wide bandwidth. To the best of our knowledge, a single circularly polarized omnidirectional waveguide antenna covering both transmitter and receiver frequencies of satellite communication is not found in literature. In this thesis, as the last and most novel design among three designs, a single antenna structure is also carried out to give circularly polarized omnidirectional pattern in both transmitter and receiver frequencies by using a dual band technique rather than wideband technique.

1.3. Thesis Overview and Outline of the Thesis

In the thesis, a single transmit antenna, a single receive antenna and a transceiver antenna (transmit and receive structures together) designs are proposed. The configuration of each structure is given. It is followed by the explanations about proposed antenna operations. The design steps as well as the parametric antenna structures/studies are constructed. Then, some parametric optimizations are implemented on the structures, and it is understood which antenna property is affected by which parameter in the design from the optimization study. The optimization

process continues until the desired antenna results are achieved. After the optimization process, only the prototype of the proposed receiver antenna is manufactured. The measurements of prototype are performed in Antenna and Microwave Laboratories of Yasar University and Izmir Institute of Technology (IYTE). Measurements and simulation results are compared to each other for the confirmation of results. Afterwards, the evaluation of the proposed antennas is given. Finally, the study is concluded, and the comments of proposed antennas are supplied.

This thesis can be examined in the six chapters; structures of satellite communication systems, electromagnetic mode conversions and transitions between waveguide components, separate transmit and receive antenna design, combined transceiver antenna design.

In Chapter 2, it is included overview satellite communication systems, fundamental components, required antenna parameters and electromagnetic mode conversions.

Chapter 3 focuses physically and electromagnetically transitions between rectangular waveguide to circular waveguide.

Chapter 4 explains the design of transmit and receive antennas, which have separate structures to each other.

Chapter 5 gives the design of transceiver antenna, which is obtained by the combination of transmit and receive antenna structures.

Chapter 6 concludes the thesis.

CHAPTER TWO

THE STRUCTURE OF SATELLITE COMMUNICATION SYSTEMS

2.1. Satellite Communication Systems Overview

The satellite communication systems can be divided into two main part as; space segment and the ground segment. A simple representation of a space segment is shown in Figure 3. Position information is sent from satellite to ground station by telemetry system. The position information is processed on ground station and required commands, which provide correct settlement of satellite to its orbit, are sent back to satellite from ground station by telecommand systems.
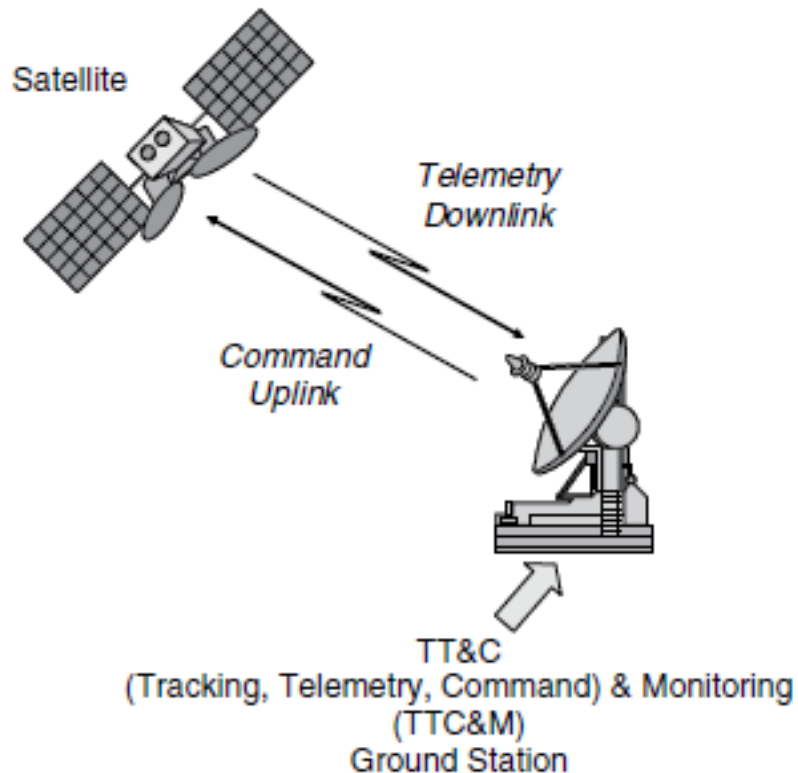
Figure 3. Satellite Communication System (Ippolito Jr, 2008).

Space segment consists one satellite or a group of satellite and ground station, which provides the operational control to keep the satellites safely in orbit. The ground station

is variously referred as the Tracking, Telemetry, Command (TT&C) or the Tracking, Telemetry, Command and Monitoring (TTC&M) station (Ippolito Jr, 2008). The satellite must contain a platform and a payload. The payload is composed from receiving and transmitting antennas with all other electronic communication equipment that provide carrier signal transmission. The organization chart of a sample payload is shown in Figure 4.
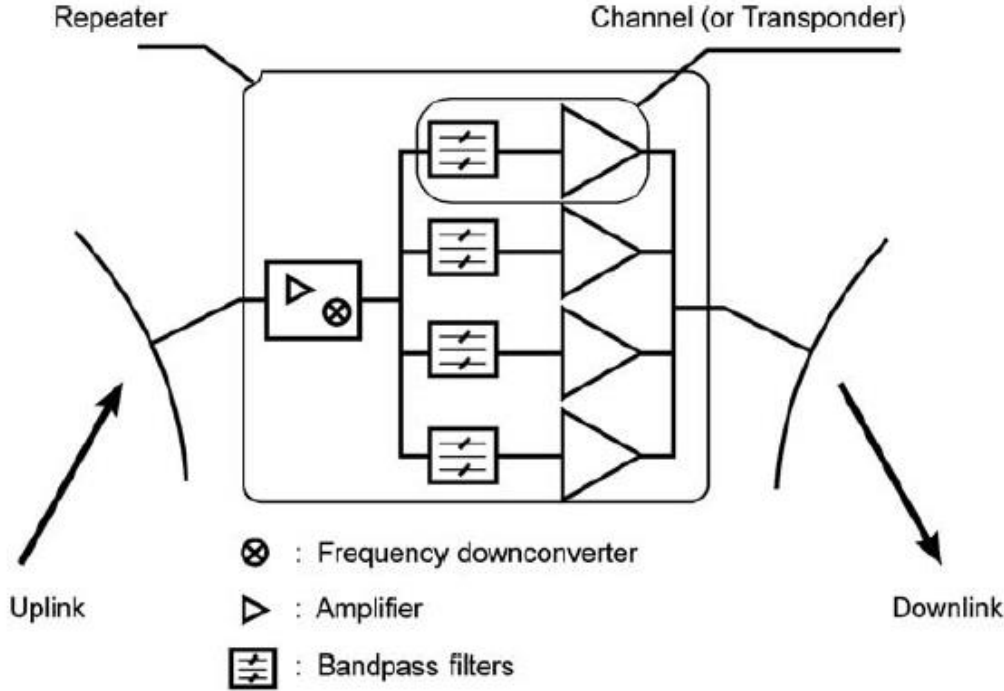
Figure 4. A Payload Organization Chart (Maral, Bousquet, 2010).

On the payload shown Figure 4 carrier signal, which comes from uplink system, is amplified, and it is frequency down converted. The isolation between input (received) signal and output (transmitted) signal is provided by this frequency conversion. Payload bandwidth is divided into some sub-bands. Bandwidth division is realized with input multiplexer (IMUX), which consists of a group of filter. Output carrier signal that are amplified are recombined via output multiplexer (OMUX).

Ground segment includes all data traffic in earth stations. It includes three basic types of terminals as; fixed (in-place) terminals, transportable terminals and mobile terminals. These terminals mostly connected to end users via terrestrial networks or small stations. An organization chart of an earth station is given in Figure 5. TTC&M ground stations are not a part of ground segment depicted in Figure 5.
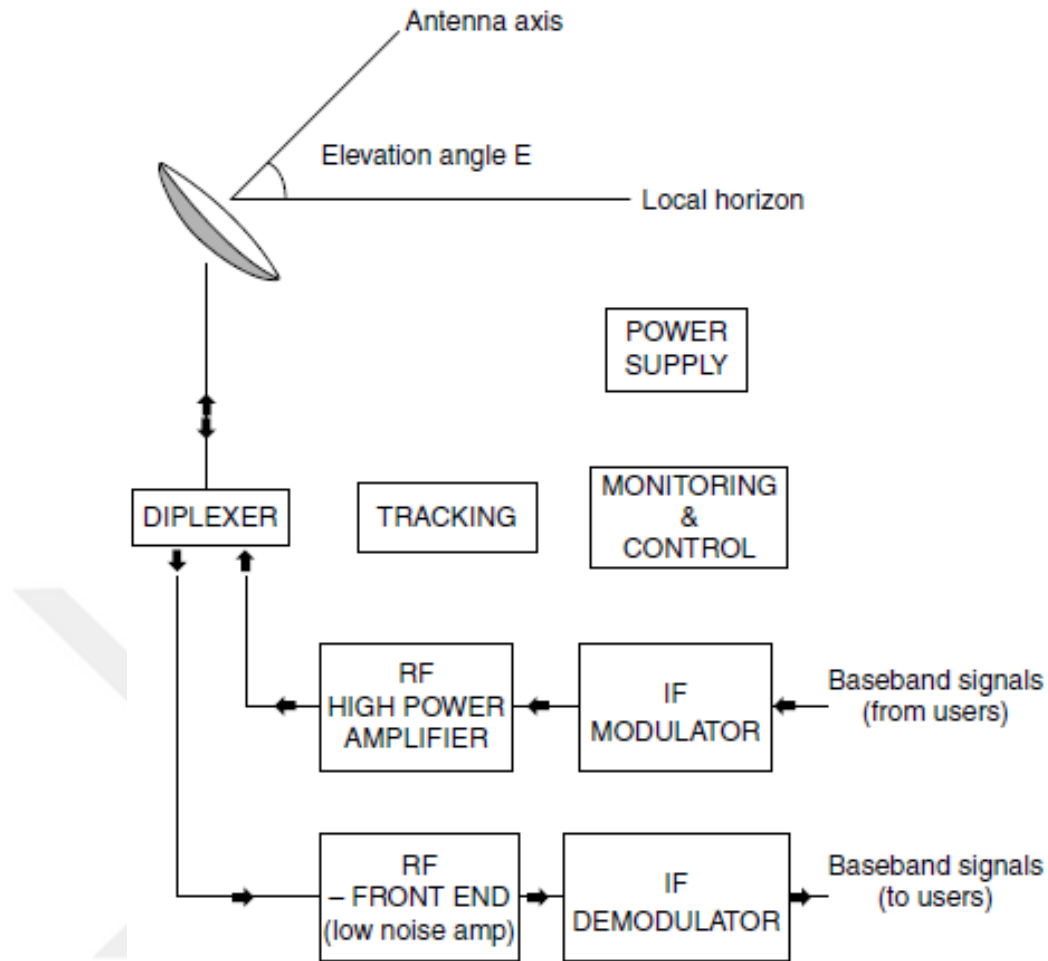
Figure 5. The Organization Chart of an Earth Station (Maral, Bousquet, 2010).

Operating frequency is one of the most important design and performance parameter in satellite communication systems. When determining the free space wavelength of carrier signals, the atmospheric effects and other losses that may be occurred in communication path must be taken into consideration. In addition, there are some international and domestic regulations about operating frequency of satellite communications. The designers of satellite communication system must comply with these restrictions.

2.1.1. The Structure with Separate Transmitter and Receiver Antennas

In satellite ground stations, separate transmitter and receiver antennas can be employed together. In Europe, Ku-band downlink (transmitter) frequency band is used from 10.7 GHz to 12.75 GHz for direct broadcast satellite services, while the usable frequency band is generally between 12.75 GHz and 14.5 GHz for uplink (receiver). In satellite communication, the frequency pair selected for downlink/uplink (or transmit/receive)

of a specific satellite application is not selected close to each other such that at least 1.5-2 GHz difference between uplink and downlink frequencies is selected both for transponder or telemetry/telecommand purposes (Ulaby, Ravaioli, 2014). By using different frequency bands for Earth-to-satellite uplink segments and for satellite-to-Earth downlink segments, it is guarded against interference between the two (transmit and receive) signals. The downlink segment uses lower-frequency carrier than the uplink segment, because lower frequencies suffer lower attenuation by Earth's atmosphere, thereby easing the requirement on satellite output power where the transmit frequency of 11.75 GHz and receive frequency of 14 GHz used in this thesis also satisfies all of these requirements/restrictions described above.

The design of two separate antennas for two different frequencies is easier than the design of a single antenna (transceiver) structure, which includes transmit and receive part of the TT&C systems. Four separate antennas, two of which should be the receiver and the other two should be transmitter, must be used in this configuration. Besides, different RF front-end topologies between antennas and payload must be used for transmitter and receiver antenna structures. The schematic views of RF front-end structures corresponding to transmitter antennas and receiver antennas of telemetry and telecommand applications are given in Figure 6 and Figure 7, respectively.

RF circuit diagram of the transmitter block is given in Figure 6. Data Handling Unit (DHU) produces two carrier signals, which have different frequencies of "*f1*" and "*f2*" within the downlink frequency band of 10.7-12.75 GHz. DHU carries data between electronic units on satellite and ground segment via TT&C subsystem. Signal processing in TT&C subsystem of satellite communication is done within the electronic circuits, which are parts of DHU. The carrier signals "*f1*" and "*f2*" is amplified inside Payload. The amplified "*f1*" and "*f2*" signals are firstly divided by two channels by hybrid coupler, which has two input and two output ports.
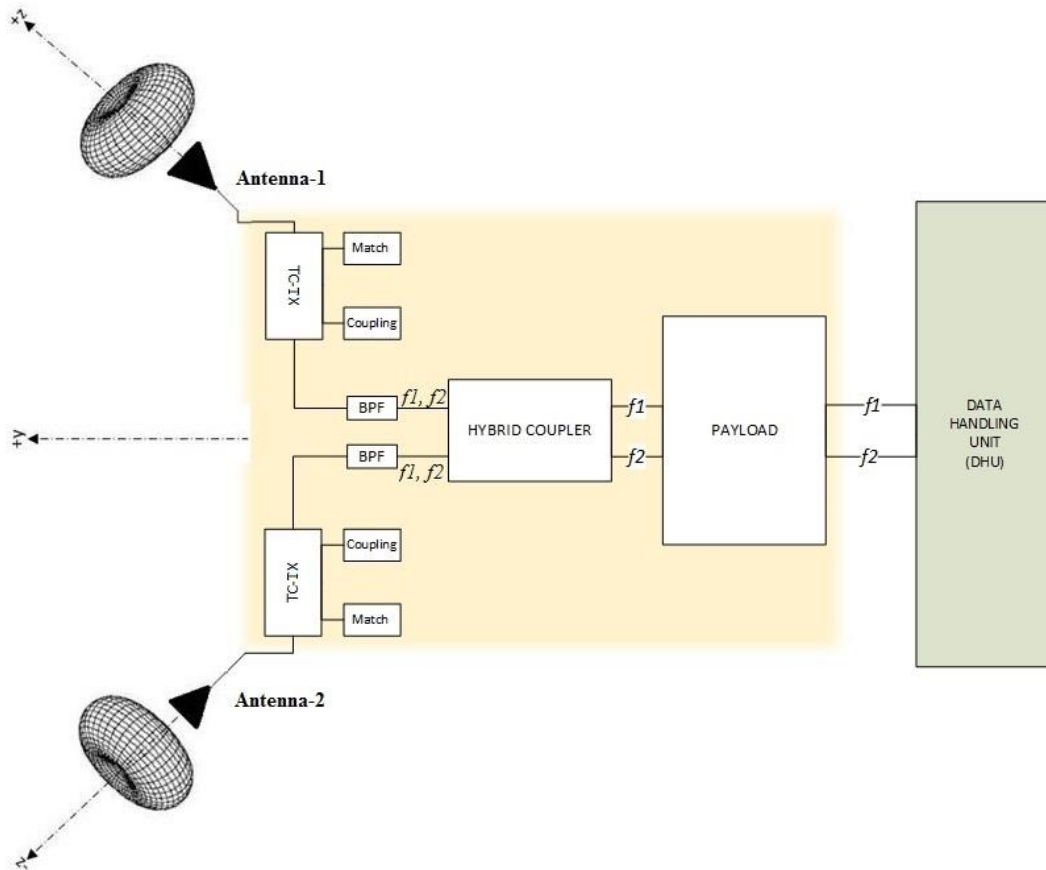
Figure 6. RF Circuit Diagram with Separate Transmit Antennas.

The hybrid coupler is also known as -3dB coupler and it divides to power of signal that travels inside of the waveguide up into two equally portions. In addition, the hybrid coupler can create phase difference that desired. Then, half of the "*f1*" and "*f2*" signals are summed on output ports of the hybrid coupler. The sum of "*f*1" and "*f*2" signals on the output ports of the hybrid coupler must be filtered with a Bandpass Filter (BPF) or a Low Pass Filter (LPF). This is because higher order harmonics of these signals may occur while they are travelling on RF circuit. Before the signals are transmitted from antenna, they pass from a test coupler that belongs to transmitter (TC-TX). Signals power values can be measured by test coupler. Finally, the signals radiate from the transmitter antennas to free space.

In the settlement of the antennas, two transmitter antennas are used, which are placed perpendicular to each other in order to provide full space coverage as shown in Figure

6. The antennas are positioned to satellite platform with 45^0 angle. Thus, the reflection from the other components of the satellite can be reduced.

RF circuit diagram of a receiver block is given in Figure 7. According to the selected uplink frequencies (*f1* and *f2*) within uplink frequency band of 12.75-14.5 GHz, the each antenna in Figure 7 can receive the signal of one frequency or multiple(double) frequencies. If the selected frequencies are very far away from each other, typically 1 GHz, such that a single antenna can not cover that kind of wide bandwidth, each antenna can receive the signal of only one of the uplink frequencies. Here, two nonidentical antennas in Figure are used, one of which operates at *f1* and the other is designed to obtain the signal of *f2*. If the frequencies are employed sufficiently close –on the order of a few 100 MHz-, each antenna in Figure can get the signals of all frequencies, and they are designed to be identical.

The receiver blocks of these two different cases can receive single carrier signal (*f1* or *f2*) or double carrier signals (*f1* and *f2*) simultaneously. These operations are required different RF circuit diagrams from each other. Receiving single carrier signal RF circuit diagram is shown in Figure 7 with black color, while receiving double carrier signals is shown in Figure 7 with blue color.
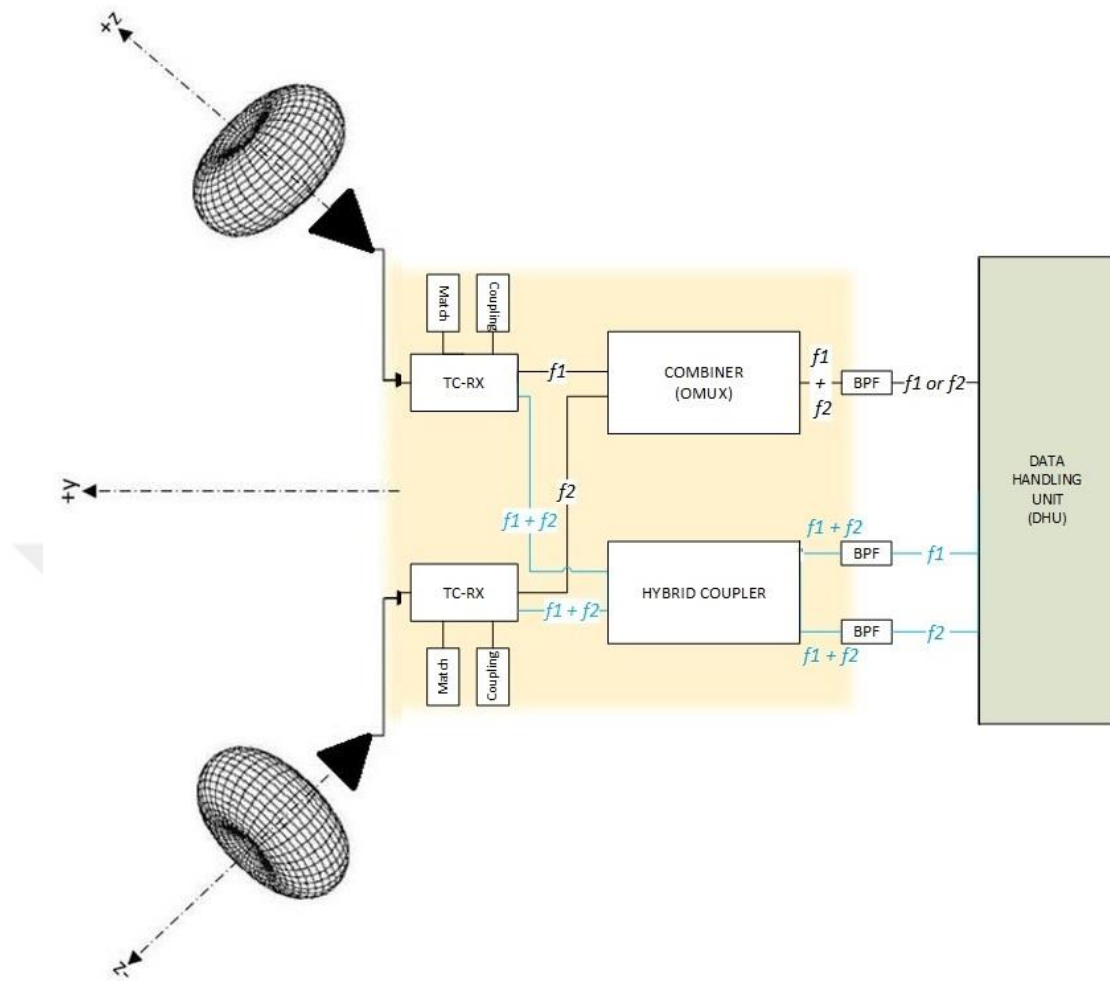
Figure 7. RF Circuit Diagram with Separate Receive Antennas.

In receiving of single carrier signal RF circuit diagram, the signal with frequency of *"f1"* is taken by one of the antennas, and *"f2"* is taken by other antenna from free space. Then, they convey to test coupler (TC-RX). Signals power values can be measured by TC-RX. *"f1"* and signals *"f2"* that come from TC-RX blocks of different and nonidentical antennas are collected in a combiner called as output multiplexer (OMUX) structures. Task of OMUX is to combine signals to feed antenna networks. As the output of combiner or OMUX, there exist the signals of *"f1"* and *"f2"*, which is obtained by combining of two incoming signals. However, the power level of one frequency is much more dominant to other according to aspect view of the antennas with respect to earth station. Therefore, practically, there is only one frequency at the output of OMUX. Before *"f1"* OR *"f2" signal* reaches to DHU, it is passed from BPF,

which should allow *"f1"* and *"f2"* in its bandpass region. Finally, *"f1"* or *"f2"*signal reaches to DHU, and it is processed in this block.

The RF circuit diagram for the receiving of double carrier signals, which is frequently preferred method as compared to that of single carrier signal, is a little bit different from the gathering of single carrier signal. The main difference between the reception of double carrier signals and the reception of single carrier is the usage of hybrid coupler instead of combiner (OMUX). Incoming signals that are *"f1 and f2"*, come from TC-RX blocks are divided by two inside hybrid coupler. It can be observed summation of half of the *"f1 and f2"* at each output ports of the hybrid coupler. BPF are applied to hybrid coupler outputs. First BPF is selected according to frequency of *"f1"* and the other is selected according to frequency of *"f2"*. As result of this filtering operation, there is only half of *"f1"* signal on one of the DHU input port and there is only half of *"f2"* signal on the other input port of DHU.

Two carrier signals can be received with a single system. But power of each carrier signals reduce to their half. In receiving single carrier process, it must be used combiner or OMUX structures instead of hybrid coupler. These structures are more complicated than hybrid coupler and cost of receiver block may be increased by using these complicated structures. There are some advantages and disadvantages of using, receive double carrier signals blocks instead of receive single carrier signal blocks. Designer have to decide which one is proper to system according to system properties.

2.1.2. The Structure with One Transceiver Antenna

In some satellite systems, transmit and receive antennas are designed as a single structure, which includes transmitter part and receiver part inside of it. This kind of structures are called as transceiver. Design and production of transceiver structures are more sophisticated than separate receiver and transmitter structures. Also transceiver RF circuit diagram is more complicated than separate transmitter and receiver structures. However, using single transceiver antenna reduces the number of the antennas that must be mounted on the satellite platform. RF circuit diagram that belongs to transceiver blocks is given in Figure 8.
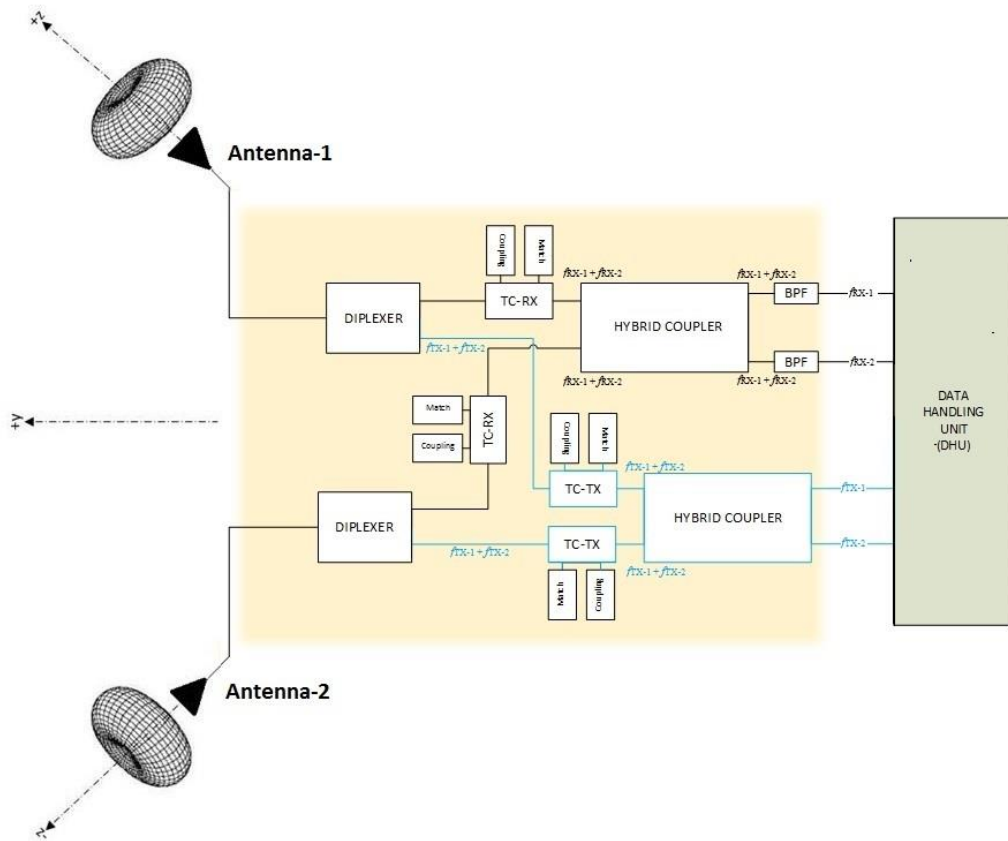
Figure 8. RF Circuit Diagram of Transceiver Antennas.

Transceiver blocks RF circuit diagram can be investigated as two parts, which are transmitter blocks and receiver blocks. Transmit part of the RF circuits is indicated with blue blocks, receive part of the RF circuits is indicated with black blocks. Receive and transmit parts of transceiver RF circuit are inverse of each other.

In transmitter part of the RF circuit, the signals are produced by the DHU. Then, the signals, which are produced by DHU, are divided into two by Hybrid Coupler, and halves of each carrier signals are summed on the output ports of Hybrid Coupler. These signals pass in TC-TX blocks. Power levels of the signals can be measured in these blocks. Then the signals convey to diplexers, which are a crossover filters. Diplexers are employed for decoupling two channels via frequency difference. Thus, different signals that have different frequencies can be transmitted and received in a single antenna as in Figure 8.

As it is mentioned before, receiver part of the RF circuit operates as inverse of the transmitter part that is explained. Carrier signals from the antennas convey to diplexers.

Diplexers provide decoupled two different frequency channels, which are transmitter channel and receiver channel. Received carrier signals go through in receiver channel of the diplexers. Then carrier signals pass inside TC-RX blocks. Power levels of carrier signals can be measured in these blocks. Carrier signals, which include two different frequency components, are divided into two inside of Hybrid Coupler. Half of the each frequency components of the carrier signal are summed on the output ports of Hybrid Coupler. These signals that summed are filtered by BPF. This filtering operation separates frequency components of the carrier signals to each other. Half of the each frequency components of the carrier signals are given to DHU as inputs.

2.2. General Antenna Parameters

Aperture type antennas are commonly employed in satellite communication systems. Generally, antenna apertures are placed XY plane in coordinate system, which is shown in Figure 9.
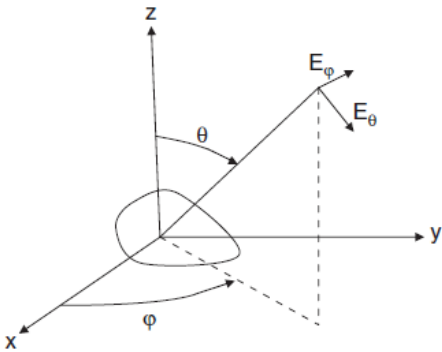
Figure 9. Aperture Antenna Coordinate System (Dybdal, 2009).

XY plane in this figure is scanned by ϕ angle ($0 \leq \phi \leq 360°$), and called as azimuth plane. The other fundamental plane is represented with θ angle ($0 \leq \theta \leq 180°$), and called as elevation plane. These terms are frequently used for explaining properties that related with radiation pattern. Besides, S-parameters are often used for representations of return loss.

2.2.1. Return Loss

All component in electronic have an impedance value. In satellite communication systems, it is aimed to transmit a signal with low loss as much as possible. For providing maximum power transfer, impedance of components that connected to each other must be match. Mismatch loss is generally expressed with scattering matrix

parameters. The reflected signals can be expressed in terms of voltage or power value. Coefficients that belong to reflection are denoted by S_{11} parameter. Coefficients that belong to transmission are denoted by S_{21} parameter. Relation between impedances and S_{11} parameter is expressed as;

$$|S11| = \frac{V_0^-}{V_0^+} = \frac{Z_L - Z_0}{Z_L + Z_0} \qquad (1)$$

Return Loss (RL) in dB is expressed in terms of S_{11} parameter as;

$$RL(dB) = -20 \log(|S11|) \qquad (2)$$

At high frequencies, measurement of total voltage, current and power on a network port is very hard. It is not possible to use proper probe for each impedance value of networks. Even if a measurement probe that has proper impedance is connected to circuit, it may cause oscillation or self-destruction on the circuit. S-parameters do not required to connection of undesired loads to the device under test (DUT). In S-parameter measurement, multiple devices can be cascaded to predict overall systems performance. S-parameters are measured with network analyzers (NA).

2.2.2. Directivity and Gain

The directivity of an antenna, D, is simply defined as "the ratio radiation intensity in a given direction from the antenna to radiation intensity averaged overall directions" (Balanis, 2005). Maximum directivity, which is the maximum value of the directivity function and also usually called as the directivity, can be expressed mathematically as;

$$D_{max} = \frac{U_{max}}{U_0} = \frac{4\pi U_{max}}{P_{rad}} \qquad (3)$$

Here, in order to find average radiation intensity (U_0) in equation (3), total radiated power (P_{rad}) in equation (3) is divided by 4π.

Gain is a similar parameter with directivity. The ratio between the radiated power from the antenna of a system to the transmit (generated) power of antenna gives total system efficiency. The system efficiency represents with a coefficient, which is e_0. Gain of antenna is calculated with directivity of antenna in given direction.

19

$$G = De_0 \qquad (4)$$

2.2.3. Polarization

Radiated electromagnetic wave consists electric field component and magnetic field components. Electric field vector and magnetic field vector are orthogonal and perpendicular to the direction of the wave propagation. Polarization can be defined as orientation of the electric field in one RF cycle as it can be seen it Figure 10. There are three type of polarization, which are linear polarization, circular polarization and elliptical polarization. Linear and circular polarizations are special cases of elliptical polarization. Antenna parameter, which determines type of polarization, is axial ratio. Axial ratio is expressed as,

$$AR = \frac{E_{max}}{E_{min}} \qquad (5)$$

In general the ratio of major axis to minor axis, gives elliptically polarization. If the ratio of major axis to minor axis is zero (AR = 1 = 0dB), polarization becomes circular. If ratio of major axis to minor axis is infinity (AR = ∞, direction of the electric field is fixed), polarization becomes linear.
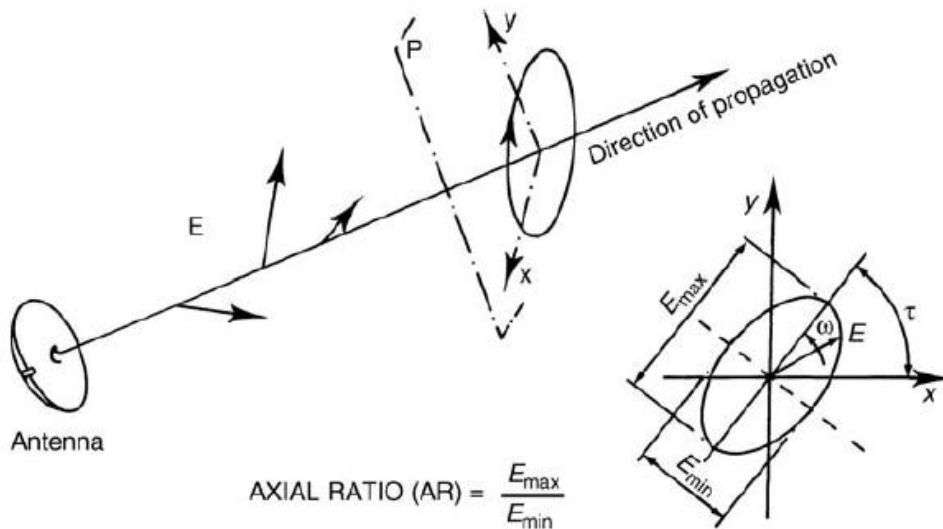
Figure 10. Polarization of Propagating Wave (Maral, Bousquet, 2010).

Ideally, a circularly polarized wave's AR must be 0 dB. In literature, electromagnetic wave, which has AR between 0 dB and 3 dB, is accepted as circularly polarized.

20

When the electromagnetic wave is travelling toward to observer, if electric field vector rotates clockwise, it is called as left-hand polarized. If it rotates counterclockwise, it is called as right-hand polarized.

Transmit and receive antennas are desired to have circular polarization. Because, the wave from a linearly polarized antenna on a spacecraft will rotate due to motion or Faraday rotation in the ionosphere, but if a circularly polarized antenna is used, the incoming linearly polarized wave orientation angle will not lead to power level fluctuations. Even though a 3- dB signal loss encountered, the received signal remains constant (Stutzman, Thiele, 2013).

2.3. Rectangular and Circular Waveguides

Structures, which enable propagation electromagnetic waves with minimum energy loss by restricting expansion dimensions, are defined as waveguide. There are many different kinds of waveguide in literature but only rectangular and circular ones are employed in this study. Electromagnetic waves can travel inside of waveguide in different modes. These modes can be listed as transverse electromagnetic (TEM), transverse electric (TE) and transverse magnetic (TM). Transition between different kinds of waveguide is possible. Also conversion between different modes can be applied with special mode converter structures.

Waveguides structures provide an interface between antennas and overall system. Different waveguide dimension standards exist for providing integration between structures that are designed and different systems. Waveguide dimensions, which are standard, are selected according to operating frequency. Operating frequency value must be between lower and upper cutoff frequencies of waveguide in desired mode. In this study, rectangular waveguide is selected as WR75, which is a standard rectangular waveguide. It is used as an interface between system and antennas.

2.3.1. Rectangular Waveguide

Rectangular waveguide is a fundamental waveguide type in transmission of microwave signals. Standard rectangular waveguides can operate from 1 to 220 GHz. In market, many rectangular waveguide components are available such as couplers, attenuators, isolators, detectors, slotted lines as commercial products. Only electromagnetic waves that have TE and TM modes can propagate inside of the

rectangular waveguide. Electromagnetic wave that has TEM mode cannot propagate inside of rectangular waveguide.
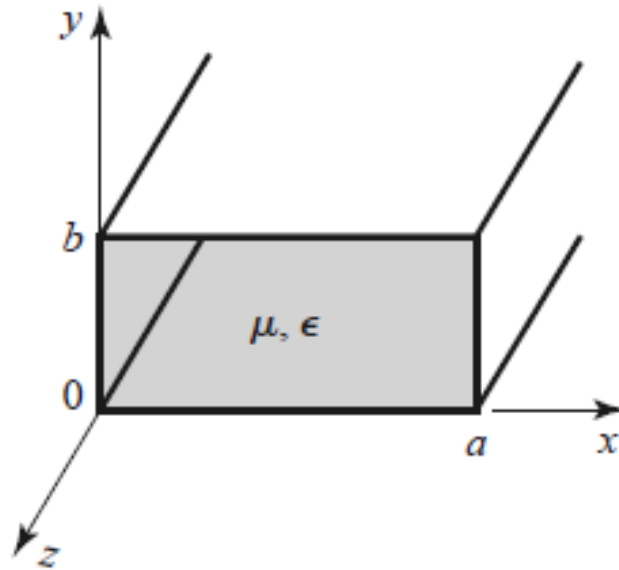
Figure 11. A Rectangular Waveguide (Balanis, 2005).

The antennas designed in thesis are designed to operate at 11.75 GHz (transmitter) to 14 GHz (receiver) at Ku-Band. WR75 rectangular waveguide is commonly used as standard waveguide in Ku-Band satellite communication, where all microwave and antenna components of the topologies described in Figure 6, Figure 7 and Figure 8 are generally connected together with these waveguides. This standard waveguide will be also used as the feeding waveguide of the antennas designed in this thesis. Thus, practically, the designed antennas can be easily connected to other components behind the antennas.

It is expected that only TE_{10} dominant mode should operate within rectangular waveguide in order to give a single mode operation. The dimensions of WR75 rectangular waveguide are given as $a = 19.05$ mm (long edge) and $b = 9.525$ mm (short edge). The lower and upper operating frequency values of a rectangular waveguide can be practically evaluated such that the operating frequency should be at least 25% above the cutoff frequency of the TE_{10} mode but no higher than 95% of the next higher cutoff frequency which is TE_{20} or TE_{01} mode for WR75 rectangular waveguide (Cheng, 1993). By using this explanation, the boundaries of the frequency band is calculated as

$$\frac{c}{2a} \times 1.25 = \frac{3 \times 10^8}{2 \times 19.5 \times 10^{-3}} \times 1.25 = 9.84\ GHz \qquad (6)$$

$$\frac{c}{2b} \times 0.95 = \frac{3 \times 10^8}{2 \times 9.525 \times 10^{-3}} \times 0.95 = 15\ GHz \qquad (7)$$

As it is mentioned before, WR75 standard rectangular waveguide operates at only TE_{10} dominant mode, whose field distribution is shown in Figure 12. The frequency interval is found to be from 9.84 GHz to 15 GHz, which includes transmit (11.75 GHz) and receive (14 GHz) frequencies in this thesis.
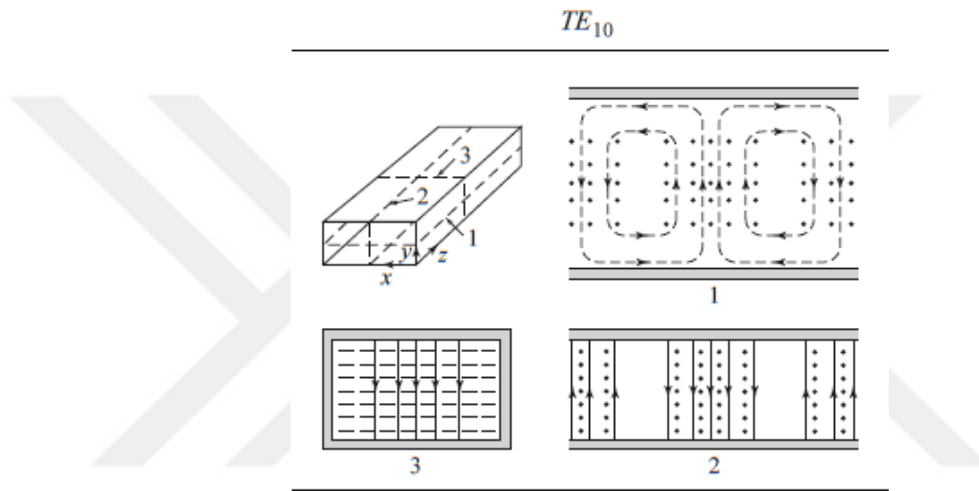
Figure 12. Electric (solid curves) and Magnetic Field (dash curves) Representation of TE_{10} Dominant Mode of a Rectangular Waveguide (Pozar, 2012).

2.3.2. Circular Waveguide

Circular waveguide is a hollow metal pipe. It supports TE and TM waveguide modes. The structure of a circular waveguide is given in Figure 13.
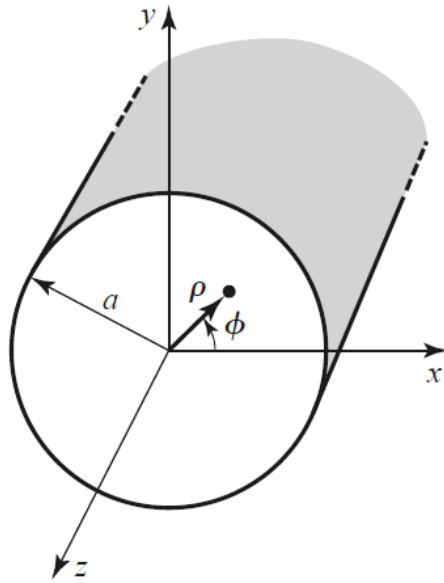
Figure 13. A Circular Waveguide (Pozar, 2012).

Inner radius "*a*" of circular waveguide determine the operating frequency and active modes that can travel inside of circular waveguide. The actual dominant mode inside of the circular waveguide is TE_{11}. Slotted antennas on circular waveguide must feed as symmetrically in order to provide non-directional radiation pattern. Slotted antennas array on circular waveguide can not be fed as symmetrically with TE_{11} mode. Therefore, slotted antennas are desired to be fed by TM_{01} dominant mode, which is known as symmetric mode. Mode conversion between dominant modes is possible via special converter structures to be explained. Three modes are going to be handled and will be important in the designs of the proposed antennas. These modes are the dominant TE_{11} mode, symmetric TM_{01} mode and the next possible higher order mode of TE_{21} according to the radius of the circular waveguide. The electric and magnetic field lines of these three modes are graphed out in Figure 14 where dash curves correspond to magnetic field lines. When the magnetic field lines of the TM_{01} mode are examined, it can be seen that these lines have circular symmetry. Therefore, these magnetic field lines create circularly symmetric current densities on the wall of the conductor of circular waveguide. Consequently, the slots placed on the circumference of a circle at the conducting wall have almost same excitations, which results in a uniform (non-directional) radiation at the plane where the slots are placed.

TE$_{11}$ TM$_{01}$ TE$_{21}$
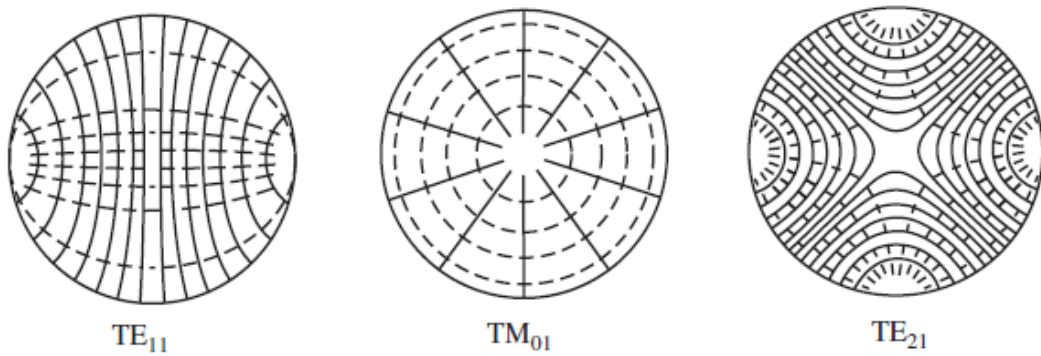
Figure 14. Field Lines of Some Circular Waveguide Modes (Balanis, 2012).

2.3.3. Rectangular to Circular Waveguide Transition

As it is mentioned before, the dominant mode without mode convertors in circular waveguide is TE$_{11}$ mode. This mode is not a symmetrical mode as shown in Figure 14. The slotted antenna array must be fed as symmetrically in order to provide non-directional radiation pattern. The most suitable mode to feed slotted antenna array on circular waveguide is TM$_{01}$ mode as described in the previous section. There are some special transition techniques, which can be employed for mode conversion while providing transition between rectangular waveguide and rectangular waveguide. Four-transition types are given Figure 15.

(a)   (b)

(c)

(d)
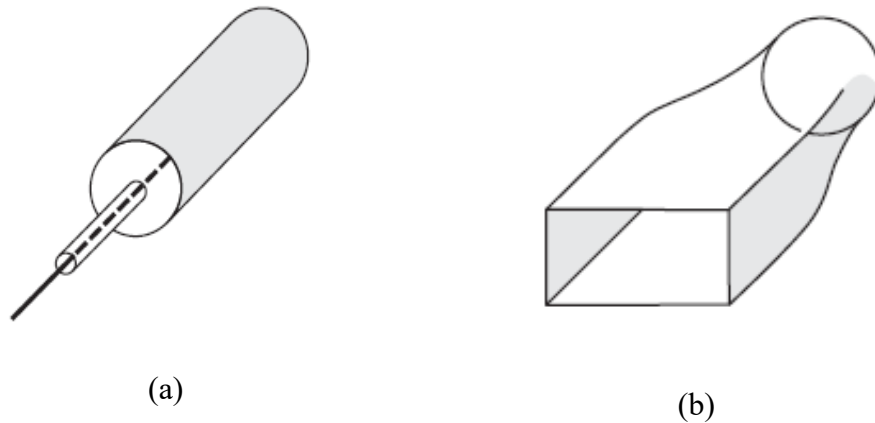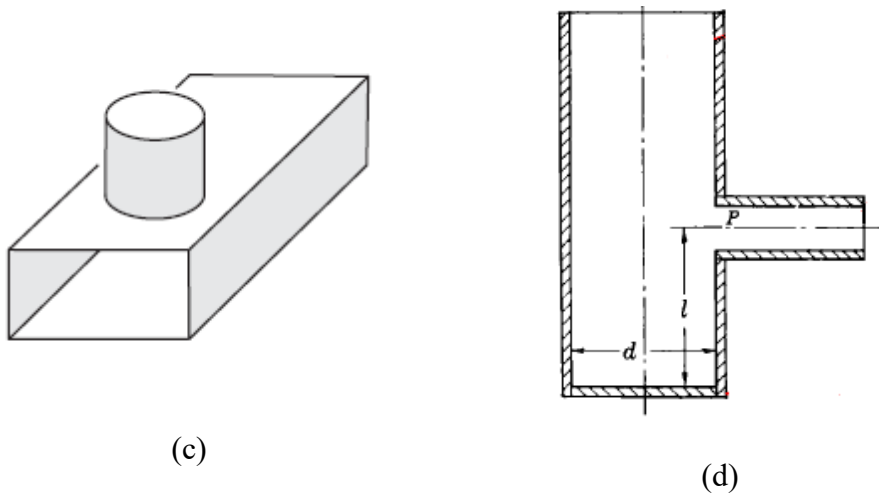
Figure 15. Excitation of TE_{mn} and TM_{mn} Modes in a Circular Waveguide (a) TM_{01}
Mode, (b) TE_{10}(rectangular) – TE_{11}(circular), (c) TE_{10}(rectangular) – TM_{01}(circular)
(Balanis, 2012), (d) TE_{10}(rectangular) – TM_{01}(circular) (Silver, 1949)

It is predicted that the structures given in Figure 15(c) and Figure 15(d) can provide
the transition between circular waveguide and rectangular waveguide for the desired
mode conversion between TE_{11} mode of rectangular waveguide to TM_{01} mode of
circular waveguide. Among these structures, the one in Figure 15(c) has the limitation
about the selection of the diameter of the circular waveguide, which can be the
dimension of the broadwall of WR75 waveguide, 19.05 mm, at most. It is going to be
shown that this diameter dimension is not enough for the designed antennas in this
thesis. Then, the study focuses on the structure given in Figure 16.
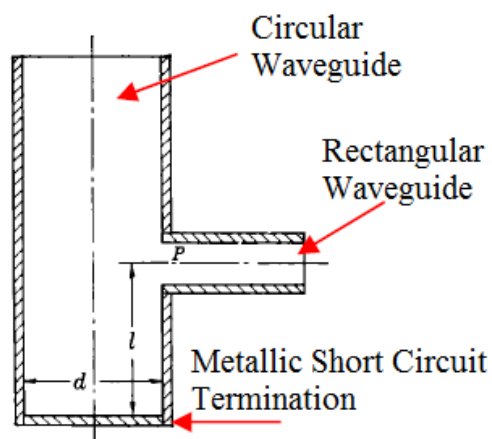
Figure 16. Transition Structure Rectangular and Circular Waveguides in This Thesis
(Silver, 1949).

26

In order to provide the desired transition between rectangular and circular waveguides, minimum return loss can be provided by adjusting two parameters. These parameters can be listed as the diameter of the circular waveguide "d" and the distance "l" between the center of the rectangular waveguide and short end of circular waveguide described in Figure 16.

CHAPTER THREE
DESIGN OF THE RECTANGULAR TO CIRCULAR WAVEGUIDE TRANSITIONS

As it is emphasized before, transition between rectangular to circular waveguides is provided by special transition structures as shown in Figure 15. In this thesis, slotted antenna array, which is on the circular waveguide walls, is decided to feed by a symmetric mode. TM_{01} mode, which is selected as symmetrical mode, is employed to feed slotted antenna array. In Figure 14 field lines of some modes that belong to electromagnetic waves, which propagates in circular waveguide, are given. From given field lines, only field lines of TM_{01} mode have symmetry property. Omnidirectionality of the antennas can be provided by symmetry property of the TM_{01} mode. Other modes that are not symmetric may disrupt the omnidirectionality of the antennas. For this reason, while electromagnetic wave propagate with TM_{01} mode inside circular waveguide, TE_{11} and TE_{21} modes, which are not symmetric, must be suppressed.

The main motivation of this chapter is to design rectangular to circular waveguide transitions for the feed of the slotted array antennas at satellite communication frequencies. In the design, it is desired to provide TM_{01} mode propagation and suppress to TE_{11} and TE_{21} modes in circular waveguide as much as possible. In this sense, two design parameters, which first one is diameter of the circular waveguide the other one is the distance between center point "P" of rectangular waveguide in Figure 16 and short circuit at the end of the circular waveguide, must be determined.

The first fundamental design parameter of rectangular to circular waveguide transition is diameter of the circular waveguide given in Figure 16. It is expected that the electromagnetic wave propagate inside of circular waveguide with TM_{01} mode. In order to provide maximum power transfer at the rectangular to circular transition, impedance value of circular waveguide should be match according to TM_{01} mode of the electromagnetic wave. In order to increase the bandwidth of the transition, the diameter of the circular waveguide *"d"* is selected as half of the guided wavelength

that belongs to symmetric mode TM_{01}, i.e. $\lambda_{g,TM01}/2$, (Silver, 1949). As a result, the diameter of *"d"* can be evaluated for any center frequency of the design by using the formula of guided wavelength and other relation equation as (Pozar, 2012);

$$\lambda_{g,TM01} = 2d = \frac{2\pi}{\beta} \tag{8}$$

$$\beta_{TM,01} = \sqrt{k^2 - k_c^2}, \begin{cases} k = \dfrac{2\pi f}{c} \\ k_c = \dfrac{p_{01}}{d/2} \end{cases} \tag{9}$$

$$\sqrt{\left(\frac{2\pi f}{c}\right)^2 - \left(\frac{2 \times p_{01}}{d}\right)^2} = \frac{\pi}{d} \tag{10}$$

This system of equations gives relation between circular waveguide diameter and specific frequency values. There is only unknown parameter in equation set, which is *"p_{01}"*. This parameter represents TM_{01} mode inside circular waveguide and it can be found from Table 1.

Table 1. TM Mode p_{nm} Values inside the Circular Waveguide.

n	P_{n1}	P_{n2}	P_{n3}
0	2.405	5.520	8.654
1	3.832	7.016	10.174
2	5.135	8.417	11.620

In the study, the circular waveguide, which is a part of transition structure between waveguides, is terminated with a short circuit as given in Figure 16. The second fundamental design parameter of this study is distance between short circuit and *"P"* point, which is rectangular waveguide center. The distance is indicated by *"l"* in Figure 16. Suppression of non-symmetric modes can be provided by the adjustment of the distance *"l"*. It is known that electromagnetic wave propagates with TE_{11} dominant mode inside circular waveguide. Therefore, in this study it is primarily targeted to suppress TE_{11} mode. The distance *"l"* can be selected as quarter wavelength ($\lambda_{g,TE11}/4$), which belongs to TE_{11} dominant mode inside circular waveguide for the suppression TE_{11} dominant mode. The suppression is provided by transforming short circuit (at the

conducting cap of the bottom side of the circular waveguide) to very large impedance (open circuit) to the output of the rectangular waveguide by selecting $l = \lambda_{g,TE11}/4$. Since this impedance should be evaluated as a series element to the circular waveguide, almost no power of TE_{11} mode propagates towards the circular waveguide. However, when l is selected as $\lambda_{g,TE11}/4$, this length corresponds to almost $\lambda_{g,TM01}/6$ for the desired TM_{01} mode. Consequently, the short circuit at the bottom wall is transformed to not exactly open circuit but again large impedance, which results in the reduction on the power of TM_{11} mode through the circular waveguide. Therefore, the selection of $l = \lambda_{g,TE11}/4$ effectively suppresses the effect of the undesired TE_{11} mode but also the desired TM_{01} mode.

The distance *"l"* can be also selected as $3\lambda_{g,TE11}/4$. Selection of *"l"* distance to be as $(3\lambda_{g,TE11}/4)$ is more effective than selection of *"l"* distance to be as $(\lambda_{g,TE11}/4)$ for suppression of non-symmetric modes. This is because when *"l"* distance is equal to $(3\lambda_{g,TE11}/4)$, it is also equal to $\lambda_{g,TM01}/2$, which makes transformation of the short circuit again to the short circuit for TM_{01} mode at the output of rectangular waveguide. Now, the selection of $l = 3\lambda_{g,TE11}/4$ effectively suppresses only the effect of the undesired TE_{11} mode but not the desired TM_{01} mode. In this situation, TM_{01} mode of electromagnetic wave is sufficiently transferred to the circular waveguide. *"l"* value can be expressed as,

$$\lambda_{g,TE11} = \frac{2\pi}{\beta} \tag{11}$$

$$\beta_{11} = \sqrt{k^2 - k_c^2}, \begin{cases} k = \dfrac{2\pi f}{c} \\ k_c = \dfrac{p'_{11}}{d/2} \end{cases} \tag{12}$$

$$\beta_{11} = \sqrt{\left(\frac{2\pi f}{c}\right)^2 - \left(\frac{2 \times p'_{11}}{d}\right)^2} \tag{13}$$

$$l = \frac{3 \times \lambda_{g,TE11}}{4} = \frac{6\pi}{4\sqrt{\left(\frac{2\pi f}{c}\right)^2 - \left(\frac{2 \times P'_{11}}{d}\right)^2}} \tag{14}$$

There is only one unknown parameter that is p'_{11}. This parameter can be found from Table 2. Different "l" values can be calculated for each frequency values from the given expressions.

Table 2. TE Mode p'_{nm} Values inside the Circular Waveguide.

n	p'_{n1}	p'_{n2}	p'_{n3}
0	3.832	7.016	10.174
1	1.841	5.331	8.536
2	3.054	6.706	9.970

Transmit and receive frequencies are selected as 11.75 GHz and 14 GHz, respectively. By using the equation set from (8)-(10), diameter values of circular waveguides are determined for transmitter structure and receiver structure respectively as d = 23.3 mm and d = 19.6 mm. Wavelengths of the propagation modes can be calculated by using Equation 8 and Equation 11. Wavelengths depended on frequency, diameter of the circular waveguide and coefficient that belongs to propagation mode. These coefficients are found from Table 1 and Table 2. Table 3 is constructed for the first three modes to be considered in the antenna designs by using all these information. Values, which are line on them, cannot propagate over given frequency and diameter values.

Table 3. Calculated Wavelength Values for Different Propagation Modes at Transmit and Receive Frequencies in Circular Waveguides.

| 11.75 GHz (Transmit)			14.00 GHz (Receive)		
d = 23.3 mm					
TE11	TE21	TM01	TE11	TE21	TM01
33.3 mm	-	46.9 mm	25.44 mm	47.83 mm	30.17 mm
d = 19.6 mm					
TE11	TE21	TM01	TE11	TE21	TM01
39.53 mm	-	342.87 mm	27.91 mm	-	39.16 mm

3.1. Design for Transmitter Structure

Transmit frequency is given as 11.75 GHz. There are two fundamental parameters in rectangular to circular waveguide transition. These are diameter of the circular

waveguide *"d"* and the distance between short circuit that is located end of the circular waveguide and rectangular waveguide center point where located intersection rectangular and circular waveguides. For calculation these parameters with respect to different frequency value and different operating modes, some MATLAB scripts are generated. As result of MATLAB calculation initial value of circular waveguide diameter is found *"d = 23.3 mm"* and *"l =25 mm"*.

The calculated *"l"* and *"d"* values are used as initial values in Computer Simulation Technology (CST) designs. CST MWS is a simulation software program, which provides design antennas or microwave components and it makes electromagnetic simulations of structures that are designed. CST MWS simulations of structures are done with a workstation, which has 128 GB RAM, in Yasar University Antenna and Microwave Laboratory.

Firstly, rectangular to circular waveguide transition structure, which is decided to employ, is drawn in CST MWS with calculated initial values of *"l = 25 mm"* and *"d = 23.3mm"*. Then structure that designed is simulated. Until simulation results are satisfied to expectations, simulations are repeated. Optimizer and parameter sweep tools of CST MWS are used in iterations of optimization.
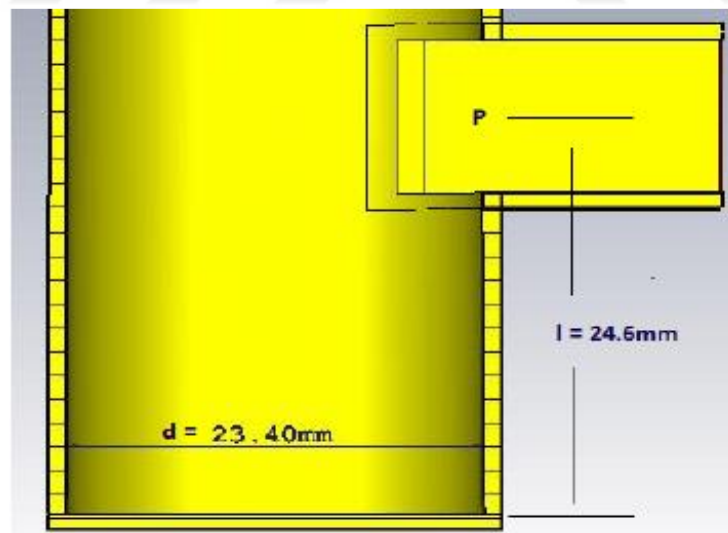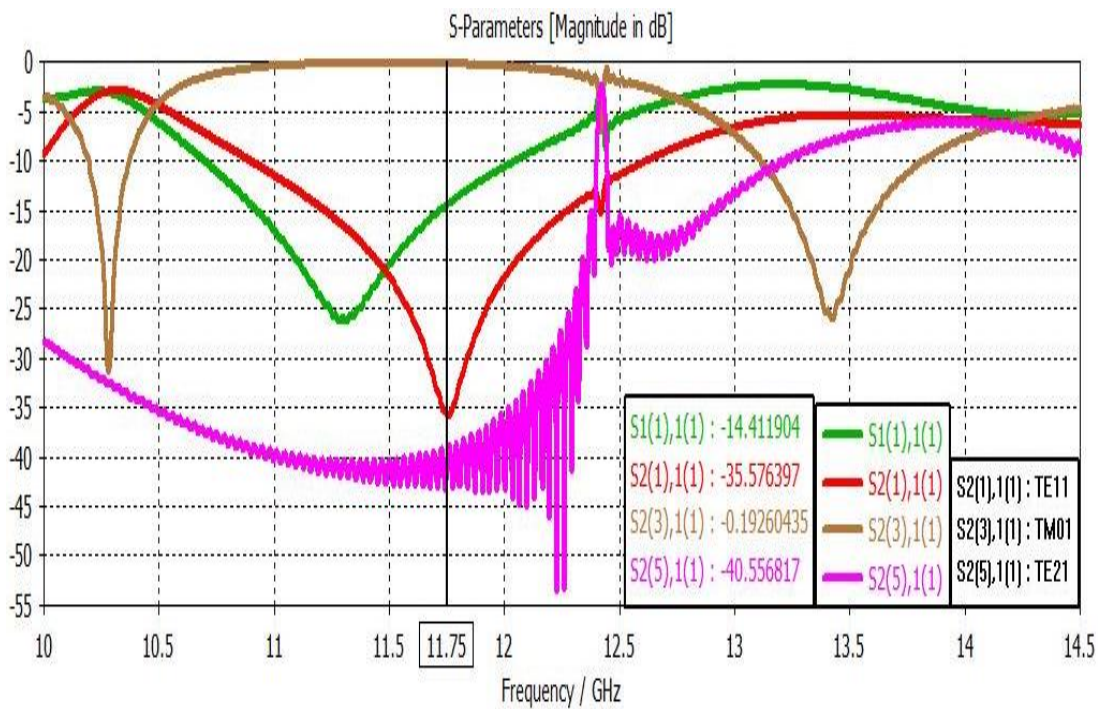

Figure 17. Rectangular to Circular Waveguide Transition That Designed for Transmitter Structure.

At the end of the iterations of optimization in CST MWS, final values of circular waveguide diameter and distance between P point and short circuit that is located end of the circular waveguide are found as, *"d = 23.4 mm and l = 24.6 mm"* as consistent

with the theoretical calculations. Final dimensions of the waveguide transition are given in Figure 17.

Transition structure has two ports. Rectangular waveguide aperture is determined as port-1 and circular waveguide aperture is determined as port-2. In simulations, S11 and S21 parameters are investigated for different operating modes. It is aimed that provide transmission of TM_{01} mode and suppression of the other modes (especially closer modes TE_{11} and TE_{21}) in circular waveguide.

In CST MWS, S-parameters of different excitation modes can be observed. CST MWS simulation results are given in Figure 18.

Figure 18. Reflection and Transmission Coefficients Belong to Rectangular to Circular Waveguide Transition Structure of Transmitter Part.

In graph that is shown in Figure 18. S1(1),1(1) is S11 parameters of TE_{10} mode in rectangular waveguide, S2(1),1(1) is S21 parameters of TE_{11} mode in circular waveguide, S2(3),1(1) is S21 parameters of TM_{01} mode in circular waveguide and S2(5),1(1) is S21 parameters of TE_{21} mode in circular waveguide. Simulation results are consistent with the targets, which are provided transmission TE_{10} dominant mode in rectangular waveguide and TM_{01} mode in circular waveguide and suppression the other modes. In this simulation, it is aimed that the transmission coefficient of TM_{01} ($S21_{TM01}$) is as much as possible, when the transmission coefficient of TE_{11} ($S21_{TE11}$)

34

is as low as possible at the operating frequency of transmitting. Reflection coefficient of signal (S11), which propagates inside rectangular waveguide with TE_{10} mode, should be low and transmission coefficient that belongs to TE_{21} mode ($S21_{TE21}$) also should be low.

S_{11} parameter of the transition structure is -14.4 dB at 11.75 GHz. This means that 3.63 percent of the transmitted signal is reflected and 96.37 percent of the transmitted signal is conveyed. In general, -10 dB S11 parameter is accepted as working standard. In simulation results, transition structure has approximately 1.3 GHz -10 dB bandwidth (10.7 GHz to 12 GHz).

Three S_{21} graphs correspond to different modes. S2(2),1(1) parameter is transmission coefficient of TE_{11} mode inside circular waveguide. S2(1),1(1) is -35.6 dB in operating frequency. It means that 99.972 percent of TE_{11} mode is suppressed. The other mode that desired to be suppressed is TE_{21}. S2(5),1(1) parameter represents this TE_{21} mode and it is -40.56 dB. 99.997 percent of the TE_{21} mode is suppressed. Only TM_{01} mode is desired to convey inside of the circular waveguide. S2(3),1(1) parameter in graph belongs to TM_{01} symmetric mode and its value is 0.19 dB. It means that 95.72 percent of TM_{01} mode is conveyed inside the circular waveguide.

Transmitter rectangular-to-circular waveguide transition structure provides transmission with low reflection and required mode conversion. Non-symmetrical modes are suppressed by adjusting two important design parameters of transition structure, which are *"l and d"*. Meanwhile, TM_{01} that is symmetric mode travels inside the circular waveguide with low loss.

3.2. Design for Receiver Structure

Design of receive transition structure is similar to transmit transition structure. Receive frequency is given as 14 GHz. There are two fundamental parameters, which are diameter of the circular waveguide and the distance between short circuit and the center point of the rectangular waveguide, in receiver transition structure like in transmitter transition structure. These parameters can be calculated same ways. As result of calculations, *"d"* and *"l"* values of receiver transition structure are found respectively 19.6 mm and 20.9 mm. The only difference between transmitter and receiver structures is the operating frequencies. Therefore, wavelength of the signals

are different to each other. The dimensions of the receiver structure can also be found by scaling dimensions of the transmitter structure.
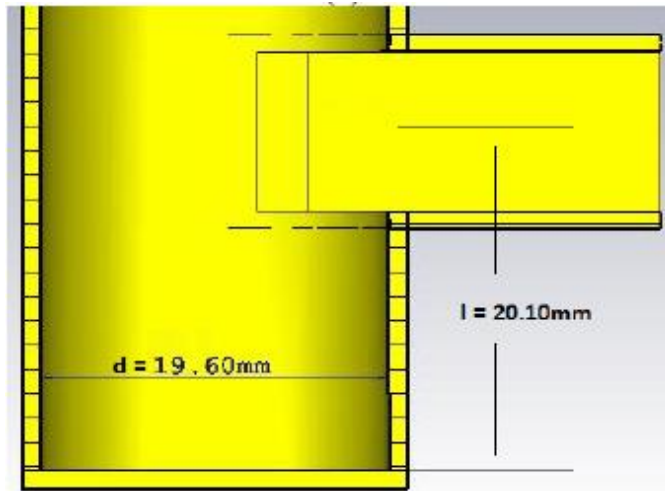
Figure 19. Rectangular to Circular Waveguide Transition That Designed for Receiver Structure.

As result of many optimization iterations in CST, final dimensions of the transmitter structure are found *"d = 19.6 mm and l = 20.1 mm"* as shown in Figure 19. Calculated values of *"d"* and *"l"* parameters are consistent with measurement results.
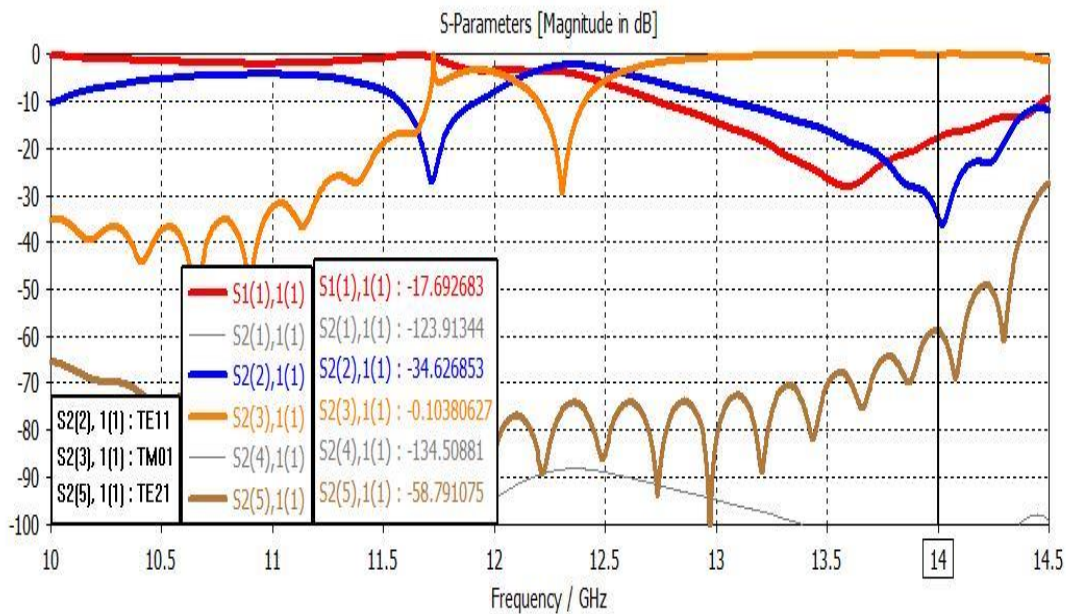
Figure 20. Reflection and Transmission Coefficients for Transition Structure of Receiver Part.

Simulation results are consistent with the targets, which are provided transmission TE_{10} dominant mode in rectangular waveguide and TM_{01} mode in circular waveguide

and suppression the other modes. S11 parameters of the transition structure is -17.7 dB at 14 GHz. This means that 1.7 percent of the transmitted signal is reflected and 98.3 percent of the transmitted signal is conveyed. In simulation results, transition structure has approximately 1.75 GHz -10 dB bandwidth (12.75 GHz to 14.5 GHz).

Three S21 graphs belong different modes. S2(2),1(1) is -34.6 dB in operating frequency. It means that 99.975 percent of TE_{11} mode is suppressed. The other parameter that desired to be suppressed S2(5),1(1) is -58.8 dB. Almost 100 percent of the TE_{21} mode is suppressed. S2(3),1(1) parameter in graph belongs to TM_{01} symmetric mode and its value is 0.1 dB. It means that 97.72 percent of TM_{01} mode is conveyed inside the circular waveguide.
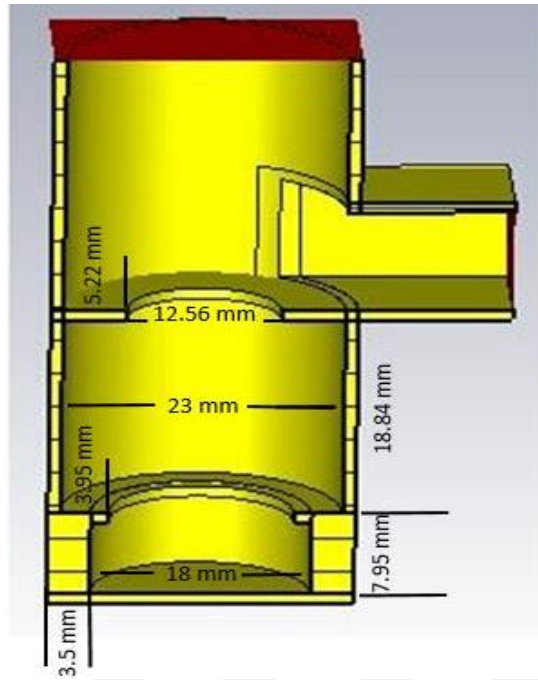
Receiver rectangular to circular waveguide transition structure provide transmission with low reflection and required mode conversion. Non-symmetrical modes are suppressed by adjusting two important design parameters of transition structure, which are *"l and d"*. Meanwhile, TM_{01} that is symmetric mode travels inside the circular waveguide with low loss.

3.3. Design for Transceiver Structure

The design of transceiver transition structure is more complicated than transmit and receive transition structures. This is because the antenna and the transition from rectangular-to-circular waveguide in transceiver structure should operate at transmit frequency (11.75 GHz) and receive frequency (14.00 GHz) simultaneously. When the transition design for the transceiver structure is considered, the difficulty in the design can be explained as follows. When the transition structure given in Figure 17 with d = 23.4 mm and l = 20.1 mm is tried to be used for the transmission of TM_{01} mode at 11.75 GHz and 14 GHz frequencies, this "l" length almost corresponds to $\lambda_{g,TM01}/2$ at f = 11.75 GHz by considering the wavelengths in Table 3. However, it corresponds to almost $3\lambda_{g,TM01}/4$ at f = 14 GHz; so, the structure in Figure 16 effectively suppresses the TM_{01} mode propagation in circular waveguide, which is not desired. Similarly, when the transition structure given in Figure 19 with d = 19.6 mm and l = 20.1 mm is tried to be used for the transmission of TM_{01} mode at 11.75 GHz and 14 GHz frequencies, the cutoff frequency of TM_{01} mode is so close to 11.75 GHz, which can be observed with very high wavelength value for this mode at 11.75 GHz in Table 3. Therefore, the wave of TM_{01} mode at 11.75 GHz experiences a significant attenuation

while propagating along circular waveguide. Thus, the structure in Figure 19 attenuates the effect of TM_{01} mode propagation at 11.75 GHz. Consequently, a single circular waveguide structure below point P in Figure 16 is not enough for the multiple frequency transmission of TM_{01} mode at 11.75 GHz and 14 GHz. For this purpose, a combination of the structures in Figure 17 and Figure 19 is considered to be used. Here, it is considered that the circular waveguide with larger diameter (about 23.3 mm) is just below point P and the one with smaller diameter (about 19.6 mm) is placed below the other. In the design, the electrical path length in terms of wavelength from the bottom wall of the circular waveguide to the point P in Figure 16 contains the sum of two lengths coming from the circular waveguides with small and large diameters. For an efficient suppression of TE_{11} mode at 11.75 GHz and 14 GHz and transmission of TM_{01} mode at 11.75 GHz and 14 GHz, total electrical path lengths should be integer multiple of (guided wavelength/2) for TE_{11} mode and odd integer multiple of (guided wavelength/4). However, although there are four parameters to be used (two from diameters and two from lengths) and there are four constraints in the design, the optimal solution is found for very long total physical length. Therefore, two irises are added to design, one of which is at the transition between smaller and larger circular waveguides, and the other is inside the larger circular waveguide at level of bottom wall of the rectangular waveguide. These irises bring an equivalent inductance circuit element, which makes an increase in the number of parameters to be used; consequently, the flexibility in the design. The initial lengths and diameters are chosen approximately as $\lambda_{g,TE11}/2$ for the larger waveguide and $\lambda_{g,TE11}/4$ for smaller waveguide at 11.75 GHz. So, the total electrical path length becomes for TE_{11} mode becomes $3\lambda_g/4$ at 11.75, which provides sufficient suppression of this mode at 11.75 GHz.

After modifications, rectangular to circular waveguide transition for transceiver structure is shaped as shown in Figure 21. The initial dimensions are used for the optimization and the final dimension given in Figure 21 are found as a result of the optimization in CST MWS simulations. Many simulation iterations are employed to reach final value of these dimensions.

Figure 21. Dimensions of Rectangular to Circular Waveguide Transition for Transceiver Structure.

After the determination of final dimensions by the optimization process, the suppression and transmission of the modes in consideration is observed by getting the corresponding S parameters results. These results are depicted in Figure 22.
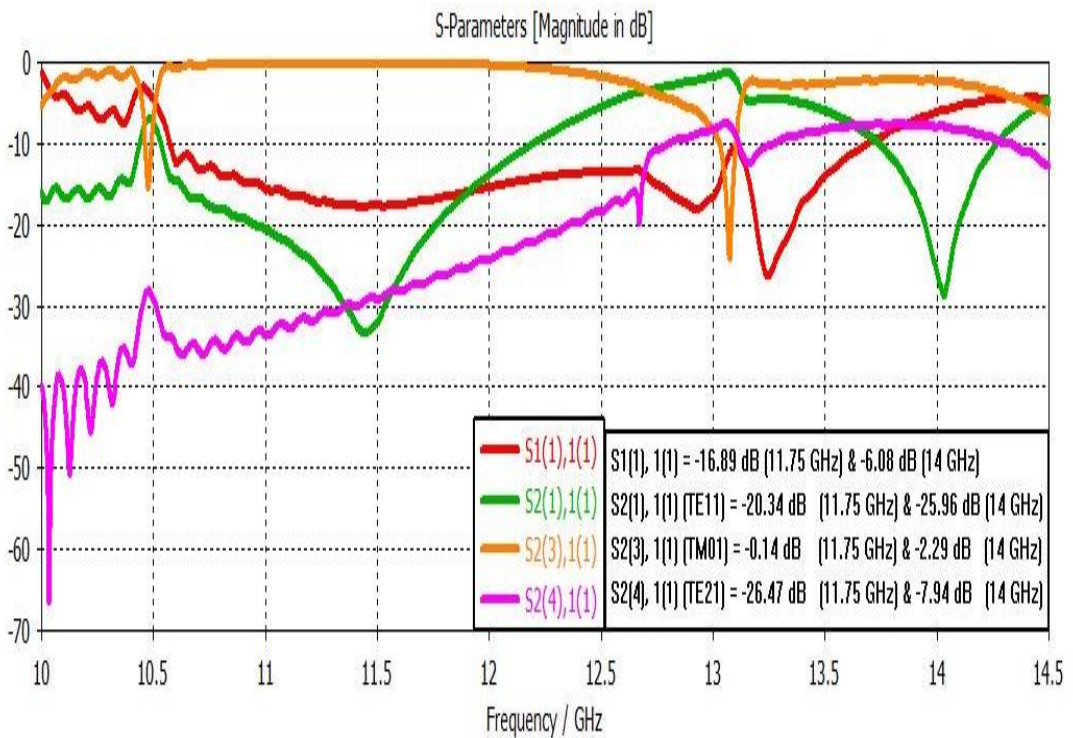
Figure 22. Reflection and Transmission Coefficients for Transition of Transceiver Structure.

When the results in Figure 22 is examined, it can be concluded that TE_{11} mode is annihilated about 20 dB at both 11.75 GHz and 14 GHz, which causes a sufficient suppression of this mode. On the other hand, the transmission coefficient of S_{21} for TM_{01} mode is about -0.2 and -2.2 dB for 11.75 GHz and 14 GHz, respectively. Therefore, the transmission of TM_{01} mode is almost perfect for 11.75 GHz. The transmission efficiency at 14 GHz is not as good as 11.75 GHz due to comparably worse S_{11} value at 14 GHz. However, the improvement of S_{11} value is not first priority of the design that it can be improved with the final antenna design, which is attached to this transition design. Finally, for the other possible mode of TE_{21} mode, it is significantly suppressed at 11.75 GHz by giving lower than -25 dB transmission coefficient since the cutoff frequency of this mode at a circular waveguide with diameter of 23 mm is greater than 11.75 GHz. So, this mode is evanescent mode at 11.75 GHz. However, the suppression of this mode at 14 GHz is not as good as 11.75 GHz since the cutoff frequency is also below 14 GHz so this mode is propagating mode. But, again the improvement of this mode is not prior in the design since as it is explained in the antenna design that this mode is effectively suppressed by using an antenna having circular waveguide with diameter of 19.6 mm.

CHAPTER FOUR

SEPARATE TRANSMITTER AND RECEIVER ANTENNA DESIGN

## 4.1. Design of Cylindrical Slotted Array Structure

In order to transmit or receive electromagnetic waves, after circular waveguide is terminated with short circuit, eight symmetrical slots are opened on the circular waveguide wall. Eight slots play important role in creating omnidirectional radiation pattern. These slots act as antenna array that radiate at center frequencies of transmitter (11.75 GHz) or receiver (14.00 GHz). Distance between center of the slots and short circuit is adjusted as radiation resistance to be maximum (Ragan, 1948). Radiation resistance has maximum values, when the distance between short circuit and center of the slots is half of the wavelength ($\lambda_{g,TM01}/2$) that belongs to TM_{01} mode or integer multiples of half of this wavelength value. Maximum power transfer is provided, when transmission line and load are match to each other. Slot antenna array and short circuit of the waveguide are designed to be match load for obtaining high radiation efficiency. With $\lambda_{g,TM01}/2$ short circuit transformation technique, the short circuit which is located at the end of the circular waveguide is moved to center of the antennas. Short circuit structure has zero impedance value. Because of this, there exists radiation resistance of antennas at the center of the slots. Thus, theoretically all power is consumed here as radiation. The distances that belong to receiver and transmitter antennas are calculated as 19.6 mm and 23.3 mm respectively.

Lengths of the slots are adjusted as half of free space wavelengths, which belong to desired resonant frequencies ($\lambda_0/2$). Width of the slots is chosen much shorter than the length of the slots (w<<l) for reducing reflections. In general, width of the slots is s as one in ten of the slots length ($\lambda_0/20$). This type of antenna is inherently matched and when the slots are resonant, about 75% of the incident waved are radiated (with a VSWR of 1.12) (Gao, Luo, Zhu, 2014). Lengths of the slots are found as 12.77 mm and 10.71 mm respectively for transmitter and receiver antennas.

To make circular polarization, slots are designed as inclined. Inclination direction of the slots determines direction of the circular polarization. In this study, antenna slots are designed as -45$^\mathbf{o}$ oblique for obtaining Left Hand Circular Polarization (LHCP). If slope of the antenna slots is +45$^\mathbf{o}$, Right Hand Circular Polarization (RHCP) will be occurred. Inclined design of slots is not enough to provide circular polarization with low axial ratio. For improving axial ratio performance of antenna structure circular polarization, metallic plates, which are located around the slots, are added to design. Electromagnetic waves that come from the slot antennas propagate towards free space from between two parallel metallic plates. In this region, vertically polarized component propagates in TEM (or TM$_0$) mode with free space wavelength. Horizontally polarized component propagates in TE$_1$ mode with wavelength given by;

$$\lambda_{HP} = \frac{2\pi}{\sqrt{k^2 - \left(\frac{\pi}{a}\right)^2}} \tag{15}$$

where *"a"* is the distance between parallel plates (Top, Dogan 2012). For creating 90$^\mathbf{o}$ phase difference between horizontally polarized and vertically polarized components of electromagnetic wave, the radius of the metallic plates and the distance between two parallel plates are optimized in CST MWS. Also, two fundamental components of the electromagnetic waves must have same amplitude values. Therefore, slope of the antenna slots is adjusted as -45$^\mathbf{o}$ or 45$^\mathbf{o}$.
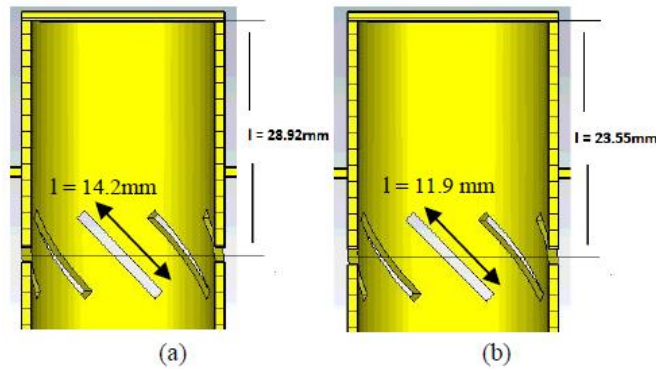
Figure 23. (a) Transmitter Antenna and (b) Receiver Antenna Slots.

Center of the slots to short circuit distance and dimensions of the slots, which are calculated via theoretical equations, are used as initial values of CST MWS design parameters. Transmitter and receiver antennas are simulated with CST MWS. For improving simulation results, design parameters of the structures are tuned with using

optimization and parameter sweep tools of CST MWS. Final values of the antenna parameters of the transmitter and receiver antennas are found as shown in Figure 23 by using CST MWS. Final values that are found by using CST MWS and evaluated values of dimensions, which belong the transmitter and receiver structures, are consistent to each other.

4.2. Overall Design

Transmitter and receiver antennas are shaped by results of design and simulation workings that are done as shown in Figure 24.
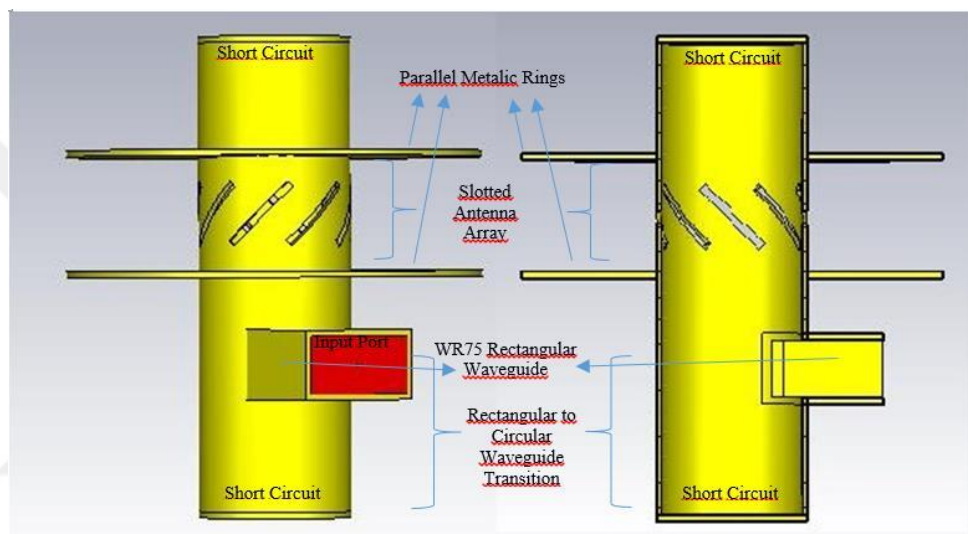

Figure 24. Overall Design of Transmitter and Receiver Antenna Structures.

Antennas have one input port. Input ports of the antennas are selected as WR75 rectangular waveguide. Antennas can be connected to satellite systems from their input ports via some flanges, which are specific for the system. The region between center of the rectangular waveguide and short circuit that is located bottom of the circular waveguide, operates as mode converter. This region may also defined as rectangular to circular waveguide transition.

Eight symmetric slots are located on the wall of the circular waveguide with 45° intervals. Electromagnetic waves radiate from these slots to free space or vice versa. Each slots are -45° inclined with respect to z-axis. Two parallel metallic plates are placed around the slots. They are symmetric to each other with respect to center of the slots.

Circular waveguide is terminated with short circuits both ends. Short circuits are modelled as a metallic cap that covers the apertures of the circular waveguide.

Thickness of the walls not dramatically affect the radiation performance of the antennas. Thickness of the walls are selected as 1 mm, which is very thin value. In production phase of the study, thickness of the walls are selected as thicker for reducing production cost and production time. In addition, using thicker structures increase durability of the antenna structures. The only disadvantage of the using thicker walls is the structures that have thicker walls are heavier than thin walled structures. In satellite communication, platform designers determine maximum weight specifications for each components. Weight of the antennas can be adjusted by changing thickness of the metallic walls. Design in CST MWS of the antennas that are produced is given in figure 25.
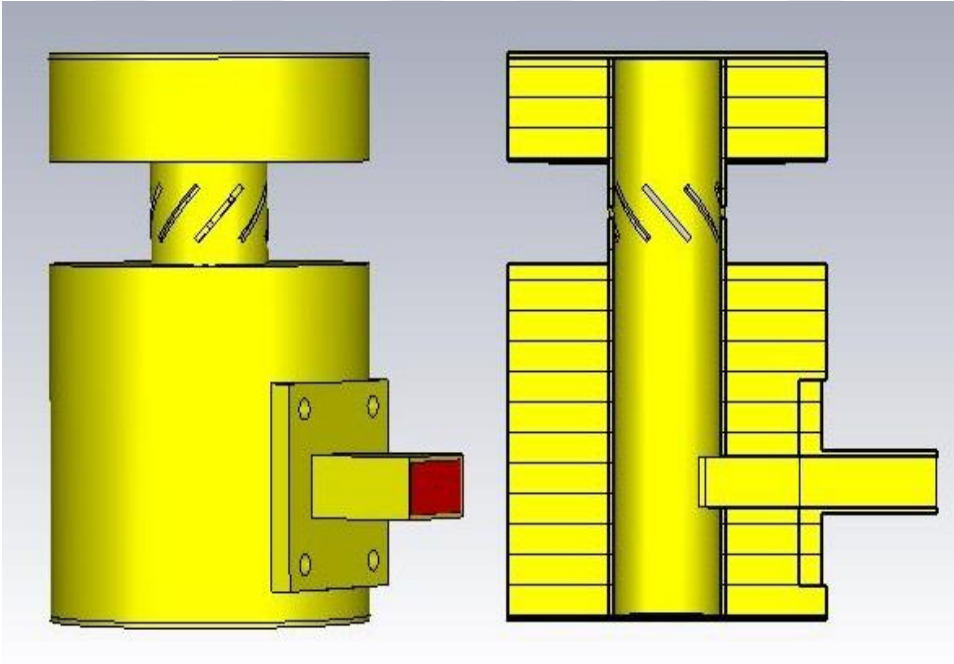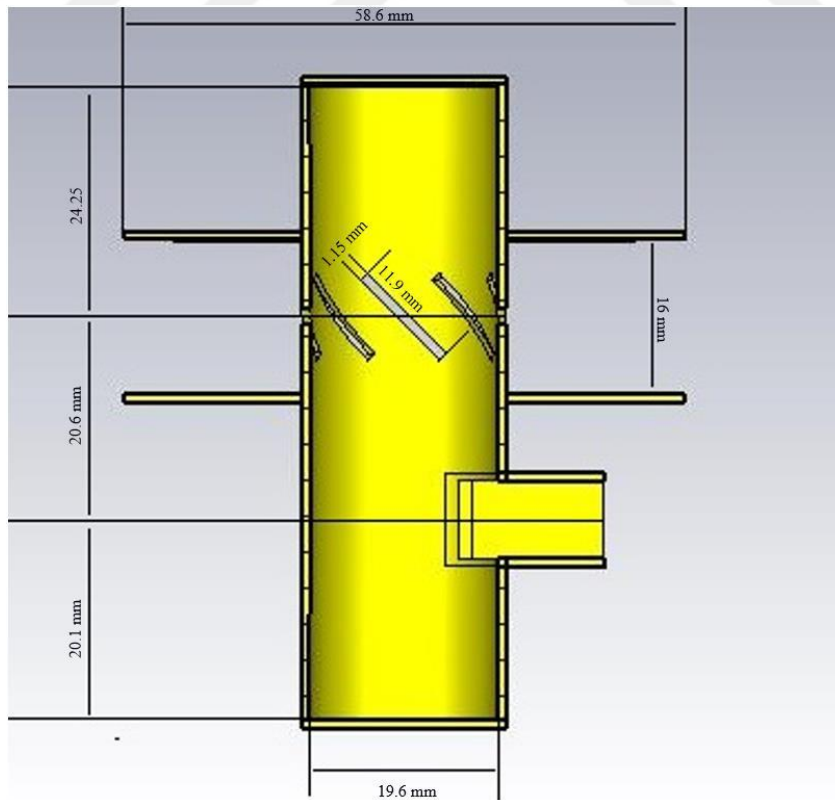

Figure 25. Production Version of Antennas' CST MWS Design.

Fundamental dimensions that effect on performance of the transmitter antenna are given in Figure 26.
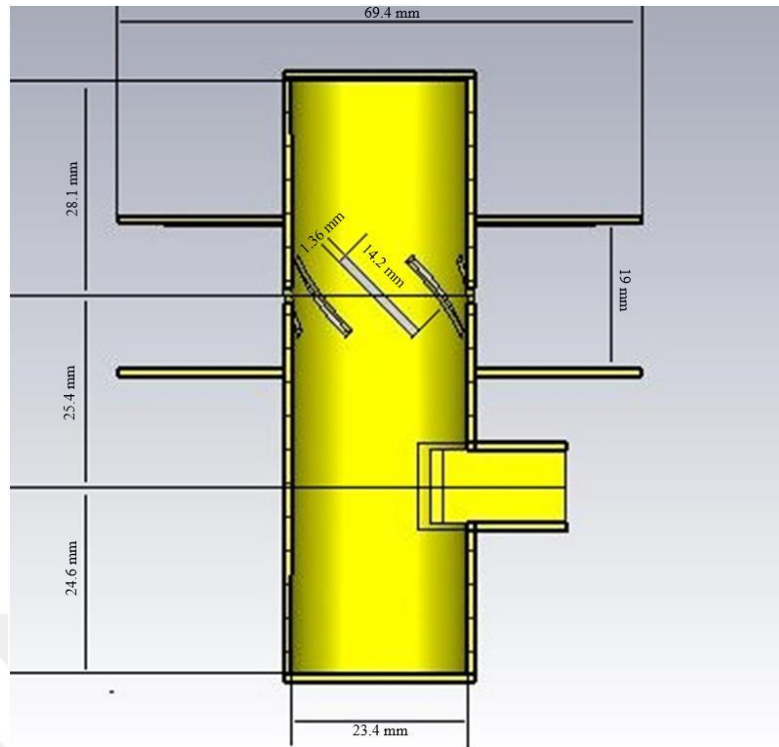
Figure 26. Fundamental Dimensions of Transmitter Antenna.

Fundamental dimensions that effect on performance of the receiver antenna are given in Figure 27.

**Figure 27.** Fundamental Dimensions of Receiver Antenna.

4.3. Simulation and Measurement Results

Antenna designs are drawn and simulated with CST MWS simulation program. Calculated design parameters with theoretical formulas are used as initial values of the antenna structure dimensions. S-parameters and farfield radiation patterns of the antennas are investigated in simulations. Frequency interval of the simulations is determined as between 10 GHz and 14.5 GHz. This frequency interval includes operating frequencies that belong receiver and transmitter antennas. CST MWS automatically produces S11 parameter of antenna as a result of simulations. Farfield monitors must be added to simulations for investigation of farfield radiation patterns of the antennas. For transmitter antennas five-farfield monitors are added to simulation at 11 GHz, 11.5 GHz, 11.75 GHz, 12 GHz and 12.5 GHz frequencies. For receiver antennas again five-farfield monitors are added to simulations at 13.8 GHz, 13.9 GHz, 14 GHz, 14.1 GHz and 14.2 GHz frequencies.

There are different kind of solver modes in CST MW Studio. In this study, Time Domain Solver is employed for simulated the antennas that are designed. In CST MWS two time domain solvers are available, which both work on hexahedral meshes. One is based on the Finite Integration Technique (FIT), just called Transient Solver, the second one is based on the Transmission Line Method (TLM) and is referred to as TLM solver. Transient Solver is used in this study. The transient solver applies advanced numerical techniques to allow accurate modeling of small and curved structures without the need for an extreme refinement of the mesh at these locations. This allows very memory efficient computation together with a robust hexahedral meshing to successfully simulate extremely complex structures.

Dimensions of meshes are selected as $\lambda/60$. Adaptive mesh refinement tool of the CST MWS is used to obtain this mesh value. For smaller mesh dimensions, difference between simulation results is smaller than the error that is determined. Default maximum error is determined as 0.02 by CST MWS.

S-parameters of the structures are primarily investigated. S-parameters of the antennas demonstrate the operating frequencies of the antennas. Only S11 graph exists for each antenna because of antennas are one-port devices. S11 parameter of the transmitter antenna, which is found as result of CST MW Studio simulations, is given Figure 28.
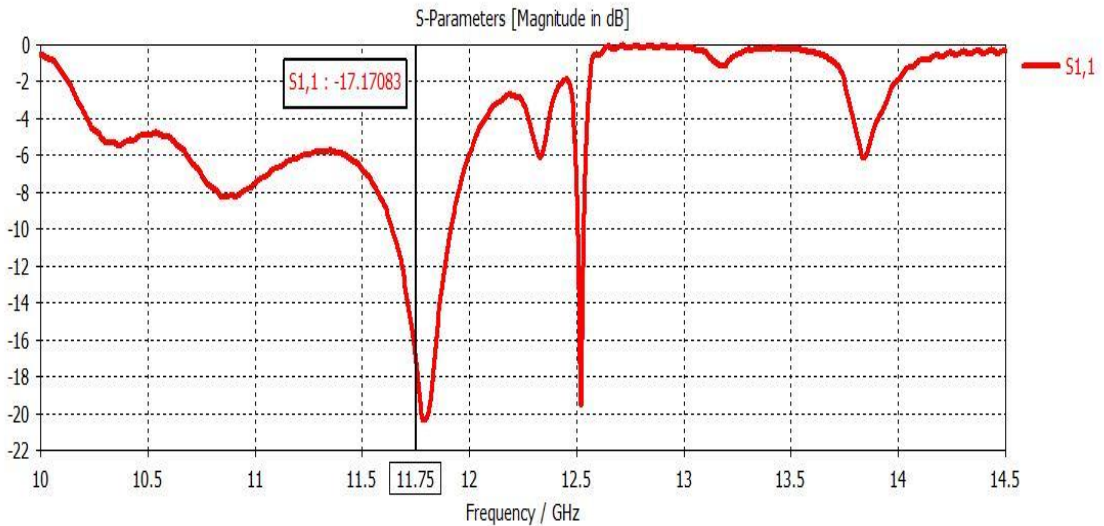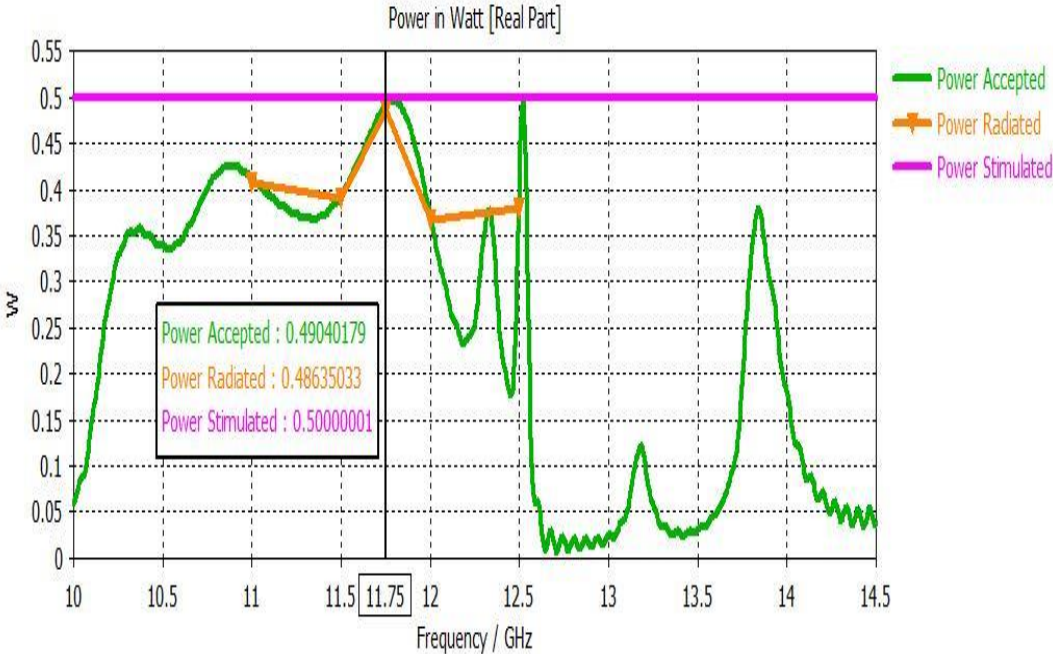
Figure 28. S11 Graph of Transmitter Antenna in CST MWS.

As it can be seen in Figure 28, S11 parameter of transmitter antenna is equal to -17.17 dB. It means, 1.92% of total power that comes from input port of the antenna is reflected back to input port of the antenna. It can be thought that non-reflecting power radiates from the antennas to free space. In this case, it can be assumed that 98.08% of the total power that comes from input port of the antenna is radiated. -10 dB bandwidth of the transmitter antenna, which includes operating transmitter frequency is 11.75 GHz, is 272 MHz (11.64 GHz to 11.912 GHz). 272 MHz bandwidth around the 11.75 GHz center frequency corresponds to 2.32% bandwidth in terms of percentage.
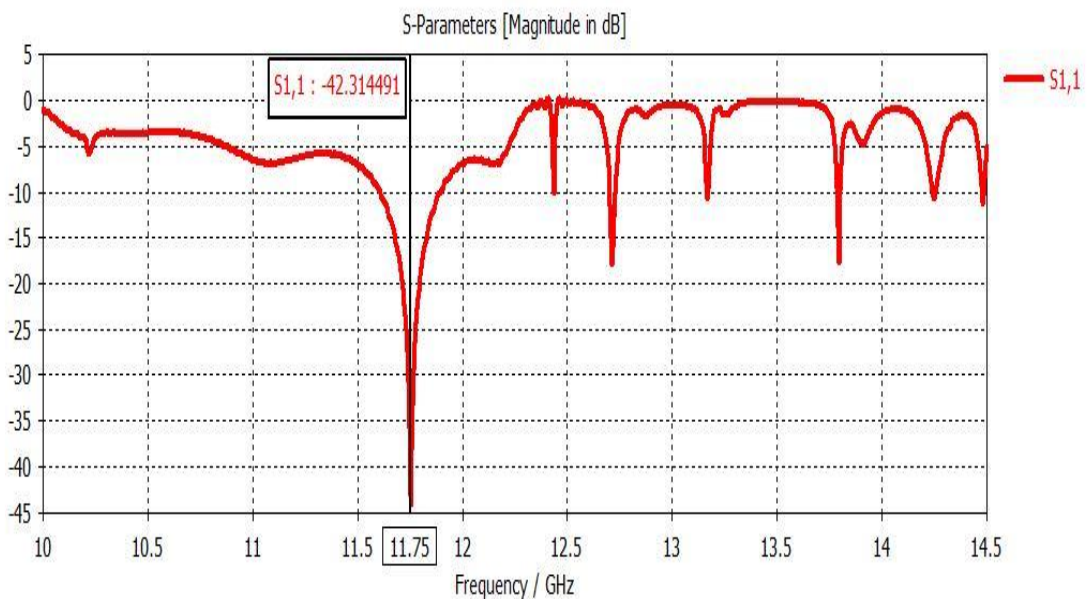
**Figure 29.** S11 Graph of Transmitter Antenna Production Version in CST MWS.

47

As it is mention before, transmitter and receiver antennas are modified for production. For increasing durability of the antennas while reducing production time and production cost circular waveguide walls are thickened. Effect of these modifications are investigated and required simulations are applied on new structures. As a result of these simulation S11 graph of transmitter antenna production version is obtained as shown in Figure 29. Production version of transmitter antenna has 289 MHz (from 11.606 GHz to 11.895 GHz) -10 dB bandwidth. 289 MHz bandwidth around the 11.75 GHz center frequency corresponds to 2.46% bandwidth in terms of percentage. -10 dB bandwidth of transmitter antenna is improved by modification, which is done for manufacturing.

Figure 30. Transmitter Antenna Power Dissipation Graph in CST MWS.

Power dissipation graph of transmitter antenna that is created by CST MWS simulations is given in Figure 30. As it can be seen in Figure 30, 98.08% of total power is transmitted to antennas and 97.28% of total power is radiated from antennas at 11.75 GHz. The power dissipation results are consistent with S11 parameter of the antenna in CST MWS simulations.
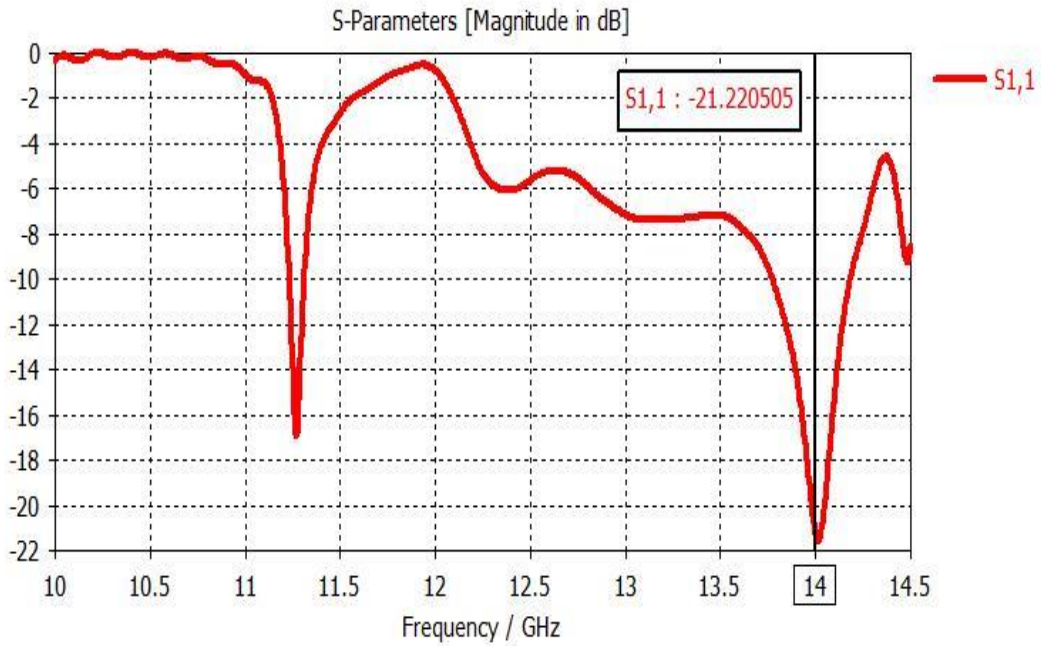
Figure 31. S11 Graph of Receiver Antenna in CST MWS.

S11 graph of the receiver antenna that is found from CST MW Studio simulations is given Figure 31. S11 parameter is equal to -21.22 dB at the 14.00 GHz, which is receiver operating frequency. 0.76% of total power that comes from input port of the antenna is reflected back to input port of the antenna. In this case, 99.24% of total power radiates from antennas. -10 dB bandwidth of the receiver antenna, which includes operating transmitter frequency is 14.00 GHz, is 406 MHz (13.774 GHz to 14.180 GHz). 406 MHz bandwidth around the 14.00 GHz center frequency corresponds to 2.9% bandwidth in terms of percentage.
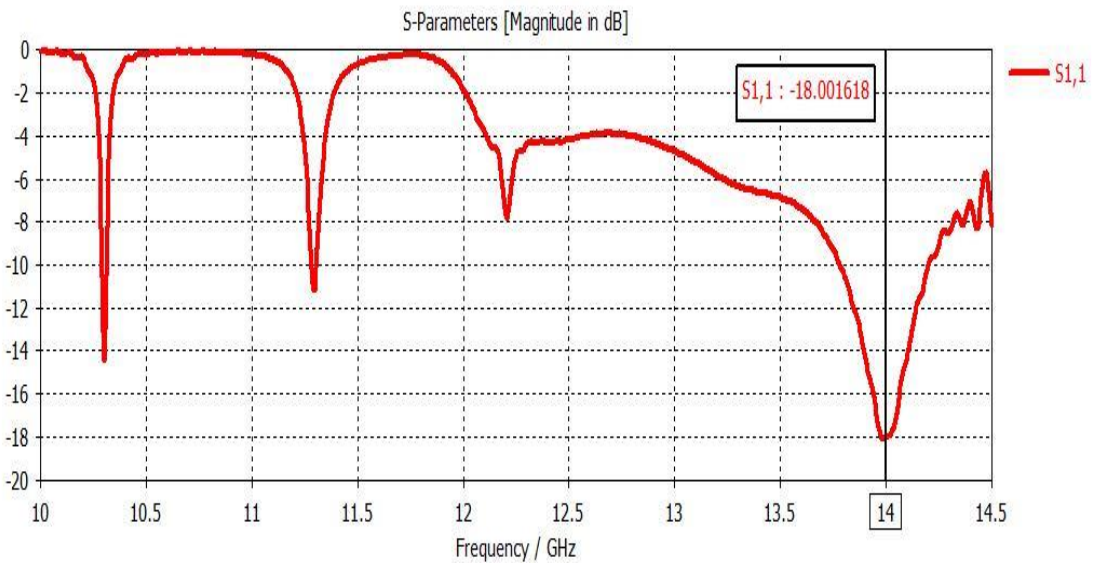
Figure 32. S11 Graph of Receiver Antenna Production Version in CST MWS.

As a result of these simulation, S11 graph of receiver antenna production version is obtained as shown in Figure 32. Production version of transmitter antenna has 481MHz (from 13.781 GHz to 14.199 GHz) -10 dB bandwidth. 418 MHz bandwidth around the 14.00 GHz center frequency corresponds to 2.99% bandwidth in terms of percentage. -10 dB bandwidth of receiver antenna is improved by modification, which is done for manufacturing.
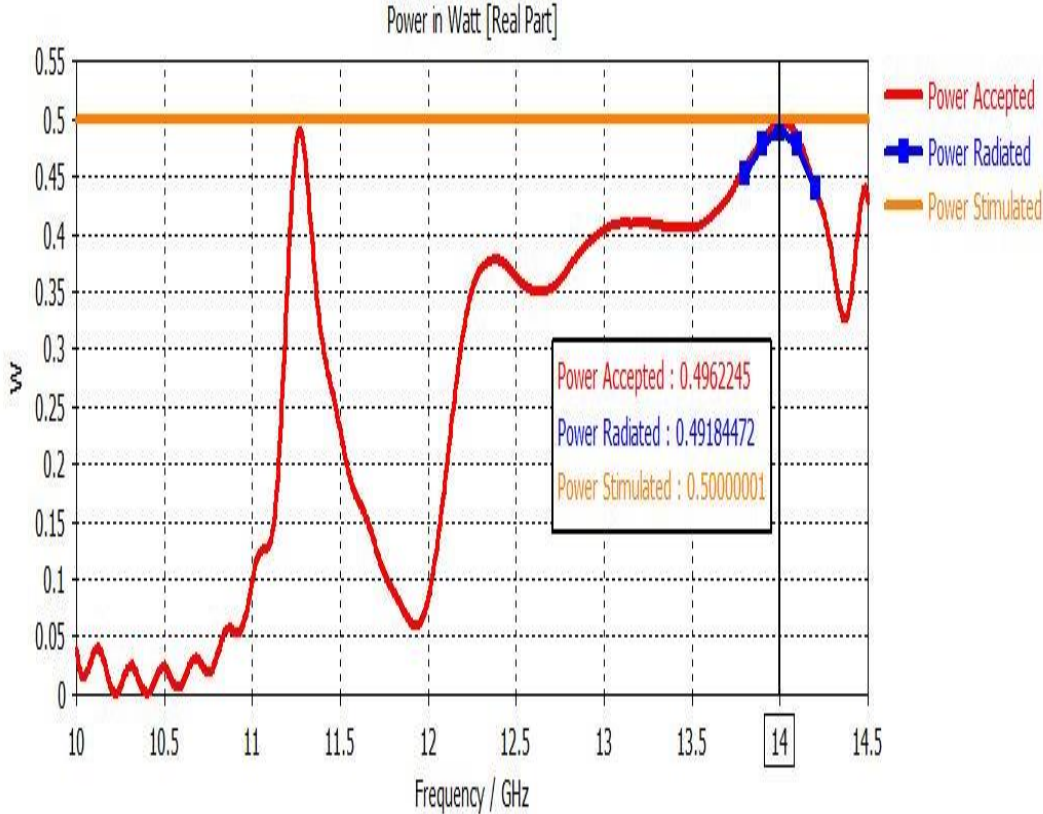

Figure 33. Receiver Antenna Power Dissipation Graph in CST MWS.

Receiver antenna power dissipation graph, which is obtained from CST MWS simulations, is given as Figure 33. 99.24% of total power that comes input port of the antenna transmits to antennas as consistent with S11 graph of the receiver antennas and 98.36% of total power is radiated from antennas to free space at 14.00 GHz.

According to CST MWS simulation results, transmitter and receiver antennas successfully provide expected transmission performance. The other important antenna parameters can be examined within farfield radiation performance of antennas. Gain and axial ratio values determine farfield radiation pattern and polarization type of antennas.
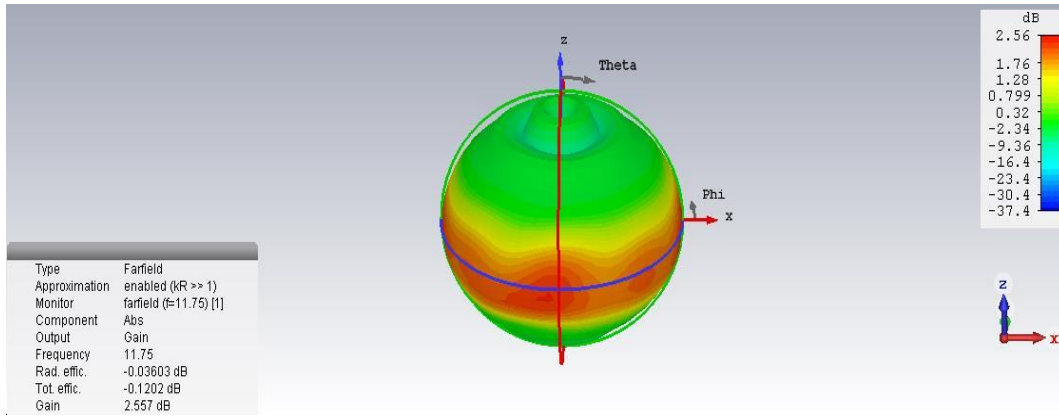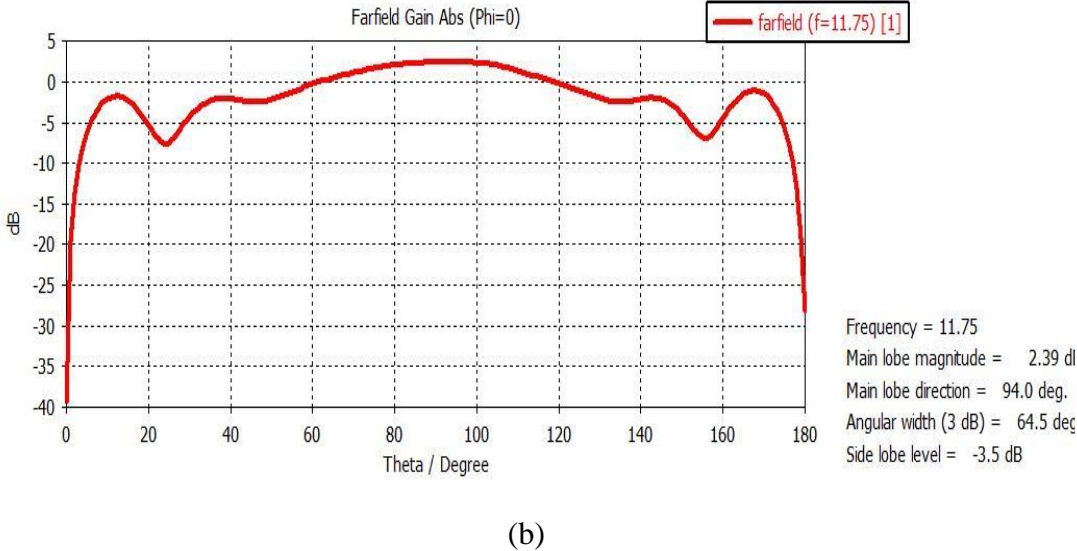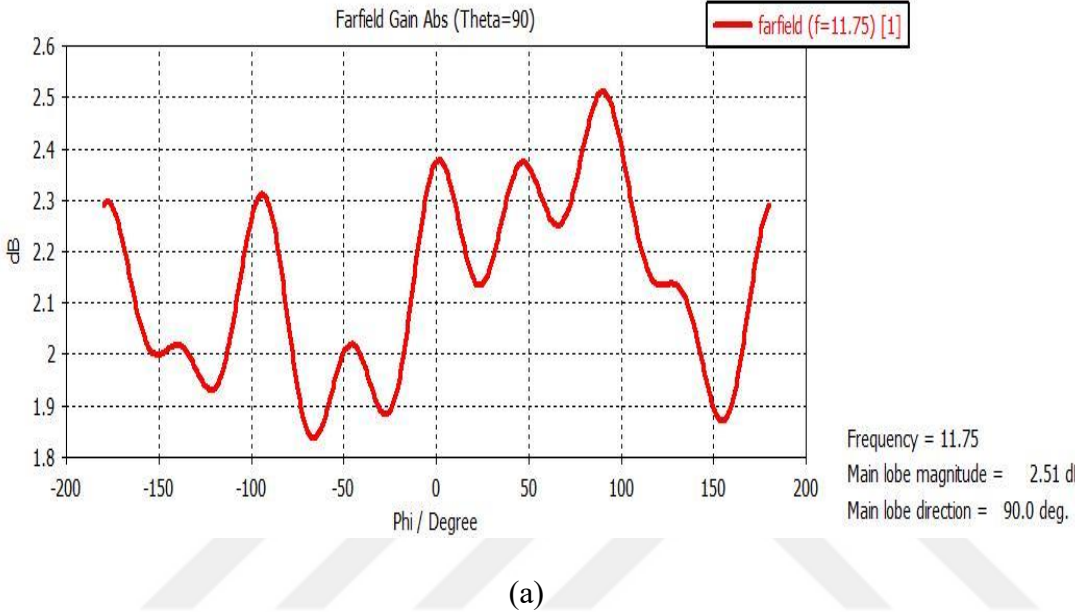
Figure 34. 3D Radiation Pattern of Transmitter Antenna in CST MWS.

3D radiation pattern of transmitter antenna is obtained as in Figure 34 via CST MWS simulations at 11.75 GHz. Transmitter antenna radiation pattern is almost perfectly match with ideal omnidirectional radiation pattern. Antenna is non-directional in one fundamental plane (azimuth plane) and directional in the other fundamental plane (elevation plane). Therefore, all farfield parameters can be examined separately for each fundamental planes.
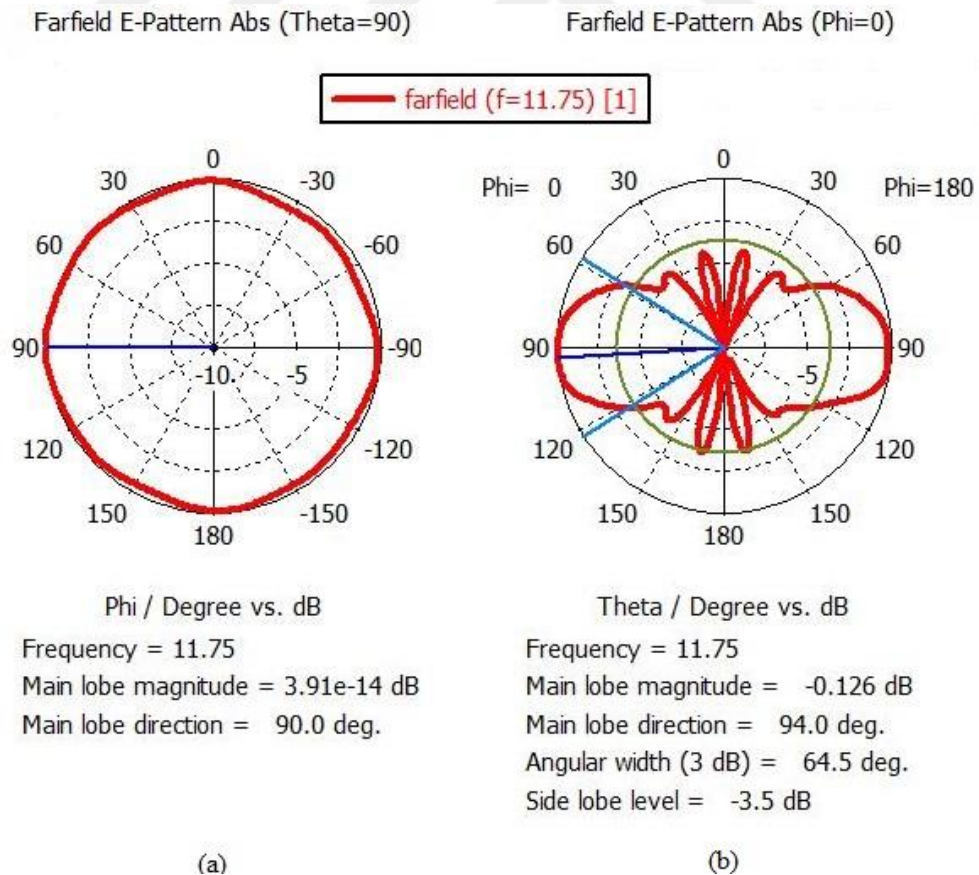
Figure 35. Polar Radiation Pattern of Transmitter Antenna (a) in Azimuth Plane and (b) in Elevation Plane in CST MWS.

Polar farfield radiation patterns of transmitter antenna in both plane are given in Figure 35. Polar farfield radiation pattern gives a clear idea about omnidirectionality of transmitter antenna. In azimuth plane, radiation pattern likes almost a circle. There is no dramatically gain change along the azimuth plane. In elevation plane, figure of eight farfield radiation pattern exists. There is no any radiation on –z and +z directions. Direction of the maximum radiations are toward to –x and +x directions.
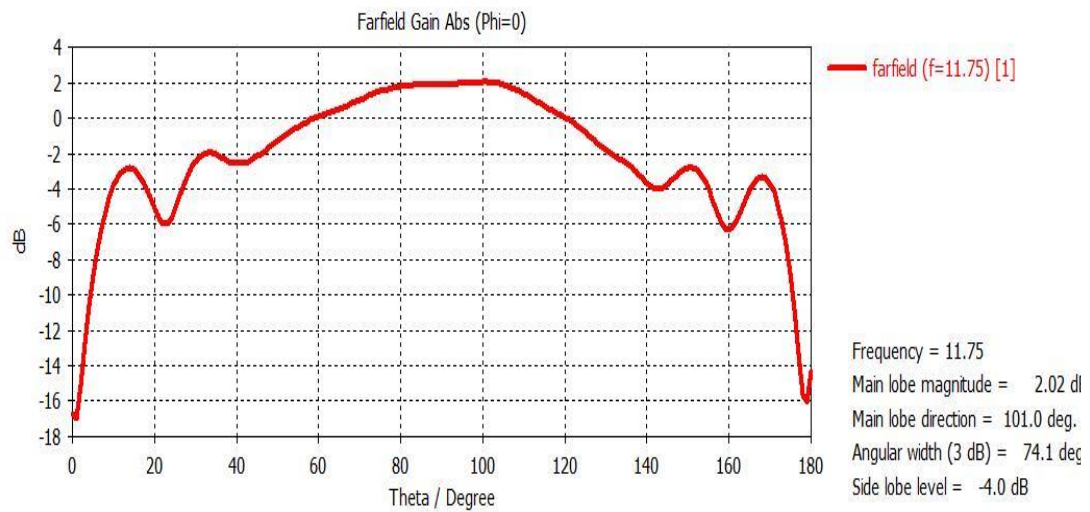

(a)

(b)

Figure 36. Cartesian Radiation Pattern of Transmitter Antenna (a) in Azimuth Plane and (b) in Elevation Plane in CST MWS.

Magnitude values of the gain in each plane can be clearly seen in Figure 36.a. In azimuth plane maximum magnitude of gain change is 0.67 dBi in all directions. 0.67

dBi is very small variation and it can be neglect. Therefore, antenna can be defined as non-directional in azimuth plane. In elevation plane, there is huge difference between maximum magnitude of gain and minimum magnitude of gain so non-directionality is not valid in this plane.
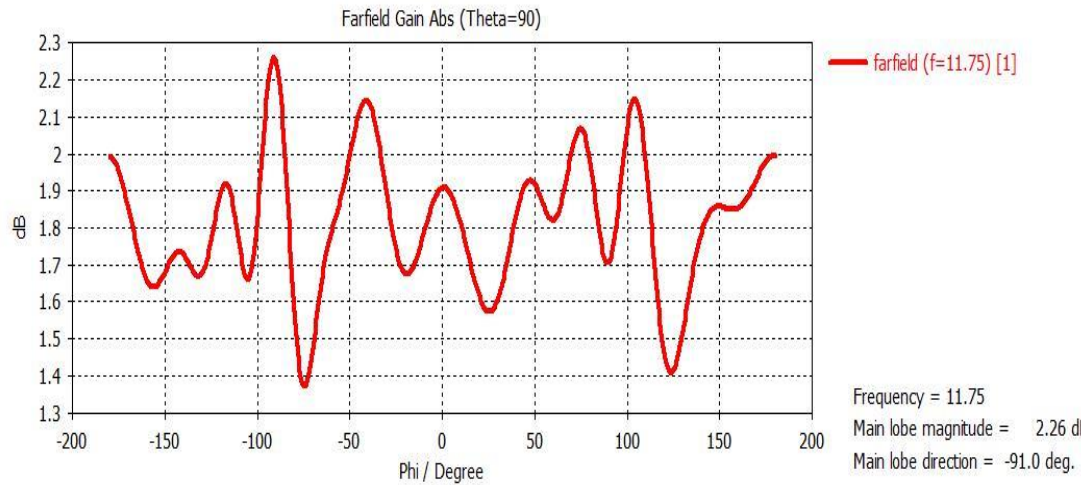

(a)

(b)

Figure 37. Cartesian Radiation Pattern of Production Version of Transmitter Antenna (a) in Azimuth Plane and (b) in Elevation Plane in CST MWS.

Maximum variation in azimuth plane is 0.89 dBi as shown in Figure 37.a. There is no meaningful difference between production version and design version of transmitter antenna for this plane. In elevation plane, simulation result of gain are similar for production version and designed version of transmitter antenna.
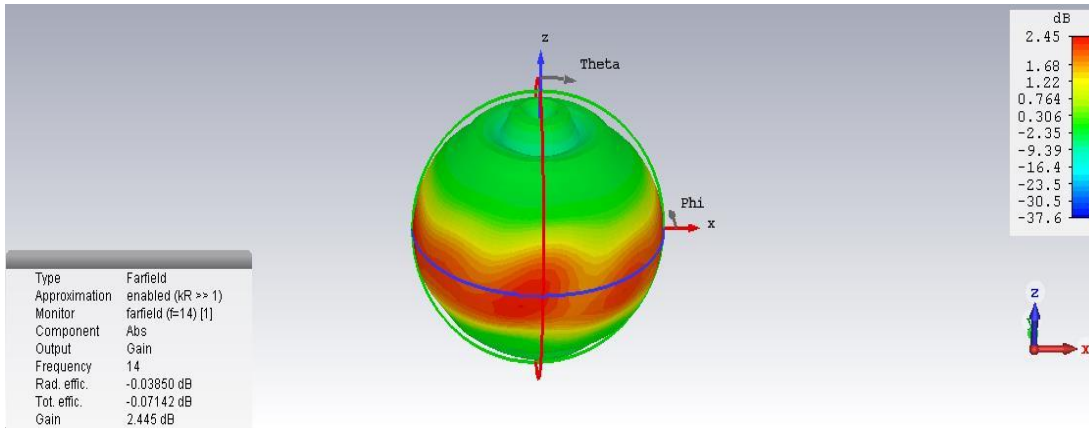
Figure 38. 3D Radiation Pattern of Receiver Antenna in CST MWS.

3D radiation pattern of receiver antenna is obtained as in Figure 38 via CST MWS simulations at 14.00 GHz. Receiver antenna radiation pattern is almost perfectly match with ideal omnidirectional radiation pattern. Antenna is non-directional in one fundamental plane (azimuth plane) and directional in the other fundamental plane (elevation plane). Therefore, all farfield parameters can be examined separately for each fundamental plane.
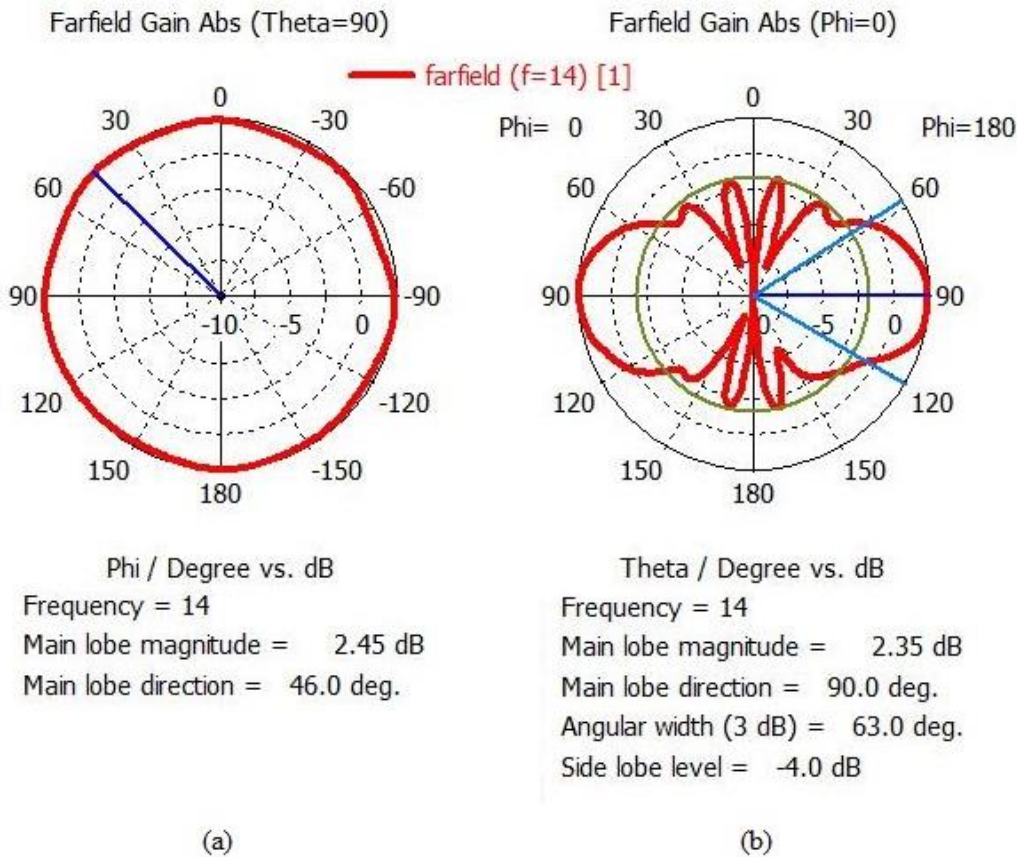
Figure 39. Polar Radiation Pattern of Receiver Antenna (a) in Azimuth Plane and (b) in Elevation Plane in CST MWS.

Polar farfield radiation patterns of receiver antenna in both plane are given Figure 39. Polar farfield radiation pattern gives a clear idea about omnidirectionality of receiver antenna. In azimuth plane, farfield radiation pattern likes almost a circle. There is no dramatically gain change along the azimuth plane. In elevation plane, figure of eight farfield radiation pattern exists. There is no any radiation on –z and +z directions. Direction of the maximum radiations are toward to –x and +x directions.

(a)

(b)
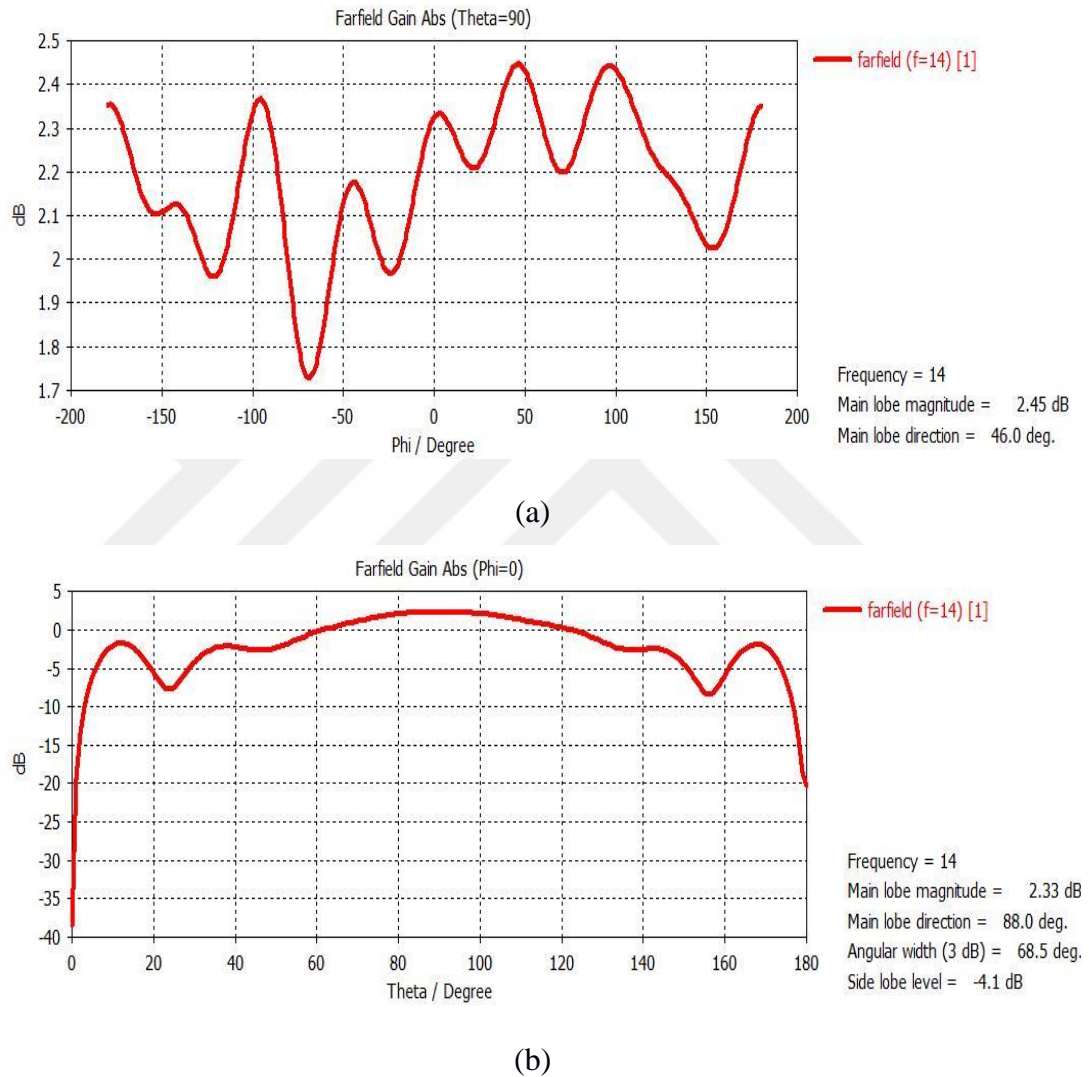
Figure 40. Cartesian Radiation Pattern of Receiver Antenna (a) in Azimuth Plane and (b) in Elevation Plane in CST MWS.

Magnitude values of the gain in each plane can be clearly seen in Figure 40. In azimuth plane maximum magnitude of gain change is 0.72 dBi in all directions. 0.72 dBi is very small variation and it can be neglect. Therefore, antenna can be defined as non-directional in azimuth plane. In elevation plane, there is huge difference between

maximum magnitude of gain and minimum magnitude of gain so non-directionality is not valid in this plane.

(a)

(b)
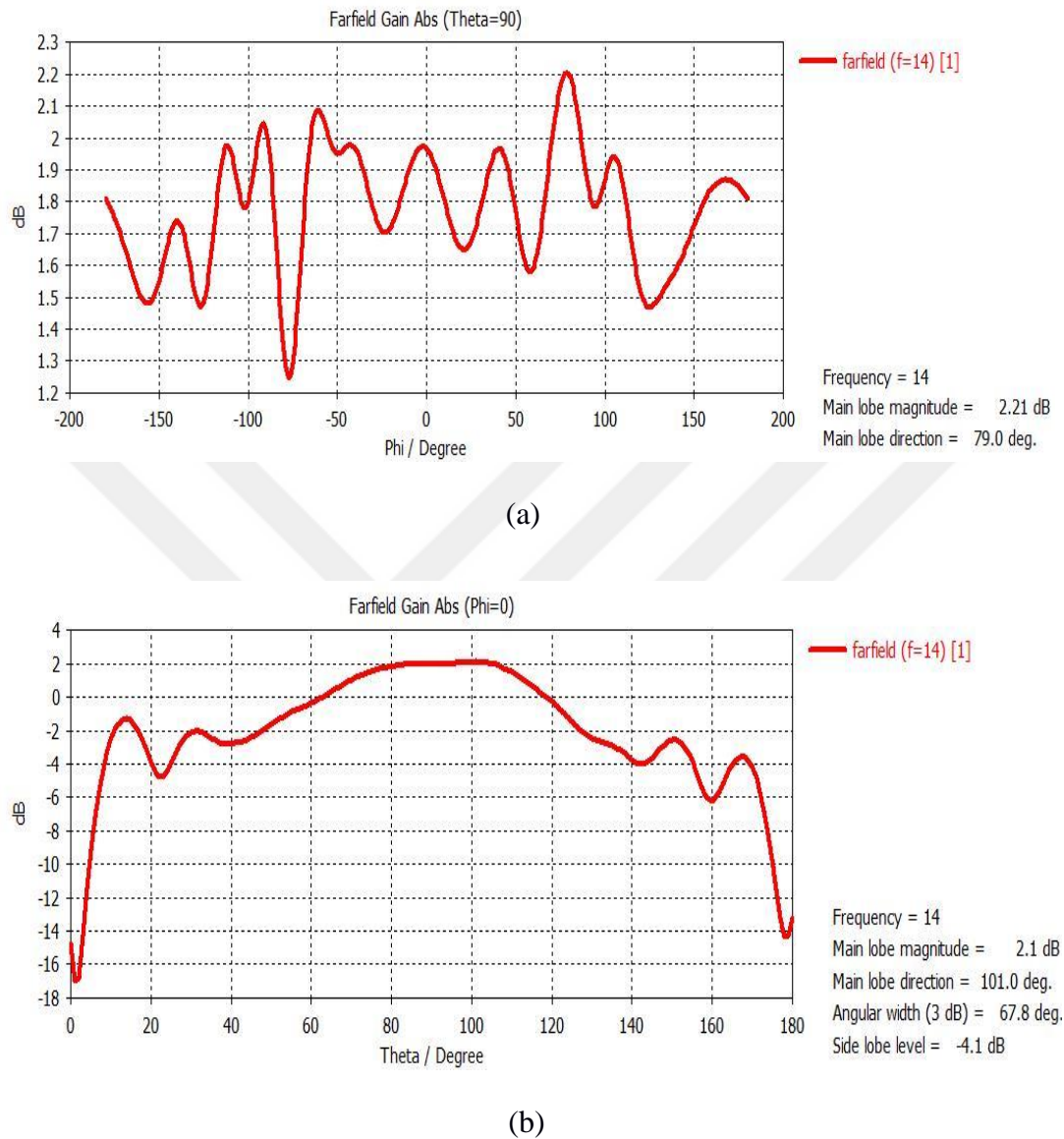
Figure 41. Cartesian Radiation Pattern of Production Version of Receiver Antenna (a) in Azimuth Plane and (b) in Elevation Plane in CST MWS.

Maximum variation in azimuth plane is 0.96 dBi as shown in Figure 41.a. There is no meaningful difference between production version and design version of receiver antenna for this plane. In elevation plane, simulation result of gain are similar for production version and designed version of receiver antenna.

In order for an antenna to be define circularly polarized, it is required that axial ratio of the antenna is smaller than 3 dB. Axial ratio of both transmitter and receiver antennas can be separately examined for azimuth and elevation planes.
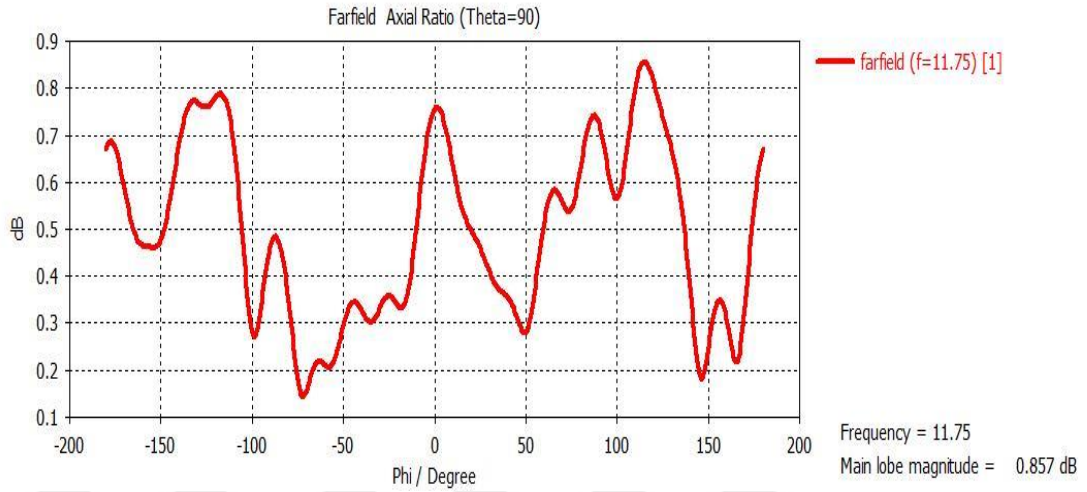
(a)

(b)

Figure 42. Axial Ratio of Transmitter Antenna (a) in Azimuth Plane and (b) in Elevation Plane in CST MWS.

Axial ratio of transmitter antenna in azimuth plane is smaller than 0.86 dB as shown in Figure 42.a. Circular polarization requires 3 dB or less axial ratio according to general standards. Even maximum value of axial ratio that belongs to transmitter antenna is much smaller than 3 dB in azimuth plane so transmitter antenna can be accepted as perfectly circularly polarized in this plane. Although axial ratio of

57

transmitter antenna is smaller than 3 dB in a large part of elevation plane, it is only smaller than 3 dB continuously between 53.72⁰ and 122.95⁰. Transmitter antennas can be assumed as circularly polarized in elevation plane with 69.23⁰ aspect angle.
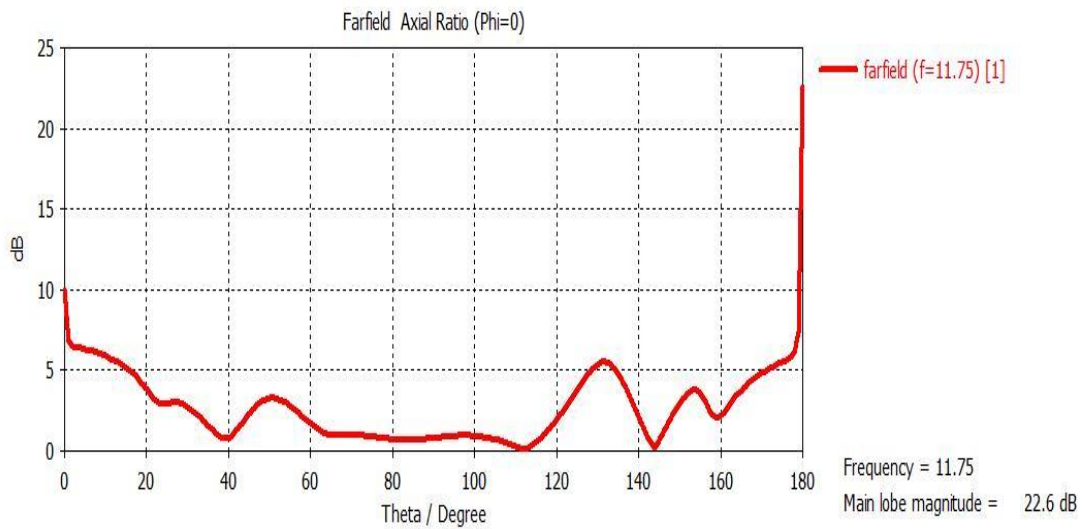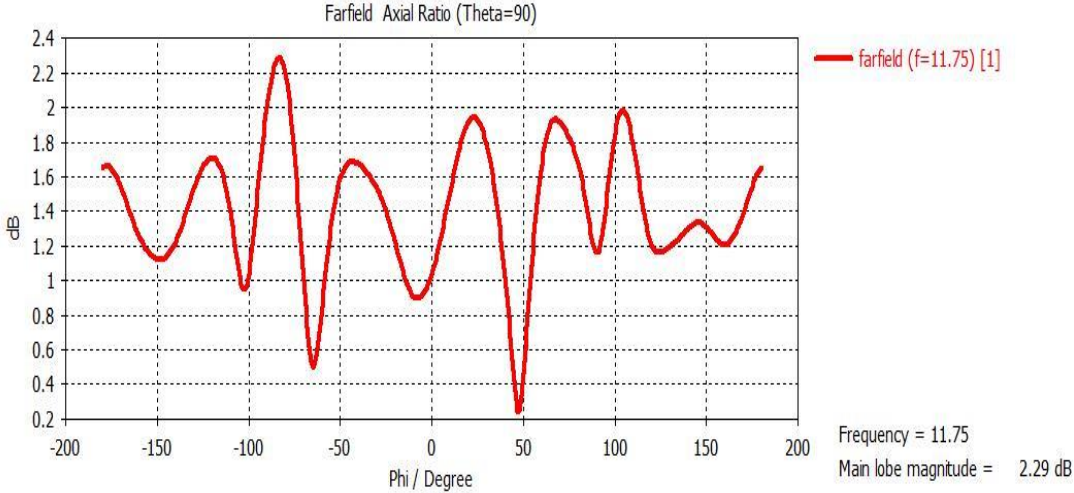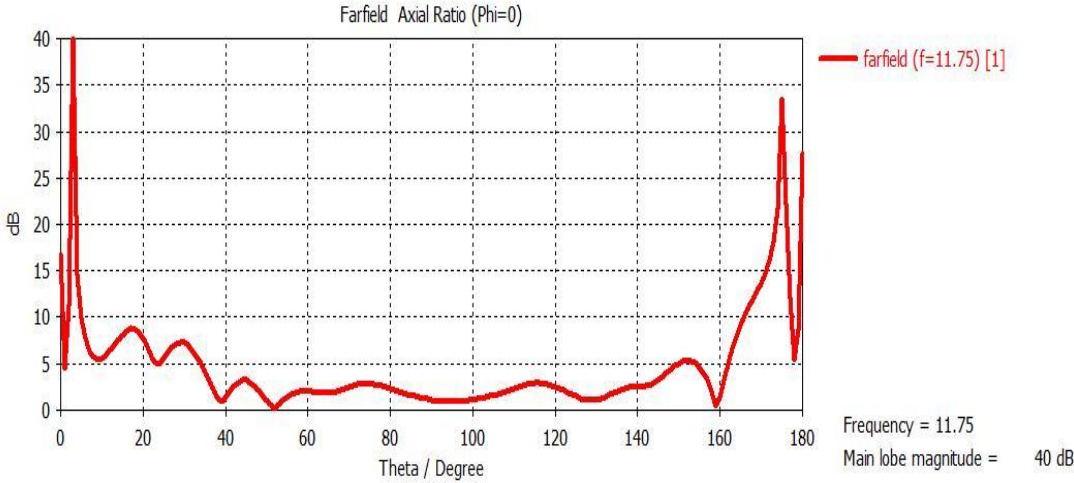

(a)

(b)

Figure 43. Axial Ratio of Production Version of Transmitter Antenna (a) in Azimuth Plane and (b) in Elevation Plane in CST MWS.

Axial ratio of transmitter antenna in azimuth plane is smaller than 2.29 dB as shown in Figure 43.a. Although production version of transmitter antenna has worse axial ratio performance than designed version of transmitter antenna, it has sufficient axial ratio performance according to 3 dB standard along the azimuth plane. In a large part of elevation plane, it is only smaller than 3 dB continuously between 45.75⁰ and 144.5⁰.

Production version of transmitter antennas can be assumed as circularly polarized in elevation plane with 98.75⁰ aspect angle. Production version of transmitter antenna is almost same with designed version.

Figure 44. Axial Ratio of Receiver Antenna (a) in Azimuth Plane and (b) in Elevation Plane in CST MWS.

Axial ratio of receiver antenna in azimuth plane is smaller than 0.98 dB as shown in Figure 44. Even maximum value of axial ratio that belongs to receiver antenna is much smaller than 3 dB in azimuth plane so receiver antenna can be accepted as perfectly circularly polarized in this plane. Although axial ratio of receiver antenna is smaller

than 3 dB in a large part of elevation plane, it is only smaller than 3 dB continuously between 54.10° and 126.38°. Receiver antennas can be assumed as circularly polarized in elevation plane with 72.28° aspect angle.
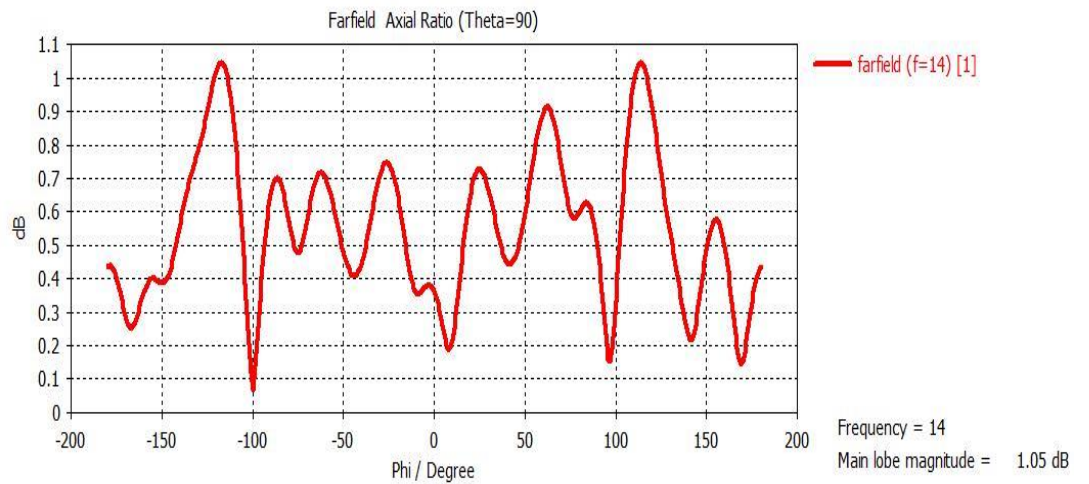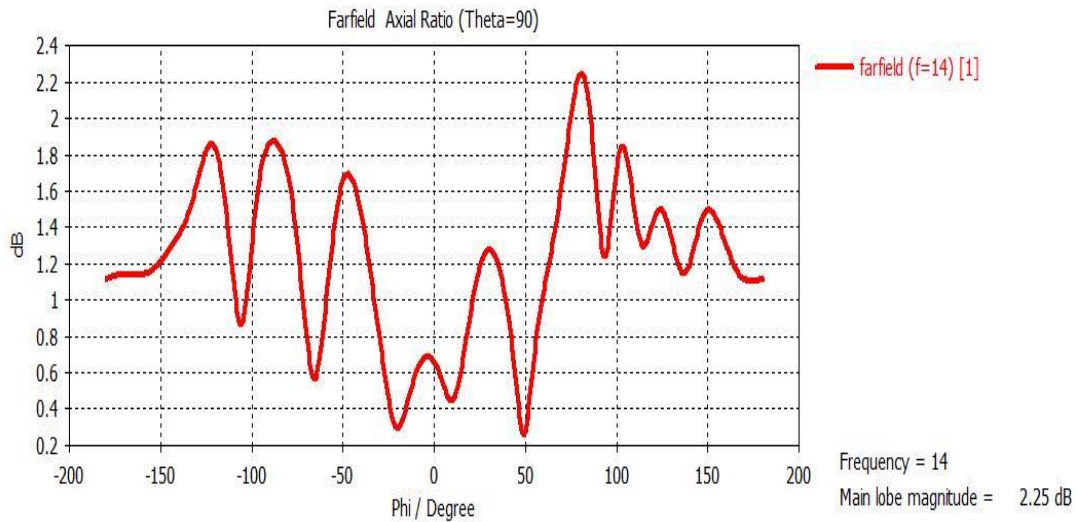

(a)
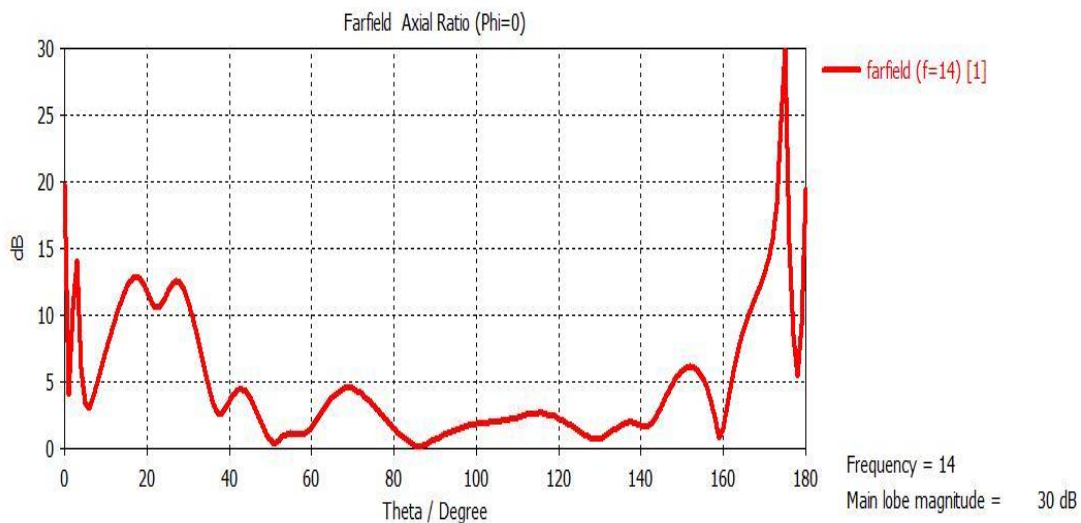
(b)

Figure 45. Axial Ratio of Production Version of Receiver Antenna (a) in Azimuth Plane and (b) in Elevation Plane in CST MWS.
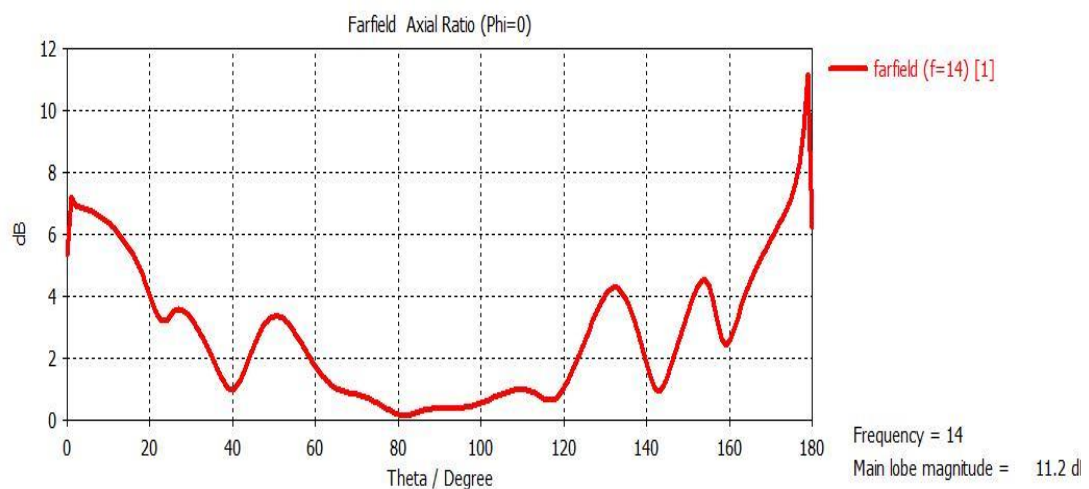
Axial ratio of receiver antenna in azimuth plane is smaller than 2.25 dB as shown in Figure 45.a. Although production version of transmitter antenna has worse axial ratio performance than designed version of receiver antenna, it has sufficient axial ratio performance according to 3 dB standard along the azimuth plane. In a large part of

60

elevation plane, it is only smaller than 3 dB continuously between 75.5⁰ and 145⁰. Production version of receiver antennas can be assumed as circularly polarized in elevation plane with 69.5⁰ aspect angle. Production version of transmitter antenna is almost same with designed version.

**Table 4.** Results of Study vs. Similar Studies in Literature.

	-10 dB Bandwidth	Maximum Variation of Gain	Maximum Value of Axial Ratio
This Study	3%	0.7 dBi	1 dB
(Top, Dogan, 2012)	1,005%	0.75 dBi	2 dB
(Masa-Campos, Fernandez, Sierra-Perez, Fernandez-Jambrina, 2006)	1,4%	1.9 dBi	3.2 dB

It is aimed that some similar studies in literature are improved with this study. Two study in literature are selected as main reference of this thesis. Comparison between results of the study and results that belong to similar studies in literature is given in Table 4. Frequency bandwidth of the first similar reference study (Top, Dogan, 2012) is improved 2%. Maximum gain variation is reduced 0.05 dBi and axial ratio is reduced 1 dB. According to the other similar reference study (Masa-Campos, Fernandez, Sierra-Perez, Fernandez-Jambrina, 2006), frequency bandwidth is increased 1.6%, maxiumum gain variation is reduced 1.2 dBi and axial ratio is reduced 2.2 dB. To be understood from the Table 4 antennas, which are designed in this study, have better omnidirectionality, wider frequency bandwidth and better circular polarization performance than the other similar studies in literature.

A prototype of receiver antenna, which is proposed in the thesis, is fabricated and measured. Receiver antenna that is fabricated shown in Figure 46.

Figure 46. Fabricated Receiver Antenna.

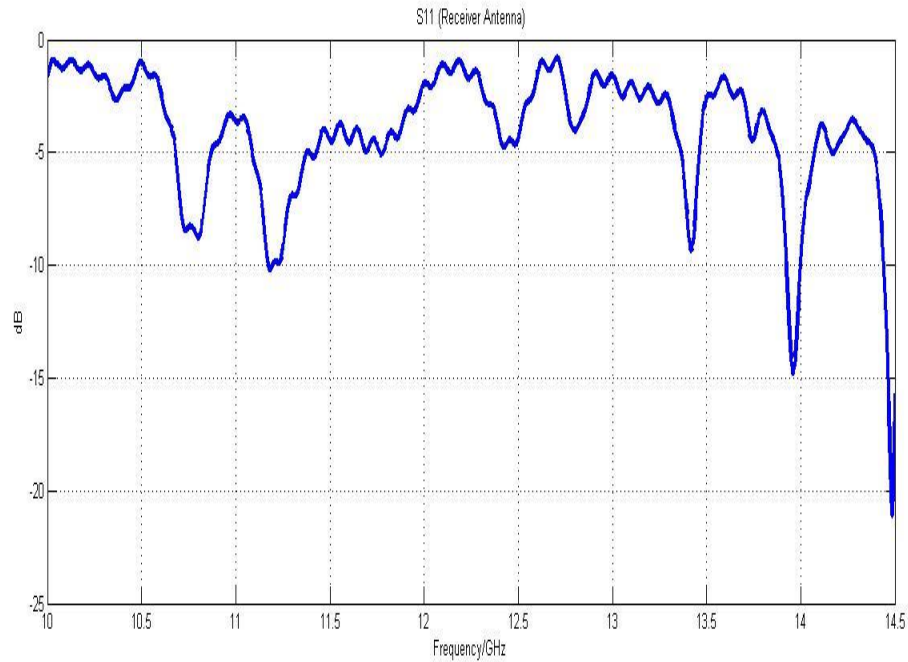S11 parameter of the receiver antenna that is fabricated is measured by a network analyzer (NA) in Yasar University Antenna and Microwave Laboratory as shown in Figure X. NA that is employed in S11 measurement can measure up to 20 GHz.
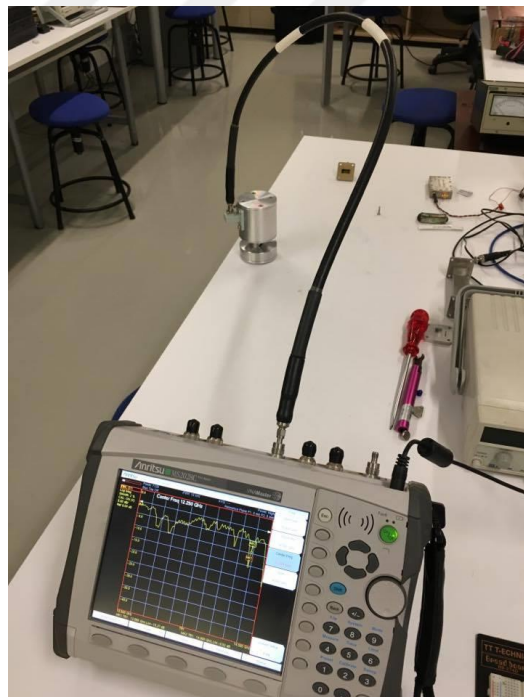
Figure 47. S11 Measurement of Prototype Receiver Antenna in Yasar University Antenna and Microwave Laboratory.

Figure 48. S11 Graph of Receiver Antenna Prototype.

S11 graph of the prototype receiver antenna is given in Figure 48. As it can be seen in the S11 graph of the antenna that is manufactured gives minimum value at the 13.972 GHz. Production version of the receiver antenna that is designed has minimum S11 value at 13.986 GHz. Minimum values of S11 parameters for prototype and design are 99.9% consistent to each other. Also as it is expected, S11 of receiver antenna that is manufactured is under -10 dB at operating receive frequency (14 GHz). Because of production faults, receiver antenna prototype has -10 dB bandwidth, which is worse than the simulation version. Manufactured antenna has about 100 MHz bandwidth around the operating frequency (14.00 GHz). The production fault that causes distortion on S11 parameter is related with the width and length of the antenna slots. Frequency bandwidth of the antenna can be fixed by more accurate manufacturing.

(a)

(b)

Figure 49. Farfield Measurements of Prototype Receiver Antenna at (a) Azimuth Plane and (b) Elevation Plane in İYTE Anechoic Chamber.

Farfield measurements of the prototype receiver antenna are realized in anechoic chamber, which is in Izmir Institute of Technology (IYTE). Farfield measurement setups are given in Figure 49.a for azimuth plane and Figure 49.b for elevation plane. Different measurement setups are constructed for azimuth plane and elevation plane measurements. For azimuth plane farfield measurements, receiver antenna prototype is placed to platform as vertical with respect to ground. When the receiver antenna prototype position is vertical, measurement antennas orientation is set as vertical according to earth. Receiver antenna prototype is turned around 360° and measurement results are taken between 6° intervals. Then measurement antenna is set as horizontal according to earth and same procedures are repeated. Suppose the gains are measured

for vertical and horizontal LP source antenna orientations, G_{Tv}, G_{Th}. These measured partial gains are combined to give total gain.

$$G_T(dB) = 10\,log(G_{Tv} + G_{Th}) \tag{16}$$

The procedure is referred as the partial gain method (Stutzman, Thiele, 2012). Axial ratio of the antenna can be found from difference between G_{Tv} and G_{Th}. For elevation plane farfield measurements, receiver antenna prototype is horizontally oriented according to earth and all procedures, which are applied for azimuth plane farfield measurements, are implemented.
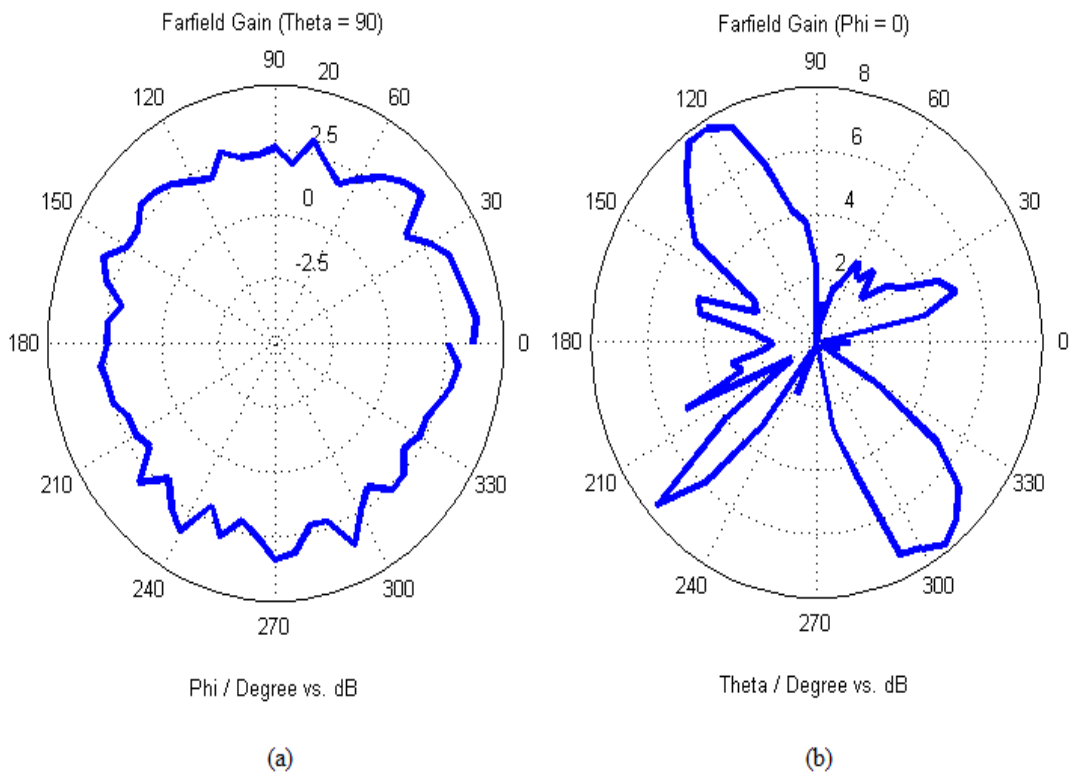
Figure 50. Polar Farfield Gain Pattern in (a) Azimuth and (b) Elevation Planes of Receiver Antenna Prototype.

Farfield polar gain patterns of receiver antenna prototype is given for in azimuth and elevation planes in Figure 50.a and Figure 50.b respectively. As it can be seen in Figure 50 antenna has almost nondirectional farfield gain pattern at azimuth plane and directional pattern at elevation plane as consistent with omnidirectional radiation pattern.
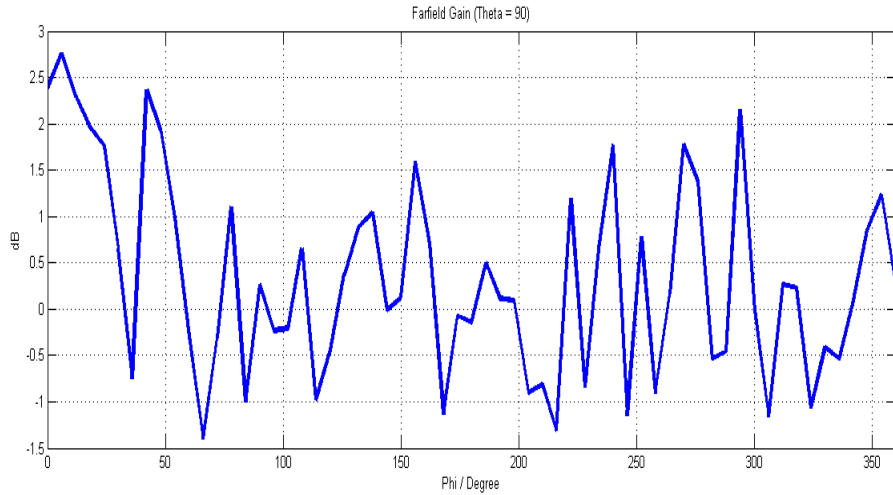
(a)
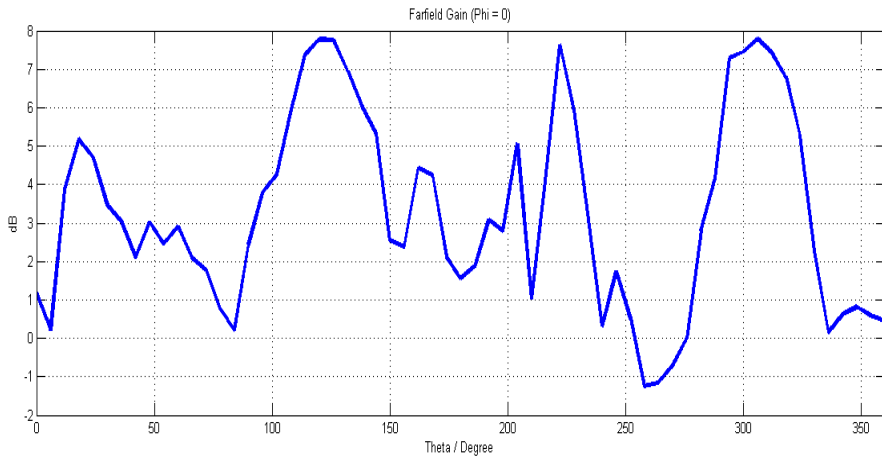
(b)

Figure 51. Cartesian Farfield Gain Pattern of Receiver Antenna Prototype in (a) Azimuth Plane and (b) Elevation Measurements.

Variations on gain patterns of receiver antenna prototype can be seen more clearly in cartesian gain pattern plots that shown in Figure 51 for both azimuth and elevation planes. In azimuth plane, maximum gain variation is desired to be as low as possible. Maximum variation of gain in azimuth plane is found as about 4 dB in Figure 51.a. The variation on gain is bigger than the simulation results. The main reason of the difference between simulations and measurements is production faults. 4 dB gain variation in azimuth plane is acceptable for omnidirectional antennas. Maximum gain variation elevation plane is given in Figure 51.b. The maximum variation in elevation

plane is seen as about 9 dB. It is believe that the actual variation on this plane is more than 9 dB. Because some measured power values fall to noise level in measurements.
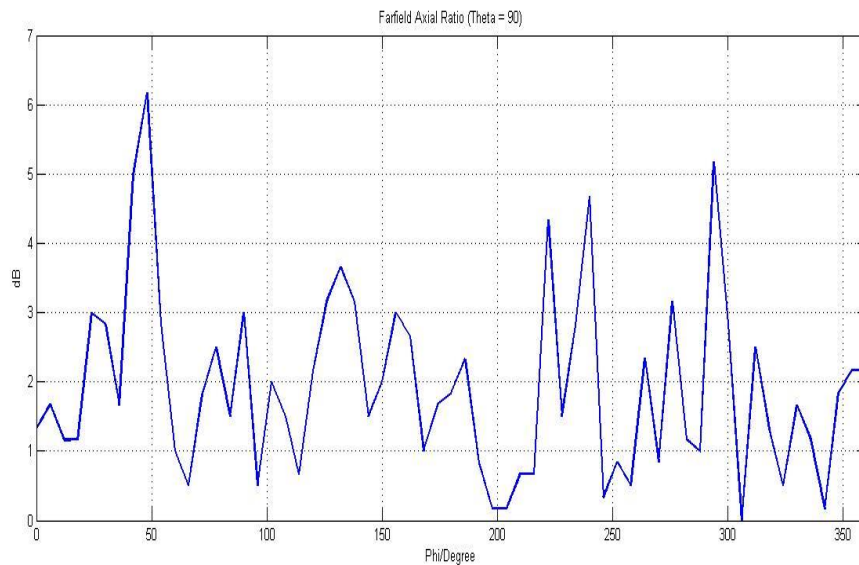

(a)

(b)

Figure 52. Cartesian Axial Ratio Graph of Receiver Antenna Prototype in (a) Azimuth Plane and (b) Elevation Measurements.

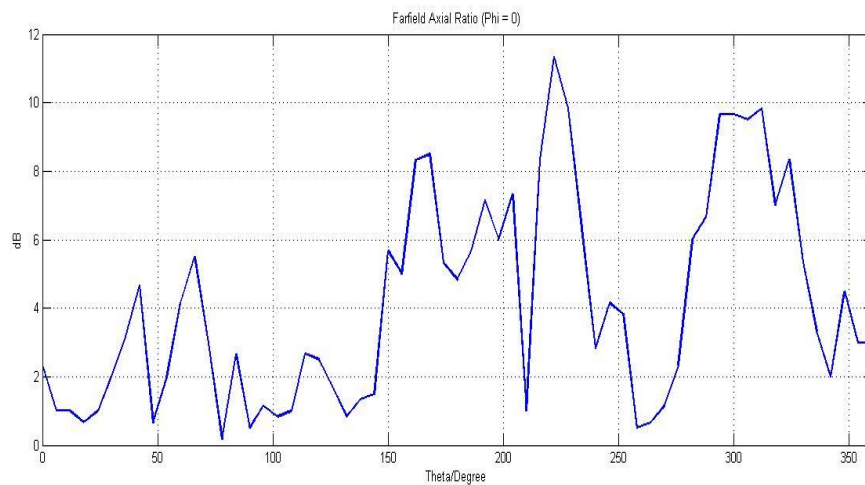Axial ratio graph of receiver antenna prototype is given for both azimuth and elevation planes in Figure 52.a and 52.b respectively. Axial ratio values are expected to be smaller than 3 dB. Even though axial ratio value are smaller than 3 dB in simulation at azimuth plane, measurement results are bigger than 3 dB in some point in azimuth plane axial ratio graph. Maximum value of axial ratio in azimuth plane is measured as

about 6 dB in azimuth plane as shown in Figure 52.a. But at large part of the axial ratio graph in azimuth plane the values of the axial ratio are smaller than 3 dB. It is believed that distortions in the axial ratio due to production faults. They can be fixed by more accurate fabrication. So axial ratio measurement results are satisfied in azimuth plane. As it can be seen in Figure 52.b, in elevation plane there is almost 60° aspect angle (75° - 135°), which axial ratio is under 3 dB as continuously. This result is consistent with the simulation results.

In general, measurement results are consistent with simulation results. It is thought that differences between measurement results and simulation results are caused by manufacture faults. Dimensions of receiver antenna prototype depend on design parameters that are calculated and optimized. Some dimensions of receiver antenna prototype are not in the desired scale. Although there are eight slot antennas in design, four slot antennas are opened on receiver antenna prototype by manufacturer. This can cause significant deterioration on antenna performance. It is believed that measurement results can be made closer to simulation results by correcting these fabrication faults.

CHAPTER FIVE
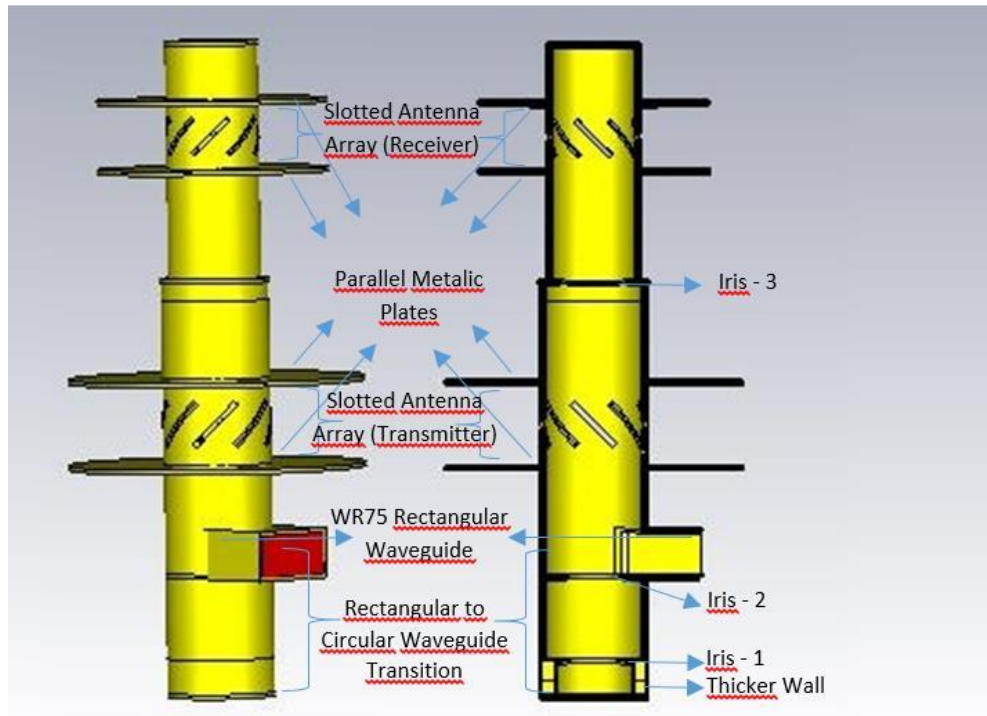# TRANSCEIVER ANTENNA DESIGN

In this chapter, the design of transceiver antenna, which works as transmitter and receiver simultaneously by providing operation at the transmitter frequency of 11.75 GHz and at the receiver frequency of 14 GHz at the same time, is explained in detail with the corresponding simulation results.

5.1. The Steps of the Overall Design

Since transceiver antenna is realized for the simultaneous operation at the transmitter and receiver frequency, the designed antenna can be actually considered as the combination of separate transmitter and receiver antennas given in Chapter 4. It can be noticed that the transition (from rectangular to circular waveguide) for transceiver structure given in Figure 18 is also a combination of separate transmitter and receiver structure. Before giving the detail steps of the design, the overall structure of the designed antenna is given in Figure 52 for better understanding of the schematic of the antenna.

When the structure in Figure 52 is investigated, it can be observed that there is a rectangular to circular waveguide transition at the bottom part of the antenna. The transition is the one described and designed in Section 3.3 (the one in Figure 18). From the results given in Section 3.3, it is found more than 20 dB suppression of dominant but undesired TE_{11} mode at both frequencies and undesired TE_{21} mode at 11.75 GHz. The transition allows the propagation of desired TM_{01} mode at both frequencies, and makes a moderate suppression of desired TE_{21} mode at 14 GHz. As it can be again seen from Figure 52, an antenna similar to separate transmitter antenna with larger circular waveguide given in Figure 26 is put just above the transition such that the antenna is connected to the output of the transition. Then, as being different from the transmitter antenna given in Figure 26, the top part of the antenna in the transceiver design is left open whereas it is closed (short wall) at the transmitter antenna.

**Figure 53.** Overall Design of Transceiver Antenna Structures.

A structure similar to receiver antenna in Figure 27 with smaller circular waveguide is connected to the open part of transmitter antenna in the transceiver antenna. Thus, both transmitter and receiver antenna is connected together to form a transceiver antenna. The top of the receiver antenna part is kept as closed, and an iris (iris 3 in Figure 52) is inserted at the transition between larger circular waveguide and smaller waveguide to provide a better matching. The overall structure can be described as rectangular-to-circular waveguide transition, transmitter antenna and receiver antenna from bottom to top. The combination of rectangular-to-circular waveguide transition, receiver antenna and transmitter antenna from bottom to top is not possible since TM_{01} mode at 11.75 GHz passing from first smaller circular waveguide attenuates significantly and can not reach the upper transmitter antenna. Therefore, the transmitter antenna with larger circular waveguide should be close to the transition (feed) than receiver part with smaller circular waveguide.

By considering, the transition designed in Section 3.3 and used here only allows the propagation of TM_{01} mode at 11.75 GHz/14 GHz and TE_{21} mode at 14 GHz within the larger circular waveguide for transmitter antenna, the choice of the given configuration is also found to be proper. The undesired TE_{21} mode at 14 GHz can propagate in the transmitter part; but, can not propagate in the receiver part with smaller circular

waveguide since the cutoff frequencies of this mode is higher than 14 GHz in this waveguide. So, the wave of this mode can not reach the antennas in receiver part, which are tuned to 14 GHz operation. The disturbance effect of this mode is negligible to the radiation from upper slots. This mode can only radiate from the lower slots; however, the slots in the lower part are tuned for the transmitter frequency of 11.75 GHz such that the transmitter antenna has poor match for the wave of TE_{21} mode at 14 GHz. Besides, the TM_{01} mode at 11.75 GHz, which is not suppressed in transmitter part (larger circular waveguide) encounters a significant attenuation in receiver and can not reach the upper slots.

In the design, the dimensions about the slots and disk for both transmitter and receiver part are almost chosen to be same with the ones given in Chapter 4. However, the length values along bottom-top axis are very critical for the return loss (S_{11}) and radiation pattern characteristics (gain variation, axial ratio) performances. First of all the impedance for the TM_{01} mode at 14 GHz should be matched at the position (level) of iris 3 in Figure 52. Therefore, the impedance at the position (level) of input rectangular waveguide becomes match impedance, which brings low reflected wave and S_{11} for this mode. For this purpose, the distance between the upper top wall and upper slots should be about $\lambda_{g,TM01}/2$ at 14 GHz for larger circular waveguide. Similarly, since the wavelength of TM_{01} mode at 11.75 GHz is too high for upper circular waveguide, the corresponding impedance at the level of iris 3 becomes close to the short circuit. The impedance seen at the lower slot level should be also match for this mode at 11.75 GHz in order to provide lower reflected wave and better radiation at the lower slots. For this purpose, the distance between the iris 3 and lower slots should be about $\lambda_{g,TM01}/2$ at 11.75 GHz for smaller circular waveguide. The undesired TE_{21} mode having a moderate power after the transition can propagate inside the lower waveguide and causes unintended radiation at lower slots at 14 GHz. The effect of this radiation and power level can be further suppressed by arranging the equivalent impedance of this mode at 14 GHz to the large impedance as much as possible at the lower slots and rectangular waveguide levels. For this purpose, the distance between lower slots and rectangular waveguide level can be chosen about $\lambda_{g,TE21}/2$ at 14 GHz for smaller circular waveguide. The large impedance at the lower slot level can be arranged with the distance upper slots and iris 3 level in addition to the dimensions of iris 3 in Figure 52. Besides, the effect of TE_{11} modes might be better suppressed by realizing large

impedances at the rectangular waveguide level for both 11.75 GHz and 14 GHz. It can be carried out again by the proper arrangement of distance upper slots and iris 3 level in addition to the dimensions of iris 3. By considering above explanations and corresponding suggested dimensions, the structure is constructed and simulated in CST MWS by using optimizer tool to give lowest reflection at 11.75 GHz and 14 GHz with wide frequency bandwidth as possible. The dimensions after the optimization process are given in Figure 53.
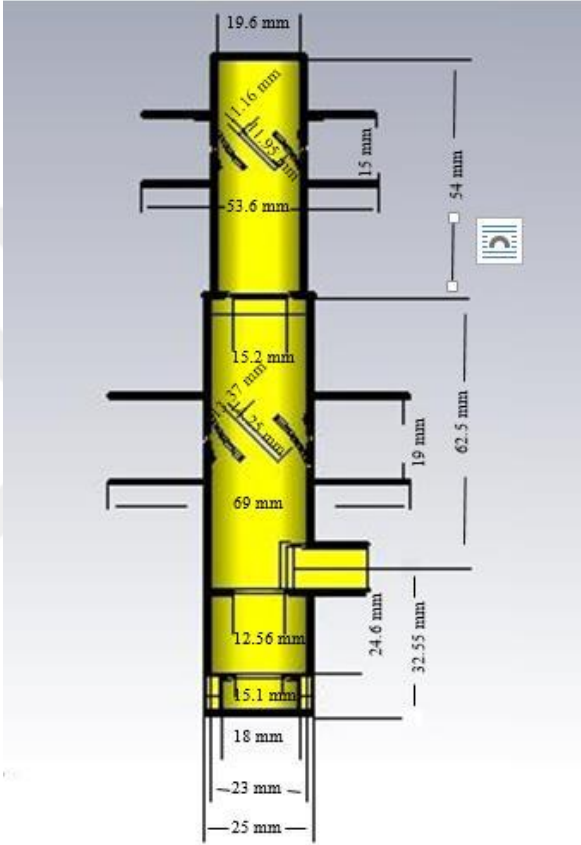

Figure 54. The Dimensions of Transceiver Antenna.

5.2. Simulation Results

S-parameters and farfield radiation patterns of the antennas are investigated in CST MWS simulations. Frequency interval of the simulations is determined as between 10 GHz and 14.5 GHz. This frequency interval includes operating frequencies that are receiving and transmitting. CST MWS automatically produces S11 parameter of antenna as a result of simulations. Farfield monitors must be added to simulations for create of farfield radiation patterns of the antennas. For transmitting frequency a farfield monitor is added to simulation at 11.75 GHz. For receiving frequency, again a farfield monitor is added to simulations at 14.00 GHz.

Firstly, S-parameters of the antenna is investigated. Because S-parameters of the antenna demonstrate the operating frequencies of the antennas. There exists only S11 parameters because of antennas are one port devices. Transceiver antenna S11 graph, which is found as result of CST MW Studio simulations, is given Figure 54.
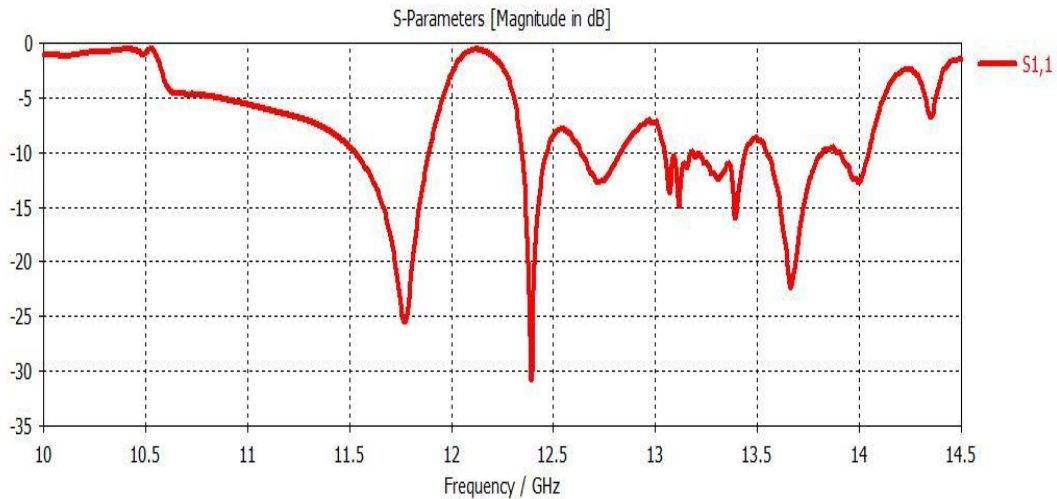

Figure 55. S11 Graph of Transceiver Structure.

As it can be seen in Figure 54, S11 parameter of transceiver antenna is equal to -25.63 dB at transmitting frequency (11.75 GHz). It means, 0.27% of total power that comes from input port of the antenna is reflected back to input port of the antenna at this frequency. -10 dB bandwidth of the transceiver antenna, which includes operating transmitter frequency is 11.75 GHz, is 330 MHz (11.52 GHz to 11.85 GHz). 330 MHz bandwidth around the 11.75 GHz center frequency corresponds to 2.81% bandwidth in terms of percentage. The -10 dB frequency bandwidth of the transceiver antenna is wider than the transmitter antenna that is designed in this study.

S11 parameter of transceiver antenna is equal to -22.21 dB at receiving frequency (14.00 GHz). It means, 0.6% of total power that comes from input port of the antenna is reflected back to input port of the antenna at this frequency. -10 dB bandwidth of the transceiver antenna, which includes operating transmitter frequency is 14.00 GHz, is 510 MHz (13.58 GHz to 14.09 GHz). About 510 MHz bandwidth around the 14.00 GHz center frequency corresponds to 3.64% bandwidth in terms of percentage. The -10 dB frequency bandwidth of the transceiver antenna is wider than the receiver antenna that is designed in this study.
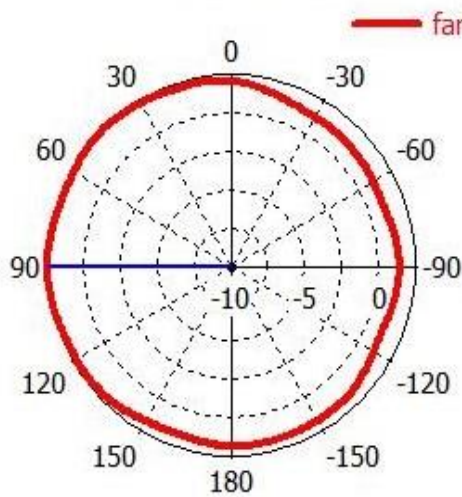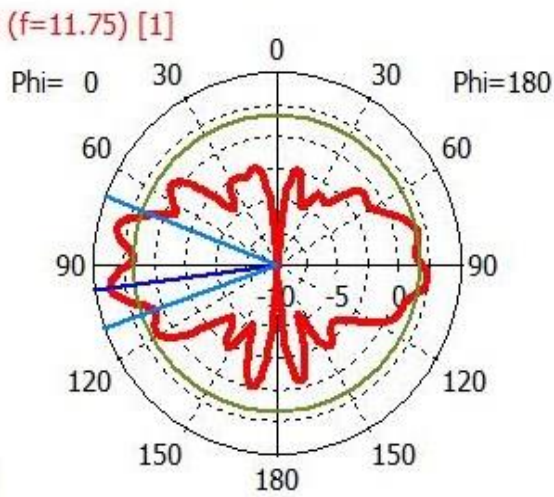
Figure 56. Polar Farfield Gain Graph of Transceiver Structure in (a) Azimuth and (b) Elevation Planes at 11.75 GHz.

Polar farfield radiation patterns of transceiver antenna in both plane are given at transmitting frequency (11.75 GHz) in Figure 55. Polar farfield radiation pattern gives a clear idea about omnidirectionality of transmitter antenna. In azimuth plane, radiation pattern likes almost a circle. There is no dramatically gain change along the azimuth plane as shown in Figure 55.a. In elevation plane, figure of eight farfield radiation pattern exists. There is no any radiation on –z and +z directions. Direction of the maximum radiations are toward to –x and +x directions as given in Figure 55.b.
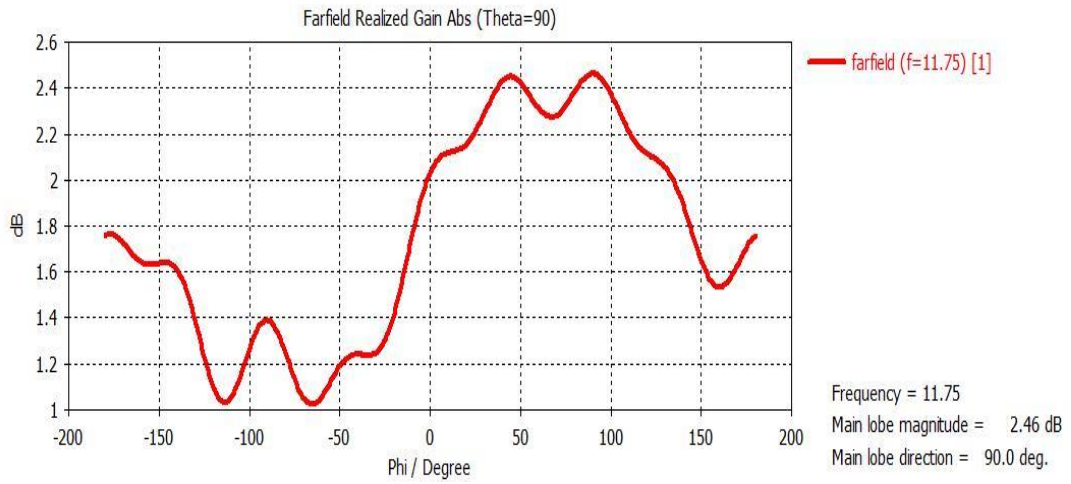
(a)
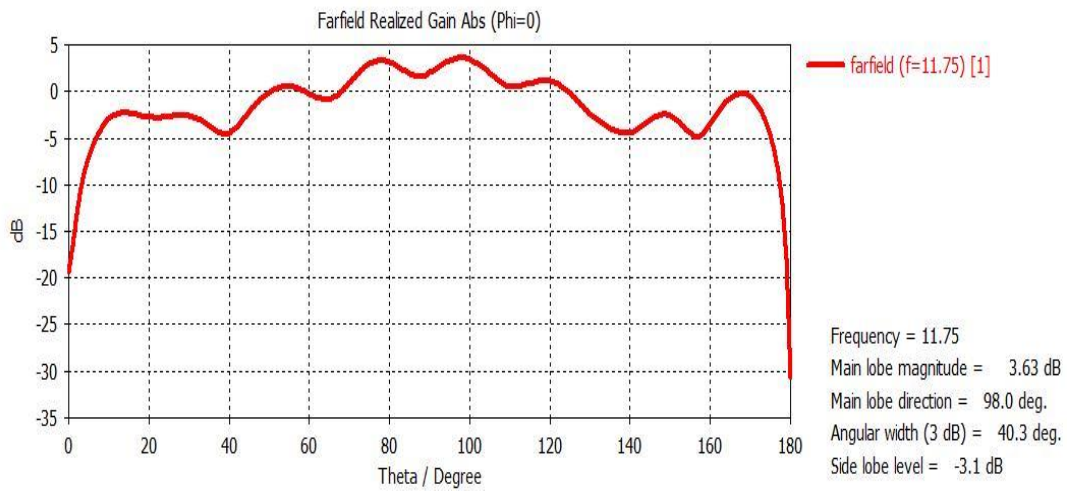
(b)

Figure 57. Cartesian Gain Graph of Transceiver Structure in (a) Azimuth and (b) Elevation Planes at 11.75 GHz.

Magnitude values of the gain in each plane can be clearly seen in Figure 56. In azimuth plane maximum variation of gain is 2.5 dBi in all directions. 2.5 dBi gain variation is worse than the single transmitter antenna design. But 2.5 dBi gain variation in azimuth plane can be acceptable for omnidirectional radiation pattern. Therefore, antenna can be defined as non-directional in azimuth plane. In elevation plane, there is huge difference between maximum magnitude of gain and minimum magnitude of gain so non-directionality is not valid in this plane as it can be seen in Figure 56.b.
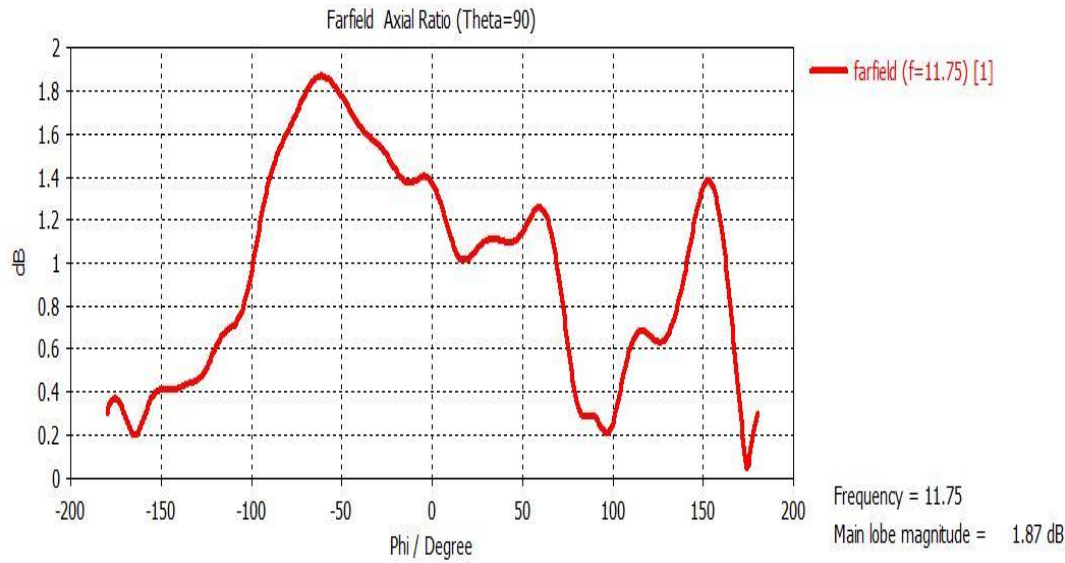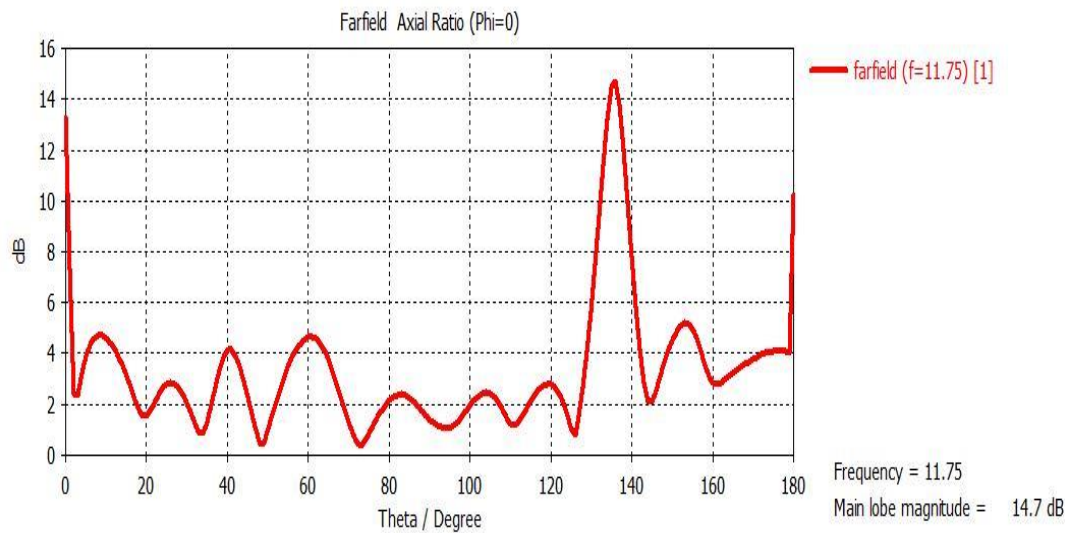
Figure 58. Axial Ratio of Transceiver Structure in (a) Azimuth and (b) Elevation Planes at 11.75 GHz.

Axial ratio of transceiver antenna in azimuth plane at transmitting frequency (11.75 GHz) is smaller than 1.87 dB as shown in Figure 57.a. Even maximum value of axial ratio that belongs to receiver antenna is much smaller than 3 dB in azimuth plane so receiver antenna can be accepted as perfectly circularly polarized in this plane. Although axial ratio of receiver antenna is smaller than 3 dB in a large part of elevation plane, it is only smaller than 3 dB continuously between 68.10^0 and 126.57^0 as in

Figure 57.b. Receiver antennas can be assumed as circularly polarized in elevation plane with 58.47° aspect angle.

Farfield Realized Gain Abs (Theta=90)   Farfield Realized Gain Abs (Phi=0)

farfield (f=14) [1]

Phi / Degree vs. dB
Frequency = 14
Main lobe magnitude =   5.82 dB
Main lobe direction = -126.0 deg.
Angular width (3 dB) = 330.7 deg.

(a)

Theta / Degree vs. dB
Frequency = 14
Main lobe magnitude =   3.97 dB
Main lobe direction =   91.0 deg.
Angular width (3 dB) =   10.2 deg.
Side lobe level =   -0.8 dB

(b)
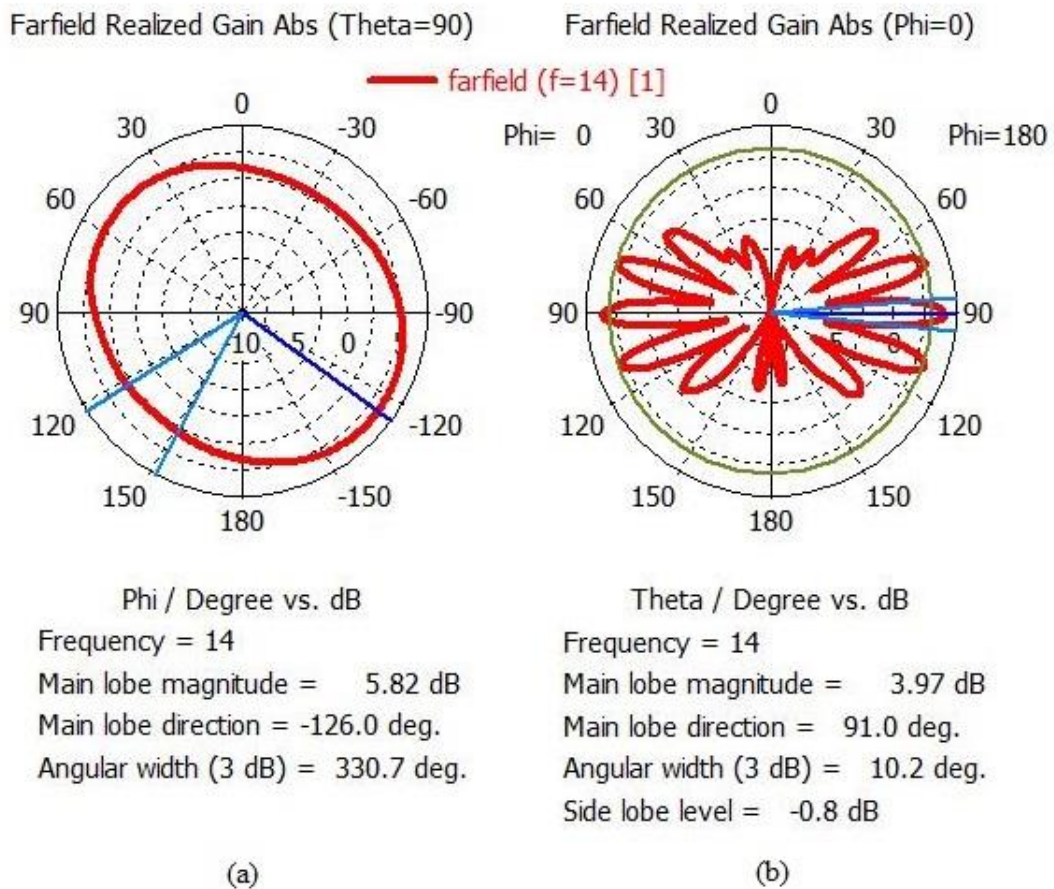
Figure 59. Polar Gain Graph of Transceiver Structure in (a) Azimuth and (b) Elevation Planes at 14.00 GHz.

Polar farfield radiation patterns of transceiver antenna in both plane are given at receiving frequency (14.00 GHz) in Figure 58. Polar farfield radiation pattern gives a clear idea about omnidirectionality of transmitter antenna. In azimuth plane, radiation pattern have elliptically pattern. There is no huge gain change along the azimuth plane as shown in Figure 58.a. In elevation plane, there is no any radiation on –z and +z directions. Direction of the maximum radiations are toward to –x and +x directions as given in Figure 58.b. farfield radiation pattern of these two planes give almost omnidirectional radiation pattern at 14.00 GHz.
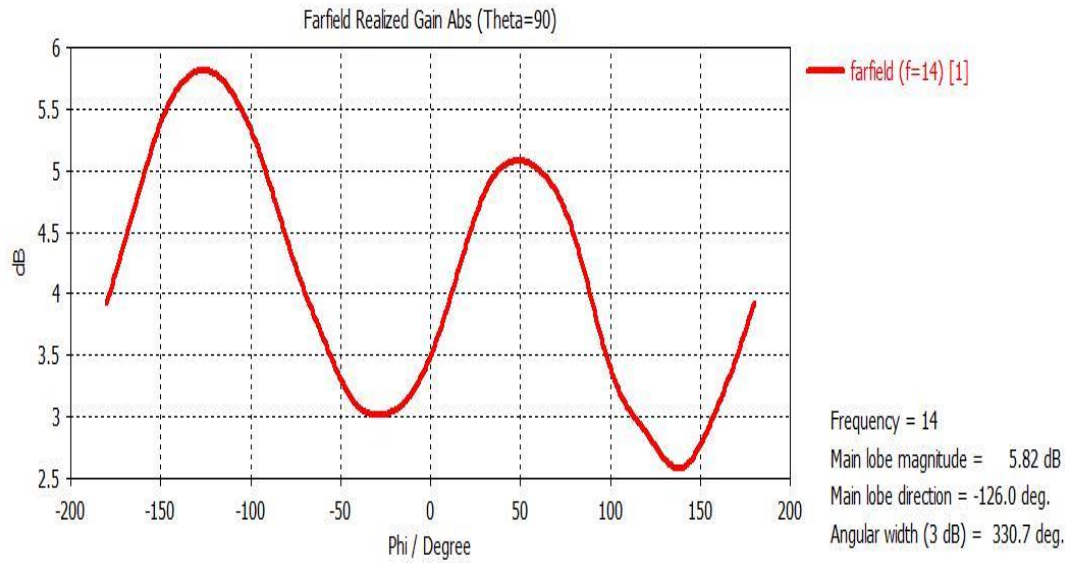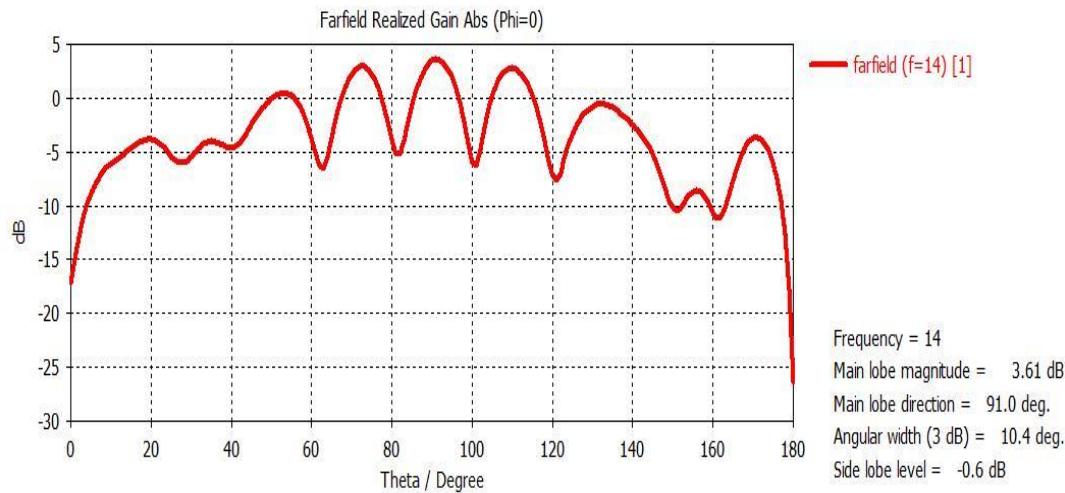
Figure 60. Cartesian Gain Graph of Transceiver Structure in (a) Azimuth and (b) Elevation Planes at 14.00 GHz.

Magnitude values of the gain in each plane can be clearly seen in Figure 59. In azimuth plane maximum variation of gain is 3.2 dBi in all directions. 3.2 dBi gain variation is worse than the single receiver antenna design. But 3.2 dBi gain variation in azimuth plane can be acceptable for omnidirectional radiation pattern. Therefore, antenna can be referred as non-directional in azimuth plane. In elevation plane, there is huge difference between maximum magnitude of gain and minimum magnitude of gain so non-directionality is not valid in this plane as it can be seen in Figure 59.b.

Farfield Axial Ratio (Theta=90)

farfield (f=14) [1]

Frequency = 14
Main lobe magnitude =   1.97 dB

(a)

Farfield Axial Ratio (Phi=0)

farfield (f=14) [1]

Frequency = 14
Main lobe magnitude =   23.5 dB
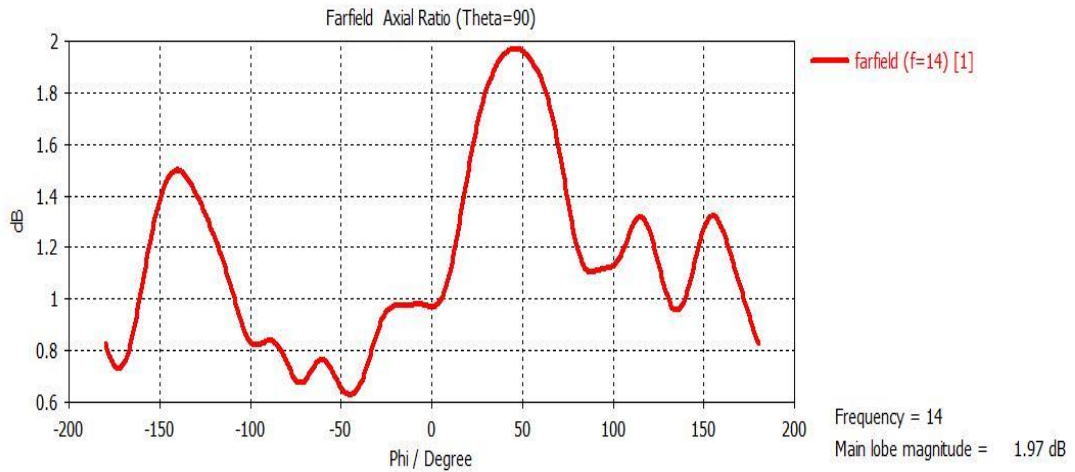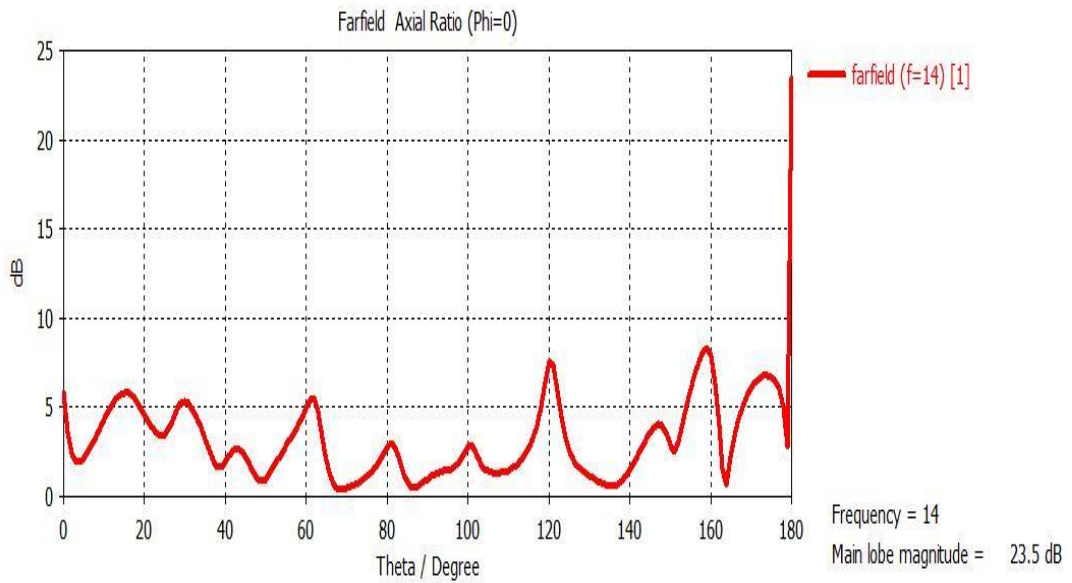
(b)

Figure 61. Axial Ratio of Transceiver Structure in (a) Azimuth and (b) Elevation Planes at 14.00 GHz.

Axial ratio of transceiver antenna in azimuth plane at receiving frequency (14.00 GHz) is smaller than 1.98 dB as shown in Figure 60.a. Even maximum value of axial ratio that belongs to receiver antenna is much smaller than 3 dB in azimuth plane so receiver antenna can be accepted as perfectly circularly polarized in this plane. Although axial ratio of receiver antenna is smaller than 3 dB in a large part of elevation plane, it is only smaller than 3 dB continuously between 65.14^0 and 117.48^0 as in Figure 60.b.

Receiver antennas can be assumed as circularly polarized in elevation plane with 52.34^0 aspect angle.

CHAPTER SIX
CONCLUSIONS AND FUTURE RESEARCH

In this thesis, omnidirectional and circularly polarized transmitter (11.75 GHz), receiver (14.00 GHz) and transceiver (11.75 GHz and/or 14.00 GHz) antennas that can be used in satellite communication applications are designed simulated. Only receiver antennas from these antennas is fabricated and measured. Types of antennas that can be used for this study are found as result of literature search. It is aimed that improve performance of antenna structures that are found in literature in terms of bandwidth, gain and axial ratio. For this purpose, antenna dimensions are reconfigured by optimization iterations in CST MWS.

Antennas that are designed consist inclined eight slots. These slots are placed on circular waveguide and they are fed by a symmetrical mode that is TM_{01} for providing omnidirectional farfield radiation pattern. Dominant mode propagation mode inside circular waveguide is TE_{11}. In order to provide mode conversion, which is from TE_{11} to TM_{01}, special transition structures are designed. It is aimed that provide suppression of dominant mode TE_{11} and other higher order modes such TE_{21}, which are no nonsymmetrical, and transmission of TM_{01} that is symmetrical mode with the transition structure. To make circular polarization, antenna slots are designed as inclined and some metallic plates are added around the antennas.

Antennas are fed by WR75 standard rectangular waveguide. WR75 rectangular waveguide is commonly used in Ku-Band satellite communication applications. To antennas work compatible with satellite communication systems is provided by selecting input port as WR75 standard rectangular waveguide.

In simulations, separate transmitter and receiver antennas have about 2.5% -10 dB bandwidth. The -10 dB bandwidth of these antennas are wider than the similar antennas in literature. Axial ratio performance of these antennas are also better than the antennas that are compared in literature. Axial ratio of separate transmitter and receiver antennas have almost perfect circular polarization in azimuth plane. Axial

ratio of these antennas lower than 1 dB in this plane. In elevation plane axial ratio of these antennas lower than 4 dB with wide beamwidth at operating transmit and receive frequencies.

Only receiver antenna is fabricated and measured. Although measurement results are not as well as simulation results, they are consistent with each other. Differences between simulation results and measurement results due to production faults. In receiver antenna prototype, four antenna slots are implemented instead of eight antenna slots and dimensions of these slots are not comply exactly with design. Parallel metallic plates that are placed around the antennas are not produced with desired dimensions. These production faults cause important disruption on antenna performance. It is believed that prototype antenna performance can be improved with more accurate fabrication.

Transceiver antenna that is proposed has wider -10 dB frequency bandwidth with respect to separate transmitter and receiver antennas. -10 dB bandwidths for transmitting and receiving frequencies are respectively 330 MHz and 510 MHz. Axial ratio values in both transmitting and receiving frequencies are lower than 2 dB in azimuth plane. Variations of gain is lower than 3.2 dBi in this plane.

Transceiver structure can be more improved. Studies continue in order to increase frequency bandwidths and reduce axial ratio and variations of gain. Design of dual polarized transceiver structures are thought as future work.

REFERENCES

Balanis, C. A. (2012). *Advanced Engineering Electromagnetics* (2nd ed.). Wiley.

Balanis, C. A. (2005). *Antenna Theory Analysis and Design* (3rd ed.). Wiley.

Bertin, G., Piovano, B., Accatino, L., & Mongiardo, M. (2002). Full-wave Design and Optimization of Circular Waveguide Polarizers with Elliptical Irises. *IEEE Transactions on Microwave Theory and Techniques 50(4),* 1077-1083. http://doi.org/10.1109/22.993409

Bornemann, J., Amari, S., Uher, J., & Vahldieck, R. (1999). Analysis and Design of Circular Ridged Waveguide Components. *IEEE Transactions on Microwave Theory and Techniques 47(3),* 330-335. http://doi.org/10.1109/22.750235

Cheng, D. K. (1993). *Fundamentals of Engineering Electromagnetics* (1st ed.). Addison-Wesley.

Dybdal, R. (2009). *Communication Satellite Antennas: System Architecture, Technology, and Evaluation* (1st ed.). McGraw-Hill.

Elbert, B. R. (2000). *The Satellite Communication Ground Segment and Earth Station Handbook.* (1st ed.). Artech House.

Galindo, V., & Green, K. (1965). A Near-Isotropic Circulary Polarized Antenna for Space Vehicles. *IEEE Transactions on Antennas and Propagation 13(6),* 872-877.

Gao, S., Luo, Q., & Zhu, F. (2014). *Circularly Polarized Antennas* (1st ed.). Wiley.

Ippolito Jr., L. J. (2008). *Satellite Communications System Engineering* (1st ed.). Willey.

Kolawole, M. O. (2014). *Satellite Communication Engineering* (2nd ed.). CRC Press.

Lim, J. Y., Nyambayar, J., Yun, J. Y., Kim, D. H., Kim, T. H., Ahn, B. C., & Bang, J. H. (2014). High Performance Dual-Circularly Polarized Reflector Antenna Feed. *ETRI Journal 36(6),* 889-893. http://dx.doi.org/10.4218/etrij.14.0114.0118

Masa-Campos, J. L., Fernandes, J. M., Sierra-Perez, M., & Fernandez-Jambrina, J. L. (2006). Omnidirectional Circularly Polarized Slot Antenna Fed by a Cylindrical Waveguide in Milimeter Band. *Microwave and Optical Technology Letters 49(3)*, 503-742. http://doi.org/10.1002/mop.v49:3

Maral, G., & Bousquet, M. (2010). *Satellite Communication Systems* (5th ed.). Willey.

Milligan, T. (2005). *Modern Antenna Design* (2nd ed.). Wiley&Sons.

Pozar, D. M. (2012). *Microwave Engineering* (4th ed.). Wiley.

Ragan, G. L. (1948). *Microwave Transmission Circuits* (1st ed.). McGraw-Hill.

Rao, S., & Sharma, S. K., & Shafai, L. (2013). *Handbook of Reflector Antennas and*

Feed Systems vol.2 (1st ed.). Artech House.

Rao, S., & Sharma, S. K., & Shafai, L. (2013). *Handbook of Reflector Antennas and Feed Systems vol.3* (1st ed.). Artech House.

Sakaguchi, K., & Hasabe, N. (2002). A Circularly Polarized Omnidirectional Antenna. In 1993 Eighth International Conference on Antennas and Propagations. IET. http://ieeexplore.ieee.org/document/224858/

Silver, S. (1949). *Antenna Theory and Design* (1st ed.). McGraw-Hill.

Stutzman, W. L., & Thiele, G.A. (2013). *Antenna Theory and Design* (3rd ed.). Wiley.

Top, C. B., & Dogan, D. (2012). A Circularly Polarized Omni-Directional Low Loss Ka-Band Slot Antenna. In 2012 *IEEE Antennas and Propagation Society International Symposium (APSURSI)*. IEEE. http://doi.org/10.1109/APS.2012.6348032

Turkmen, C., & Secmen, M. (2016). Circularly Polarized Hemispherical Antennas for Telemetry and Telecommand Applications in Satellite Communications. In 2016 *10th IEEE European Conference on Antennas and Propagation (EuCAP)*. IEEE. http://doi.org/10.1109/EuCAP.2016.7481486

Uher, J., Bornemann, J., & Rosenberg, U. (1993). *Waveguide Components for Antenna Feed Systems: Theory and CAD* (1st ed.). Artech House.

Ulaby, F. T., & Ravaioli, U. (2014). *Fundamentals of Applied Electromagnetics* (7th ed.). Pearson.

Zhong, W., Li, B., Fan, Q., & Shen, Z. (2011). X-Bnad Compact Septum Polarizer Design. In 2016 *International Conference on Microwave Technology & Computational Electromagnetics (ICMTCE)*. IEEE. http://doi.org/10.1109/ICMTCE.2011.5915191